АКАДЕМИЯ НАУК СССР

ИЗВЕСТИЯ КРЫМСКОЙ АСТРОФИЗИЧЕСКОЙ ОБСЕРВАТОРИИ

ТОМ I
Часть I

ИЗДАТЕЛЬСТВО АКАДЕМИИ НАУК СССР
МОСКВА — 1947 — ЛЕНИНГРАД


АКАДЕМИЯ
НАУК
СССР

ACADEMY OF SCIENCES OF THE USSR

PUBLICATIONS OF THE CRIMEAN ASTROPHYSICAL OBSERVATORY

VOL. I

Part 1

PUBLISHING HOUSE OF THE ACADEMY OF SCIENCES OF THE USSR

MOSCOW — 1947 — LENINGRAD

G. A. SHAJN,

Editor in chief

The present edition is a translation of the text issued in parallel in Russian.

Настоящее издание является переводом текста, выпускаемого параллельно на русском языке.

PREFACE

The Simeis Observatory was founded as a southern branch of the Pulkovo Observatory in 1908. The work consisted in the main in observations of minor planets, comets and variable stars and in determinations of photographic magnitudes of stars. This work was done with the double 120 mm astrograph.

In 1925 was mounted the 40 inch reflector by Grubb, and the laboratory equipped with some new measuring apparatus. Since then Simeis became the main astrophysical observatory in USSR. Up to the beginning of the war there were secured some thousands of spectrograms of stars mostly fainter than 6.00. Radial velocities of about 700 stars were published or are prepared for press. Attention was paid also to diverse problems of modern astrophysics (rotation of stars, emission spectrum of long period variable stars, molecular spectra, supergiants a. o.). A number of papers on this subject are now ready for publication. About 110 minor planets, 8 comets, about 40 spectroscopic binaries and more than 300 variable stars were discovered at the Observatory.

In the middle of October 1941 at the approach of the fascist invading armies to Crimea the scientific staff of the Observatory was evacuated and an insignificant part of the equipment and scientific material was carried away. In autumn 1943 the Germans took away the whole equipment including the 40 inch reflector. The main building of the Observatory was burned in January 1944, other buildings and domes were strongly damaged or destroyed by the invaders.

The Observatory lied outside the zone of war operations whatever and its looting and destruction is to be regarded as a forethought will to injury cultural institutions of a foreign country.

Soon after the end of the war our instruments were found at the Potsdam Observatory. As was duly stated, the dismounting of the instruments at Simeis, their transport to Germany and keeping there were done in so barbaric a manner that they present now no more than a heap of rusty scrap of no value whatever. The greater part of the spectroscopic material is lost.

The fascist invasion caused us also harm in another respect. From the very small scientific staff of the Observatory two young astronomers V. G. Shaposhnikov and M. V. Volkov perished on the front, and the scientific mechanician A. A. Kotov was shot by the Germans at Simeis.

Instead of the destroyed Simeis Observatory will be built a new Astrophysical Observatory equipped with modern powerful instruments including a big reflector. By a Government decree the Simeis branch of the Pulkovo Observatory is now reorganized to an independent Crimean Astro-

physical Observatory of the Academy of Sciences of the USSR. Henceforth this Observatory will issue the «Publications of the Crimean Astrophysical Observatory of the Academy of Sciences of the USSR».

It was known long ago that the site of the Simeis Observatory is unfavourable as regards the astronomical conditions for large instruments. The Observatory (360 m height) lies in a fair site on a rather steep slope between a plateau of about 1000 m. height and the sea. The character of this place is favourable for the origin of frequent disturbances in the atmosphere and local turbulent phenomena, which often spoil the stellar images. After all, the place for the Simeis Observatory was chosen accidentally: here was located a small private observatory passed on to the Pulkovo Observatory in 1908. The question of the erection of a new large astrophysical observatory in a more favourable site in the Crimea was settled long ago. Special explorations made before the war, during it and completed after the war allowed to state that the foot-hills of the Crimean mountains present serious advantages as compared with the southern shore or the slopes directed to the sea. For the sake of illustration we give below in Fig. 1 a comparison of the quality of diffraction images of stars (after Danjon and Couder) observed in 4 points in the Crimea. The full line curve and the dotted one relate to the foot-hills of the Crimean mountains (Partizanovka and Buragan respectively), the curve represented by heavy dots relates to Simeis, and the one — by dots and crosses — to Urkusta, a site located in the Central Western part of the Crimean mountains on the slope towards the sea, 26 km. south-east from Sebastopol. The observations were done simultaneously and were reduced to one system by means of a comparison of instruments with account of the personal difference. The curve relates to zenith distance 20°. A detailed paper on the comparison of different sites in the Crimea from the standpoint of astronomical observations will be published in the second part of this volume.

The site chosen for the new Observatory represents a plateau of 560 m. height and lies 27 km south-west from Simferopol and 41 km north-east from Sebastopol between the villages Partizanovka (formerly Mangush) and Bia-Sala.

The old Simeis Observatory now being reestablished will be a branch of the new Observatory. The plan of erection of the Crimean Astrophysical Observatory is reckoned upon 4—5 years. Already in 1947 we hope to mount a 50 m. spectrograph for the study of interstellar diffuse matter.

G. Sh.

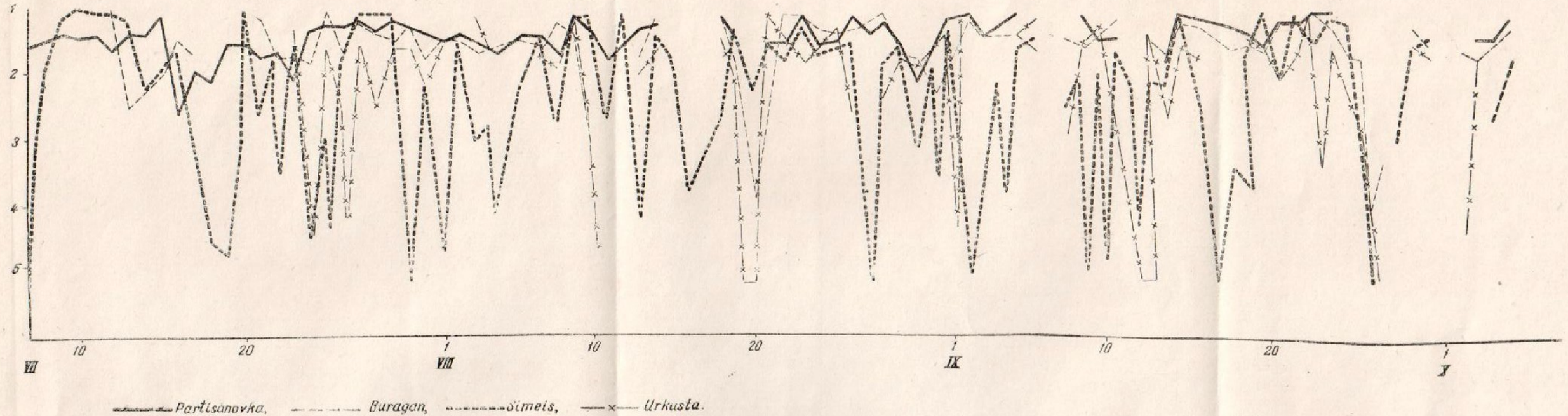

Fig. 1. Comparison of quality of stellar images

EMISSION LINES OF H, Fe II AND Fe I IN SPECTRA OF LONG PERIOD VARIABLE STARS

First paper

G. SHAJN

In this paper are given some results with respect to the emission lines in the spectra of long period variable stars.

Hydrogen. The width of the emission lines in the region 3700—3900 A turns out to be about 0.6 A, that is several times as great as the Doppler thermal width for T adopted for these stars. The extreme non-uniformity of hydrogen emission lines H_5—H_{16} with respect to structure, intensity and anomaly in wave-lengths may be explained without serious exceptions in terms of the hypothesis of physical screening or blending, the absorbing material being TiO, V I, Fe I, Cr I, Ca II, H. The discussion of the intensity of hydrogen lines in terms of the theory of the curve of growth leads to the conclusion that the exciting radiation for the emission hydrogen spectrum is very strong and has properly no relation to the usual photosperic radiation of these stars.

Ionized iron. Several anomalies are discovered in the behaviour of the emission Fe II lines, and the main of them are: 1) The anomaly in the intensity ratio 4233 : 4179 : 4173. 2) The absence of emission lines in the green region. 3) Several peculiarities in the intensity of the lines within the region 4300—4600. All the numerous anomalies may be explained in terms of the hypothesis of physical screening, the absorbing material being TiO, Fe I and Ca I. The anomaly in the intensity ratio 4233 : 4179 gradually decreases with advancing phase. It is found that near the epoch of maximum there is no reason to speak of any difference between the radial velocities of the Fe II ions and the atoms of H.

Neutral iron. An intensity anomaly is found for the lines belonging to the multiplet $a^5D - z^7P^0$. The decrease of the anomaly with increasing phase has much in common with that for the known anomaly for the multiplet $a^3F - z^3G^0$. The tendency to the formation of emission lines is found also for the multiplet $a^3F - y^3F^0$. There are serious reasons to suggest that all the low temperature multiplets of Fe I display to some degree a tendency to emission, especially in more distant phases. Even for obvious emission lines of Fe I one can always trace a gradual transition from absorption into emission. Within a multiplet it is properly not easy to divide the lines into emission and absorption ones.

The numerous and highly various anomalies in the behaviour of the emission lines of Fe I may be generally reconciled, at least in the majority of cases, with the hypothesis of physical screening, if one assumes that the main rôle in the screening effect belongs to the absorbing atoms of Fe I.

The problem of emission lines in the spectra of long period variable stars must be intimately connected with the general problem of these stars. Hitherto the origin of emission lines in these cold stars remains quite enigmatic. The problem of emission lines in these stars outgrows the limits of a

special problem, and three lines of research may be marked therein. 1) The nature of emission lines in spectra of cold stars. 2) Emission lines as a method of study of the structure of atmospheres of these remarkable stars and the processes going on in them. 3) The emission spectrum as an indicator of the special rôle of high frequency radiation in the processes taking place in these stars.

Not only the very presence of emission lines in spectra of such cold stars is a mystery, — we meet in the study of their spectra with surprising anomalies in the relative intensities of the emission lines — a phenomenon observed neither in stars of other classes with emission lines (Be, Novae, a.o.), nor in laboratory.

It was known since long that the hydrogen emission lines in the spectra of Me stars display remarkable anomalies. The Fe I emission lines are also known to be subject to some anomalies, but our information is here much less certain than for hydrogen. As to Fe II emission lines, it remains even unknown whether there are any anomalies at all.

By elucidating the general nature of these anomalies one can hope to find a clue for understanding the structure of the atmospheres of these stars, as well as of the complicated processes that take place there.

The present paper contains the results of the study of these anomalies for H, Fe I and Fe II based chiefly upon original observations of the spectrum of o Ceti. In the second part of this research, which will appear in the next issue of these publications, the material will be treated from the standpoint of interpretation of the observations. A brief account of the results of this work was read before the Session of the Academy of Sciences of the USSR. (1).

HYDROGEN

The width of the hydrogen emission lines in the spectra of long period variable stars is unknown. It is self-evident that very much would be gained even if only the order of this quantity were estimated. This was done by the author in the following three ways: a) In the region 3800—3900 the dispersion used at Simeis Observatory is about 22 A per mm., and the hydrogen emission lines in the spectra of o Ceti and χ Cygni appear to be sensibly wider than the iron lines of the same intensity in the comparison spectrum. Allowing in a rough manner for the influence of the instrumental profile, we found the width of H_{11} and H_8 to be about 0.6 A. b) It is further a well known fact that some emission lines appear to be double or even triple. The cause of the decrease of emission in the central portion of the profile is due, at least for some of the lines, to the influence of absorption lines. For instance, the doubling of H_{16} is due to the low temperature V I line at 3703.6. Even when using a moderate dispersion, the distance between the components of H_{16} and H_{10} may be measured with certainty. This distance which turned out to be about 0.6 A evidently represents the minimum value of the line width. c) At last one may judge on the width from the excellent large scale spectrogram of o Ceti, recently obtained by A d a m s (2). Selecting not overexposed emission lines not affected sensibly by absorption ones we find their width to be of the order of 0.6 A. Therefore the width of the hydrogen emission lines in the region 3700—3900, as estimated independently in three different ways, turns out to be about 0.6 A, that is several times as great as the Doppler thermal width for T adopted for these stars.

The known anomalies in the intensities of H_ε, H_γ, H_β, H_α, have long been interpreted in terms of the hypothesis of overlying absorption (TiO, Ca II),

though the phenomenon is much more complicated than it appears at first sight. The Balmer decrement within H_8 — H_{16} seems to be more «normal», though several lines show a fairly notable anomaly. The term «anomaly» is understood here in a wider sense than usually. In addition to the intensity anomaly one must also consider the anomaly in wave-length and the anomaly in the structure of the lines. Below in Table I are confronted these three characteristics for H_8 — H_{16}, using for the first two of them our own measurements and estimates. With respect to the measured deviations in λ we have a good agreement with Merrill (3). As to the line structure the above mentioned spectrogram by Adams has proved to be very useful.

TABLE I

Lines	Deviation in λ	Weakening	Structure
H_{16} 3703.85	—	very strong	Distinct doubling
H_{15} 3711.97	0?	0?	Possibly insignificant asymmetry V
H_{14} 3721.94	0?	very strong	Width nearly twice as small as for other lines
H_{13} 3734.37	—0.04	small	Small asymmetry R
H_{12} 3750.15	+0.28	very sensible	Strong asymmetry V
H_{11} 3770.63	0.00	0	Complete symmetry
H_{10} 3797.90	—0.20	small	Sensible asymmetry R, double or triple
H_9 3835.39	0.00	small	Insignificant asymmetry V
H_8 3889.05	+0.13	0?	Small asymmetry V

Remarks. H_{16}. The doubling is due to V I 3703.59, E. P. 0.299. H_{15}. There [are] no lines for sensible influence. H_{14}. The strong weakening and the anomaly in the width are due to 7 faint Fe lines near the centre and to the wings of the distant, but very strong Fe I line 3720.0, E. P. 0.000 and the blend 3722.6. H_{13}. In the solar spectrum a very strong line Fe I 3734.88, E. P. 0.855 is observed, which might be supposed to have an appreciable effect. But in M stars this line seems to be somewhat fainter, and the small weakening of H_{13} is probably justified. H_{12}. Evidently a very sensible influence of the strong Fe I line at 3749.50, E. P. 0.911. H_{11}. There are no lines for sensible influence. According to Merrill, sometimes double. This is probably due to a faint blend 3770.5 observed in M stars. H_{10}. The faint absorption lines near the centre cause probably the doubling (according to Adams, H_{10} is triple). The influence of the low temperature blend 3798.3 seems to be sensible. H_9. A very small influence is possible only from Fe I 3834.23, E. P. 0.954. H_8. Double according to Adams (possibly owing to the faint line Fe I 3888.53).

When comparing the wave-lengths it is necessary to allow for the relative shift of the emission lines (about —0.2 A).

As to the low members of the Balmer series it is preferable to use the data obtained with high dispersion. According to the older data, the structure of H_δ and H_γ is composite. The best modern observations show these lines to be only double, and the comments by Adams (2) may be interpreted to some extent as an indication that this doubling is due to hydrogen absorption lines. In this connection it is of interest to note a very considerable negative displacement for H_α in Me stars (Shane —1.0, Merrill's recent result —0.4 A). We think that this may be due to the influence of an absorption line H_α (see below). Comparing now the numerous data, we must conclude that the extreme non-uniformity of hydrogen emission lines with respect to structure, intensity and anomaly in the wave-lengths may be explained, at least in the majority of cases, without serious exceptions in terms of the hypothesis of overlying absorption, the absorbing material being not only TiO and Ca II but also V I, Fe I, Cr I, H. As we shall see later when

discussing the emission lines of Fe II, the absorbing material includes also the Ca I atoms.

This result seems to be an extension of that found previously with respect to this point (M e r r i l l and B u r w e l l, S h a n e (4)).

Attention must be paid to the observed fact that the emission line H_β is sometimes not seen and H_α is seen but very seldom, while the adjacent continuous background is quite perceptible. One may think that the optical depth for the emission lines H_α and H_β is not greater than that for the adjacent continuous background. It is true that the rotational structure of the TiO bands favours the smaller absorption for the continuous background since the atmosphere may be relatively transparent in the intervals between the rotational lines. But the rôle of these intervals is probably small, since, otherwise, the emission lines would sometimes coincide with them and therefore the intensities of the emission lines would show a great range for individual stars even within one subclass. In fact, the observations do not show this. If so, the emission lines may strongly decrease absolutely in intensity but the total intensity, expressed in units of the continuous background, cannot decrease. In fact, this does not hold for H_β and H_α, at least sometimes, and for this reason some additional absorption for these lines may be suggested. One may think here of a self-absorption properly said and of a decrease of radiation flowing through overlying layers which contain the absorbing hydrogen atoms. We think, though this is possibly in disagreement with the adopted opinion, that the hydrogen absorption lines are present in the spectra Me. It is true, the theory predicts at temperature about 3000° a negligible percentage of hydrogen atoms in the second quantum state, but as a matter of fact, the hydrogen absorption lines in gM 5 — and especially in cM 5 — are exceptionally strong. This anomaly may be partly connected with the very low value for g_{eff} and with the great extension of the atmosphere. This is probably also of importance to some extent for Me stars.

It is to be also noted, that when T and g are low, the Balmer decrement for the absorption lines must be considerable. Therefore, if even H_δ and H_γ are faint, the absorption line H_α may be still strong enough. The following arguments are to be brought in favour of the presence of hydrogen absorption lines in the Me spectra: 1) Systematic displacement (about —0.4 A) for H_α in emission, which apparently is very difficult to explain otherwise than by the influence of an absorption component H_α. 2) According to J o y (5) near the epoch of minimum, when the emission hydrogen lines disappear, hydrogen is observed in absorption. 3) Some possibilty of the interpretation of the doubling of H_δ and H_γ as an effect of corresponding absorption lines of H. 4) Some analogy between the absorption spectra of Me and gM — cM.

The presence of hydrogen absorption lines seems to be much less probable in Se and still less in Ne stars.

The possibility of the presence of overlying absorbing hydrogen atoms in Me seems to be interesting in itself. But in connection with this it is very difficult to draw some conclusion with respect to the self-absorption properly said. It seems to be probable that both effects are present: in favour of the former speaks the observed systematic displacement —0.4 A for H_α and other facts; in favour of the self-absorption—the probable weakening of H_α in Ne and Se stars.

However from the point of view of the study of the self-absorption it is worthy to pay attention to the violet region. It was already mentioned that the anomalies within $H_6 - H_{16}$ find a satisfactory explanation in that the Balmer decrement here is more or less «normal», say, as in Be stars

or in the chromosphere. This points out to an emission under conditions of an optically thin layer, when

$$A_\lambda = \frac{\pi e^2}{Mc^2} \lambda^2 . 10^8 . NHf$$

But the most interesting fact is that in addition to the «normal» decrement the observed total intensities of high Balmer members are considerable. This is seen at once, since, while the line-width is of the order 0.6 A., the contrast between such lines as H_{11} and the continuous background is high. Our measurements gave E. W. $\geqslant$ 1.0 A for H_ζ and even for H_{11}. It is evident that, though the accuracy of such measurements may be only low, the order of the value found for E. W. is correct. For the case of an optically thick uniform layer the total intensity is expressed by

$$E = B \int_0^\infty (1 - e^{-NHf}) \, d\lambda .$$

In the general case B may be considered as the mean intensity of the exciting radiation, which may be found from the study of the profile of the spectral line (6). In the case of thermal equilibrium B_λ is Kirchhoff — Planck's function for T_0 (according to the theory of radiative equilibrium, the intensity of radiation from the limb). Therefore expressing the measured E in units of intensity of the continuous background (reducing the latter to the value for the limb) we obtain E/B (in our case here is evidently presumed the thermal equilibrium for T_0 of the order of 2700°).

The integral $\int_0^\infty (1 - e^{-NHf}) \, d\lambda$ was discussed in detail in the theory of the curve of growth for the absorption lines, and these results may be applied immediately to the measured values of E/B for the emission lines. Turning now to the curve of growth connecting $\log \frac{NHf}{\Delta\omega_D}$ with $\log \frac{E}{B 2 \Delta\omega_D}$, one may see that at a given E the self-absorption is the stronger, the less is $B . 2 \Delta\omega_D$. The lower is the temperature, the earlier will take place the transition from the 45° branch to the intermediate one of the curve of growth. In the application of these reasonings to the Balmer lines it is supposed that the portion of the spectrum under consideration is very limited. At $T = 3000°$ the self-absorption must be still appreciable for E. W. about 0.50 A, and therefore in our case for H_ζ and even for the higher members. However, as this was mentioned earlier, the conditions of the optically thin layer hold at least as far as H_δ. The explanation must be probably looked for in that the value $2 \Delta\omega_D B$ is in fact much higher than $2 \Delta\omega_D \times$ Kirchhoff-Planck's function for T of the order of 2700°. One might think here of some analogy with the phenomenon of «turbulence», recently discovered by S t r u v e and E l v e y (7) in the rare objects of early class. In the latter case the cause is to be looked for probably in the large macroscopic movements greatly increasing the value $\Delta\lambda_D$. But in the case of emission lines in question the transition to the intermediate branch of the curve of growth will depend on the function $B \; 2 \Delta\omega_D$. The observed width of the H emission lines of order of 0.6 A does not still predestine the predominant rôle of the macroscopic movements. It will be shown elsewhere that the large width of the emission lines of H is probably partly due to the outward motion of gases. The main cause of the «normal» decrement in Me stars is probably in that the exciting radiation for the emission spectrum is much stronger than that corresponding to the thermal equilibrium for T of the order of 3000°, if one

may think at all of the formation in any way of emission lines at such a low temperature.

One may bring several arguments in favour of the suggestion that in Me stars the absorption and emission spectra are generally independent, and that the origin of either is due to different physical processes and conditions. Here we have found in the behaviour of the Balmer lines an evidence that the emission spectrum in Me stars is properly not connected with the photospheric radiation, determining mainly the temperature of atmospheric layers and the general character of the absorption spectrum. This result is in agreement with the extreme difficulty to understand the appearance of the emission lines in the ordinary conditions at low temperature, especially of lines of such high excitation as H and Fe II.

IONIZED IRON

For the hypothesis of the physical screening it is of high importance to know the behaviour of the lines belonging to the ions Fe II. It remained until now uncertain whether there are any anomalies for these lines at all.

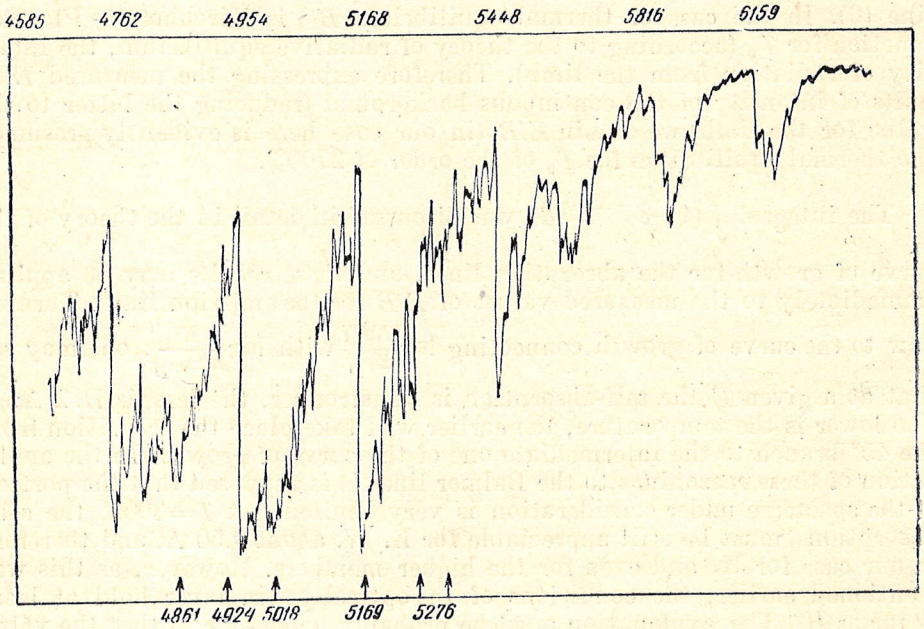

Fig. 1. Microphotogram of o Ceti

A thorough investigation of the Fe II lines intensities, mainly in the spectrum of o Ceti, led to the discovery of several conspicuous anomalies. Particularly remarkable is the nearly total absence of Fe II emission lines in the green region of the spectrum of the Me stars. The lines 4924, 5018, 5169, 5276 and 5316, which in laboratory and in the spectra of other celestial bodies are scarcely fainter than 4233, are lacking here. Of these lines are very seldom observed only 4924 and 5018, which seem to be stronger on those spectrograms on which H_β is the most strong.

A part of a microphotogram of the M5 spectrum is given in Fig. 1. In the above mentioned region the position of the lines, we are interested in, is indicated by arrows. It may be seen that all emission lines lie within strong absorption bands of TiO [α (5,3), α (2,1), α (1,0), α (0,0), α (3,3) and others];

it appears that for 4924 this effect is expressed the most weakly. The probable cause of the anomaly in question is that in certain frequencies the radiation of Fe II ions is hindered on its way out by the absorption by the TiO molecules, a hypothesis which was formerly put forward to account for the anomaly in the intensity of hydrogen lines. From this it may be inferred that the emitting H atoms and Fe II ions are at least not located in the upper shell of the atmosphere of Me stars and so there is no analogy in this respect with Novae, Novae-like and Be stars.

Now it is of interest to know whether the behaviour of other Fe II lines is in harmony with this result. We shall first consider those Fe II lines, which in other objects are, as a rule, scarcely weaker than the 4233 line. These lines are 4352, 4508, 4522, 4549 and 4584. Of them 4508 and 4549 are not observed in Me spectra at all, and the lines 4584 and 4352 are observed very rarely and then only as faint lines. Contrary to this, the line 4521 is observed often as a rather strong line. All this is to be considered as an anomaly compared to what we have in laboratory and in other celestial objects. For 4584, 4549, 4508 and 4352 the anomaly may be explained by the influence of the bands TiO α (3,0) R_a, α(7,3) R_c, α(6,2) R_c and α(7,2) R_c. In the case of 4352 one may also suppose the low temperature line Cr I 4351.77 to play a substantial rôle. But the presence of 4352 in the Me spectra is doubtful, and so is its identification with Fe II. Neither may the rather strong line 4521.4 observed in Me spectra be properly identified with Fe II 4522.6. The line is notably stronger than Fe II 4233. Whatever the origin of the line observed in the neighbourhood of 4522, it is worthy of attention for its considerable strength which may be connected with the absence here of TiO bands (the nearest is α (6,2) R_c 4506).

Finally we have to point out an anomaly in the lines 4233, 4179 and 4173, for which the upper and lower energy levels are nearly equal. While in laboratory and in the spectra of other celestial objects the intensity ratio of these lines is about 10 : 8 : 5, in the stars Me (o Ceti) it is nearly 10 : 20 : 8 respectively (in both cases the intensity of the 4233 line is arbitrarily assumed to be 10). Of these three lines 4179 appears to be free from any influence and 4173 is possibly influenced in a slight degree by a very faint TiO band α (7,1) R_a. As for the line Fe II 4233, it is probably affected by the wing of the strong resonance line Ca I 4226 and is also under the influence of the low temperature line Fe I 4232.7 (the latter effect is evident from the apparent asymmetry of the emission line Fe II 4233).

We refrain here from the consideration of the fainter Fe II lines: they may escape observation simply on account of their faintness and not necessarily because of the screening effect. However the consideration of all stronger Fe II lines, as has been shown above, brings out a series of anomalies, which may be explained satisfactorily in terms of the hypothesis of physical screening. This will be equivalent to the assumption that the mean effective level of the emitting ions is lower, or at least not higher, than that of the absorbing molecules and atoms which in our case are TiO, Ca I and Fe I. The radiation of Fe II ions is weakened in such frequencies as happen closely to correspond to certain absorption frequencies for TiO, Ca I and Fe I.

An argument in favour of the hypothesis under consideration is derived from a comparison of the behaviour of Fe II lines in the spectra of Me and Se stars. In the latter the TiO bands are known to be faint or even absent. Unfortunately, the material secured by observations at Simeis (R Gem., R And.) and elsewhere (8) is very scanty and poor. There is no sufficient evidence for the conclusion that the anomaly in 4233 : 4179 does take place in the Se stars also. On the other hand, one may point out here the presence of the emission lines Fe II 4584, 4924, 5018 and possibly 4549, which are

just the lines invisible or barely visible in Me spectra owing, apparently, to the screening effect of the TiO bands. It may well be remarked that 4352 is much stronger in Se than in Me spectra. Irrespective of whether this line is or is not due to Fe II, its strengthening in Se appears to be connected with the weakening or absence of the α (7,2) R_c band. All this is in line with the fact that the Balmer decrement $H_\beta : H_\gamma : H_\delta$ is nearly normal in Se, whereas in Me, especially in later subdivisions, the anomaly with regard to H is very strong.

We have strong reason to suppose that at least near the epoch of Max. the matter responsible for the emission lines moves radially outward, and in this case the difference in the radial velocities of different atoms and ions wlll probably mean the difference in their effective level in the atmosphere. It is customary to consider the radial velocities for H and Fe I as equal. For Fe II lines a positive shift of about 0.09 A with respect to hydrogen and low temperature emission lines was reported in o Ceti by J o y (9). The importance of this statement is obvious.

It is only for o Ceti, that we have sufficient data on individual lines (Mt. Wilson and Simeis). What is given below are deviations from the laboratory values of λ for Fe II or, in other words, the deviations for Fe ll relatively to H and Fe I.

TABLE II

λ (laboratory)	Mt. Wilson (Joy)	Simeis (author)	Weight	λ (laboratory)	Mt. Wilson (Joy)	Simeis (author)	Weight
4138.38 (pred.)	0.17 A	0.21 A	2	4583.84	0.04	—	1
4173.47	0.00	0.01	1	4923.91	—0.12	—0.09?	—
4178.86	—0.04	—0.06	2	5018.43	0.01	—	—
4233.16	0.17	0.15	4				

The last two lines are discarded by J o y, and his conclusion as to the positive shift of Fe II is practically based on the 4138 and 4233 lines. The observations made at Simeis likewise testify to the presence of a large positive shift in the case of these lines. Yet, there are serious arguments against the identification of the first line with Fe II: 1) This line has never been observed in other celestial objects (chromosphere, Novae, Be a. o.) whereas all the other lines of Fe II mentioned above, are easily seen. 2) Nor was this line observed in the laboratory, and its λ was computed from the known terms. Of the other analogous lines predicted no one was observed in laboratory or in spectra of celestial objects. 3) 4138 is a very strong line in Me, at any rate much stronger than 4233.

As to the line 4233, it may be remarked that at a distance of about 0.15 A (after allowance for the usual shift of emission lines) there is a strong low temperature absorption line Fe I 4232.74 which may affect the position of the line Fe II 4233. In fact, even at moderate dispersion, the line 4233 appears narrower than the other Fe II emission lines and displays an obvious asymmetry on the large scale spectrogram of o Ceti (10). From all of this we are bound to conclude that there is no reason to speak of any difference between the radial velocities of the Fe ll ions and the atoms of H and Fe I. It will however be shown in a later communication that this conclusion does not necessarily apply to more distant phases.

What may be argued from the fact of equal radial velocity and more or less equal screening effect for H, Fe I and Fe II is that at least about Max.

the emitting atoms and ions in question are nearly in the same layer, which in any case is not higher than the layers responsible for the absorption spectrum.

Since, judging by the K-term (11) and the velocity difference between the emission and absorption lines, the emission matter is in radial motion outward, we may expect the screening effect to vary with phase.

Therefore the study of the variation of the anomaly with phase may serve as a basis for our judgement about the change of the relative level of the matter responsible for the emission lines. Of the available data the most numerous refer to the lines Fe II 4233, 4179 and 4173. Using the Simeis observations and also J o y's estimates (12) we were able indeed to discover a quite appreciable variation with phase in the relative intensities of these three lines. Smoothed values for the log of the ratio 4233 : 4179 are represented in Fig. 2. Though we have here to deal with estimates instead of measured intensities, yet the reality of the decrease of the anomaly with advancing phase may hardly be called in question. Eventually the intensity ratio is likely to become normal. It may be shown that the effect in question cannot be ascribed to the change of the number of the absorbing atoms and molecules as function of phase. The observed effect is to be probably interpreted in the sense that the relative level of the emitting Fe II ions is subject to more or less continuous changes with advancing phase with the result that in the distant phases the level of these ions in the atmosphere is generally much higher than the mean level of absorbing atoms and molecules. This and the fact that at least about Max. the Fe II ions and atoms of H and Fe I are not separated but rather lie in the same level (probably in the lower one) throws light on the processes taking place in the atmospheres of Me stars.

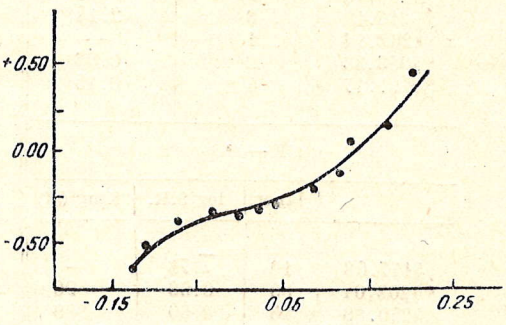

Fig. 2. The change of the intensity of the Fe II lines 4233 : 4179 with advancing phase (o Ceti)

NEUTRAL IRON

In the problem of emission lines the study of Fe I is especially interesting particularly with respect to the possibility to apply the hypothesis of physical screening. This effect must be of special importance for the Fe I emission lines, as quite close to them must always be located rather strong corresponding absorption lines of Fe I. The physical screening of Fe I (Em.) by Fe I (Abs.) is possibly in many cases more considerable than the screening by TiO a. o. Much depends also on the shift of Fe I (Em.) relatively to Fe I (Abs.) and also on some other factors.

We have noticed above that the radial velocity for the emission lines of H, Fe II and Fe I for the epoch near Max. is the same. This fact alone gives a reason to think that at least near the epoch of Max. the corresponding ions and atoms are located approximately within the same effective level in the atmosphere and that consequently the physical screening must take place for the Fe I atoms, if it affects H and Fe II.

It is of great importance for the problem in the whole to solve the question whether the physical screening affects in the same degree the emission lines

corresponding to high and low energetic levels. For the same purpose it is equally important to know which lines of the rich Fe I spectrum are observed in emission and what anomalies can be found here.

In the spectral region $\lambda > 3600$ A there are known only three multiplets (13) with E. P. < 1.6 in which a part of the lines is observed in emission (they are marked by an asterisk in the table).

TABLE III

$a^5D - z^7P^0$ (ultimate multiplet)

λ	labor.	King (gf)
4134.34	1	—
4149.77	pred.	—
4199.99	1	—
*4206.70	3	0.60
*4216.19	8	2.14
4232.74	1	—
*4258.33	2	0.38
*4291.47	4	0.45

$a^3F - z^3G'$

λ	labor.	log S.R.	King (gf)
4147.68	10	$\bar{2}.78$	—
*4202,04	30	0.60	890
4250.80	25	0 60	880
4271.78	35	1.89	2 450
*4307.91	35	1.77	3 300
4325.78	35	1.65	3 800

$a^5D - z^7F^0$ (ultimate multiplet)

λ	labor.	King (gf)
4325.76	blend	—
4347.24	(1)	0.23
*4375.95	9	4.4
4389.26	2	0.24
4405.03	(pred)	—
*4427.32	10	4.3
4435.16	2	0.24
4445.48	(1)	—
*4461.66	8	2.9
4466.55	blend	0.31
4471.68	(1)	—
*4482.18	4	1.6
*4489.75	3	0.63

In the study of emission lines of Fe I one must keep in mind that the low temperature multiplets of Fe I are well represented in absorption in the spectra of late type stars. At moderate dispersion, generally used in these cases, say 30 A, the observed contours of the emission and absorption lines are almost purely instrumental ones, and at the comparatively small shift about 18 km. these contours will to a great extent overlap one another. It is just this factor that strongly affects the observed behaviour of the Fe I emission lines in different phases. Here we have to deal not only with the effect of physical screening but also with that of a purely geometrical blending. Moreover this circumstance strongly increases in many cases the difficulty of deciding what lines properly are emission ones.

Undoubtedly as concerns the Fe I lines in emission we have to deal with an optically thin layer. Consequently one may expect that the intensity ratio of the lines within a multiplet is $\sim Nf$. Thus, independently of any anomalies, one may expect that the fainter lines within a multiplet will not be seen. Really, for the above mentioned multiplets $a^5D - z^7P^0$ and $a^5D - z^7F^0$ this is evidently well justified. From the other side, the width of the corresponding absorption lines in spectra of these stars varies $\sim \sqrt{Nf}$ or even still slower. For certain values of the relative shifts of the emission lines it may occur that a fainter emission line of a multiplet will lie outside the corresponding absorption line, whereas a stronger line may be appreciably affected by physical screening. One must also keep in mind that, as it follows from the experiments made by King and others, for some un-

known reasons several lines of a multiplet are more sensitive to changes in excitation than other ones. The influence of all these factors in addition to the usual influence by TiO or some other lines may cause especially strong anomalies for the Fe I emission lines.

Let us consider first the multiplet $a^5 D - z^7 P^0$. From the eight lines only the four strongest ones are found in emission. This emission, generally rather weak, is seen only in more advanced phases. Using our estimates of intensity of these lines in the spectrum of o Ceti, and also in first line those by J o y for the same star we have drawn smoothed curves shown in Fig. 3. The estimates for 4216.2 are very uncertain, especially in earlier phases as this line lies between two strong absorption ones — the corresponding Fe I line and 4215.5 of Sr II. The horizontal dotted line shows the transition from absorption to emission. Although the estimates are naturally of very low accuracy, the reality of the observed picture leaves no doubt. The anomaly in the intensities of lines and its variation with phase for the multiplet $a^5 D - z^7 P^0$ is recorded here for the first time. The influence of TiO is apparently insignificant, and we may speak here only on the physical screening by the corresponding Fe I lines.

There is some analogy between the anomaly for this multiplet and the known anomaly for the multiplet $a^3 F - z^3 G^0$. As we shall see later, this is of importance for the interpretation of this phenomenon.

The anomaly for the multiplet $a^3 F - z^3 G^0$ is especially strong and was long ago noticed by J o y and M e r r i l l (14). It is thought generally that from the 6 lines only 4202 and 4308 are observed in emission. The anomaly consists in that, from one side, three strong lines are not observed in emission at all, and from the other — that the ratio 4308 : 4202 very strongly differs from the theoretical value. Smoothed curves for these lines constructed in the same manner as for $a^5 D - z^7 P^0$ are shown in Fig. 4. This Figure shows distinctly that with increasing phase, the absorption lines are gradually converted into emission ones, and the anomaly in the ratio 4308 : 4202 is weakened.

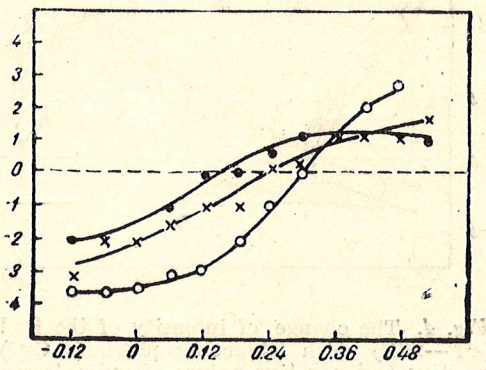

Fig. 3. The change of intensity of Fe I lines ($a^5 D - z^7 P^0$) with advancing phase (o Ceti). The positive and negative values of ordinates relate to the emission and absorption stage respectively
● — 4258, × — 4206, o — 4291

There is another important factor, which apparently holds also for the multiplet $a^5 D - z^7 P^0$. As seen from Fig. 4 there is properly no limit between emission and absorption lines. It is remarkable that when the emission at 4202 and 4308 reaches maximum, other lines at 4148, 4251, 4272 and 4326 nearly disappear as absorption lines and in more distant phases apparently show a tendency to emission. Thus, although only 4202 and 4308 are considered as emission lines, there is properly no intrinsic difference between them and the other lines of the multiplet $a^3 F - z^3 G^0$, which are known as absorption ones. Probably the same takes place within the multiplet $a^5 D - z^7 P^0$.

Let us try to interpret the observed anomalies for Fe I in the light of the hypothesis of physical screening (this is done for the first time). In the multiplet $a^3 F - z^3 G^0$ the line 4250.6 (a correction of about —0.2 A for

fhe relative shift of the emission lines is applied), unobserved in emission, must be located between two strong absorption lines Fe l 4250.80 and Fe l 4250.13, which are generally distinguished in late type spectra by very pronounced violet and red wings. At moderate dispersion these lines are unresolved, and the mean λ is about 4250.5. Thus the absence of the emission line is easily explained here within the limits of the hypothesis of physical screening.

A more striking anomaly is the absence in emission of a still stronger line 4271.78 (—0.2). But when considering that the latter lies between two very strong lines Fe I 4271.78 and Fe I 4271.17 (unresolved in o Ceti, mean λ 4271.6), one may probably also explain why this emission line escapes observation.

The emission 4325.78 (—0.2) is also unknown. Here besides the corresponding strong absorption line of Fe I is a rather strong blend centered about 4325.1. One must also keep in mind that in the region of the multiplet $a^3F - z^3G^0$ the TiO bands 4270 α (5,0) and 4315 α (6,1) may exert some influence. We recall that the strong emission line H_γ is notably weakened owing probably to TiO. It may be spoken here of the band 4340 of TiO (?), which is apparently fainter than TiO 4315. King gives for the laboratory the band 4340 in an older list (15), but does not mention this band in his new list (16). There is in this region a general depression in the continuous spectrum due probably to TiO (17). The latter can affect not only the seeing of 4271 and 4325, but also of 4308.

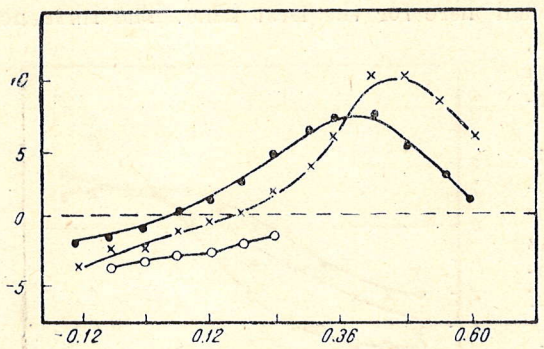

Fig. 4. The change of intensity of the Fe l lines ($a^3F—z^3G^0$) with advancing phase (o Ceti). The positive and negative values of ordinates relate to the emission and absorption stages respectively ● — 4202, × — 4308, ○ — 4251, 4272, 4326

Finally the absence of 4147.7 in emission appears natural, as independently of influences whatever its intensity according to the sum rule is very insignificant.

Thus the absence in emission of all above discussed lines of the multiplet $a^3F - z^3G^0$ can be explained in the terms of the hypothesis of physical screening.

On the other side two lines of this multiplet 4202.04 (—0.2) and 4307.91 (—0.2) are observed in emission. The first of them may be affected only by the corresponding moderately strong Fe I line and namely this may be the cause of the presence of emission here. The case of 4307.91 (—0.2) is more complicate. Here there seem to be no conspicuous lines, belonging to elements other than Fe I, but the corresponding absorption line of Fe l is very strong. Perhaps when comparing the seeing conditions of the emission lines it is proper to recall from one side the note by Miss Moore and H. N. Russell (18) that in the solar spectrum the lines 4202 and 4308 are less winged than 4325 and 4272, and on the other, the observation by King that for some unknown reason 4202 and 4308 are more sensitive to changes in excitation than the other members of the multiplet (19). As concerns 4308, some influence, as duly mentioned above, may be ascribed to TiO. It is also interesting to note, that, as seen from Fig. 4, the emission

4308 appears in a later phase than the emission 4202. On the other side, as seen from the same Figure, in very remote phases both lines 4326 and 4272 show a tendency to emission.

For the understanding of the anomaly for 4308 : 4202 it is very important to note that in the Se spectra «the relative intensities 4308 : 4202 are never extremely abnormal» (20). It must be just so, if in Se the TiO bands are considerably weaker than in Me. However the absence or faintness of emission for 4272 and 4326 shows that the rôle of the wide absorption lines of Fe I is also important here. Besides, some effect may be due also to the somewhat higher value of the relative shift of emission lines in Se spectra.

According to Thackeray and Merrill the anomaly in 4308 : 4202 may be due to the mechanism itself of formation of emission lines (fluorescence of Bowen's type). However the very strong weakening of the anomaly in 4308 : 4202 in Se spectra and also in remote phases of Me spectra suggests that Bowen's fluorescence is perhaps not the only cause of the observed anomaly.

The example of the multiplet $a^3F - z^3G^0$ shows particularly well that there is no intrinsic difference between the lines which are generally accepted as emission lines and lines of the same multiplet known as absorption ones. After all, considering the behaviour of these lines in different phases from early to late ones, one may apparently follow all the transitions from a sharp defined emission to a well pronounced absorption. The combination of all facts can apparently be satisfactorily explained within the limits of the hypothesis of physical screening, the screening material being here chiefly Fe I and perhaps TiO. Moreover it is very essential that with increasing phase the screening effect becomes considerably less (as will be shown in the second paper probably owing to the gradual increase of the effective level of matter responsible for the emission spectrum).

An important factor is also the size of the shift of the emission lines with respect to the absorption ones, as well as the width of these lines, especially of absorption ones.

The ultimate multiplet $a^5D - z^7F^0$ is generally weak. Like the multiplet $a^5D - z^7P^0$ a relatively great number of lines is in emission here. As seen from Table III these are the lines of greatest theoretic and laboratory intensity. Possibly this is due to the smaller effect of the corresponding absorption lines. This may be also partly connected with the very low level of the terms a^5D, z^7F^0 and z^7P^0. Owing to the faintness of the lines and probably to the sensible influence of the TiO bands it is more difficult here to trace the variation of intensity of lines with phase.

For separate lines we have the following. The emission 4427.3 (—0.2) is probably affected by the influence of TiO 4421.6 α (4,0) R_a and possibly the Ti I line 4427.11. The emission 4461.7 (—0.2) is apparently outside the band TiO 4462.5 α (5,1) R_a. One may also explain the emission at 4482.18 (—0.2) and 4489.75 (—0.2) apparently lying outside the sensible influence of bands or absorption lines. The emission at 4375.95 (—0.2) often stands out from the other lines of this multiplet. Possibly this is connected with that this persistent line is very sensible to the conditions of excitation. According to King (21) this line is the strongest iron line in the furnace at 1400°.

That the lines of this multiplet are affected by the TiO bands is seen from their behaviour in the Se spectra. Although the data are very scarce (estimates by Merrill (22) and Simeis ones for R Gem. and R And.) it follows that if 4376 is ever mentioned, it appears mostly together with

4427 and 4461, the difference between them being apparently less than in Me.

As concerns the faint lines of this multiplet, the data are generally scarce. The influence of TiO is apparently stronger than that of Fe I. Although the lines 4376 and 4427 display perhaps some peculiarities, the general behaviour of the multiplet $a^5D - z^7F^0$ presents no contradictions to the hypothesis of physical screening.

All three multiplets considered belong to low temperature ones. We have studied one low temperature multiplet more which was not suspected to possess emission lines. Unfortunately our observations of o Ceti are limited to the phase +100. Using α Herculis as a standard we have estimated the intensities of the absorption lines 4005, 4046, 4064 and 4072 (Fig. 5). It is seen from these comparisons that while at the epoch of Max. the intensities of the lines of the multiplet $a^3F—y^3F^0$ are nearly equal in the spectra of o Ceti and α Herculis, the same lines in advanced phases are strongly weakened in the first star. This must be apparently interpreted as a transition into emission of the lines of this multiplet in analogy to the similar effect for the lines of the multiplet $a^3F - z^3G^0$ 4251, 4272 and 4326. That we deal here with a probable tendency to emission and not with the effect of change of T and P is shown by the fact, that low temperature lines of V I as for instance 4093, 4110, 4117, 4128, 4379 a. o. lying beyond the absorption bands of TiO are nearly invariable when passing from Max. to phase +100 and even still more advanced ones.

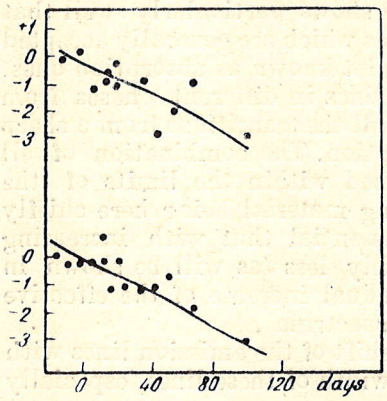

Fig. 5. The change of intensity of absorption lines of Fe I with advancing phase (o Ceti minus α Herculis). Top for $a^3F—y^3F^0$ (4046, 4064, 4072). Bottom for $a^3F—y^3G^0$ (4251, 4272, 4326)

The same effect of faintening of the absorption lines is apparently manifested, although in a lesser degree, also for the multiplet $a^3F—z^5G^0$. However, as this multiplet lies in a region of longer wave-lengths, the apparent faintening of the absorption lines may be due to the strengthening of the TiO bands in advanced phases. But in the region $\lambda > 4300$ the absorption lines of Fe I seem faintened in o Ceti relatively to α Herculis. This must be so, if o Ceti is of a somewhat later class (the bands of TiO are stronger).

We have considered in the region $\lambda > 3600$ all low temperature multiplets (excitation potential of the lower level < 1.6 V.). In these of them, where some lines are in emission, the others show tendency to emission in distant phases. But the lines in the other low temperature multiplets seem, as a rule, to tend to emission in more remote phases. This is a more general conclusion than the detection of separate emission lines in some multiplets.

The result here found may be without difficulties satisfactorily explained within the limits of the hypothesis of physical screening due chiefly to corresponding lines of Fe I and to TiO bands. The study of the behaviour of the Fe I lines must have, as it will be shown in the second paper, an extremely great importance for the solution of the question of the origin of emission lines.

REFERENCES

1. G. Shajn. Bull. de l'Acad. Scienc. URSS Sér. Phys. IX, 3, 161, 1945
2. Adams. Ap. J. **93**, 11, 1941
3. Merrill. Ap. J. **93**, 40, 1941
4. Merrill and Burwell. Ap. J. **71**, 285, 1930. Shane. Lick Obs. Bull. **10**, 131, 1921
5. Joy. Ap. J. **63**, 302, 1926
6. Ambarzumian. Theoretical Astrophysics 107, 1939 (russian)
7. Struve and Elvey. Ap. J. **79**, 409, 1934
8. Merrill. Ap. J. **65**, 23, 1927
9. Joy. l. c., p. 314
10. Adams. l. c., p. 14
11. Shajn. Bull. of the Acad. of Scienc. Georgian SSR IV, 123, 1943
12. Joy. l. c., p. 309
13. Joy. l. c., 316
14. Merrill and Burwell. l. c., 305
15. King PASP **38**, 173, 1926
16. King. P. R. **33**, 701, 1929
17. Shajn. Zs. f. Ap. **10**, 73, 1935
18. Moore and Russell. Ap. J. **63**, 6, 1926
19. Joy. l. c., 317
20. Merrill and Thackeray. PASP, **49**, 12, 1937
21. King. Ap. J. **56**, 337, 1922
22. Merrill Ap. J. **65**, 23, 1927

ЭМИССИОННЫЕ ЛИНИИ H, Fe II и Fe I В СПЕКТРАХ ДОЛГОПЕРИОДИЧЕСКИХ ПЕРЕМЕННЫХ ЗВЕЗД

Г. ШАЙН

В настоящей работе даны некоторые результаты исследования эмиссионных линий в спектрах долгопериодических переменных звезд.

Водород. Измеренная ширина эмиссионных линий в области 3700—3900 А равна около 0.6 А, что в несколько раз превышает допплеровскую тепловую ширину для температуры, принятой для этих звезд. Крайнее разнообразие эмиссионных водородных линий H_5 — H_{16} в отношении структуры, интенсивности и аномалии в длине волны может быть объяснено без серьезных исключений в рамках гипотезы о физическом экранировании через поглощение. В этом случае поглощающим материалом являются TiO, V I, Fe I, Cr I, Ca II, H. Анализ интенсивностей водородных линий в рамках теории кривой роста приводит к заключению, что возбуждающая радиация для эмиссионного водородного спектра очень сильна и, собственно, не имеет отношения к обычной фотосферной радиации для этих звезд.

Ионизованное железо. В поведении эмиссионных линий Fe II открыты некоторые аномалии. Главные из них: 1) аномалия в отношении интенсивностей линий 4233 : 4179 : 4173; 2) отсутствие эмиссионных линий в зеленой части спектра; 3) некоторые особенности в интенсивности линий в области 4300 — 4600. Все многочисленные аномалии могут быть объяснены в рамках гипотезы физического экранирования (поглощающий материал здесь TiO, Fe I и Ca I). С увеличением фазы аномалия в отношении интенсивностей 4233:4179 постепенно уменьшается. Найдено, что около эпохи максимума нет основания говорить о каком-либо различии в радиальных скоростях для ионов Fe II и водородных атомов.

Нейтральное железо. Найдена аномалия для эмиссионных линий мультиплета $a^5D - z^7P^0$. Уменьшение этой аномалии с увеличением фазы имеет много общего с известной аномалией для мультиплета $a^3F - z^3G^0$. Тенденция к образованию эмиссионных линий найдена также для мультиплета $a^3F - y^3F^0$. Имеются серьезные основания предполагать, что все низко-температурные мультиплеты Fe I выявляют в той или иной степени тенденцию к эмиссии, в особенности в более далекие фазы. Даже для явно эмиссионных линий Fe I всегда можно проследить постепенный переход из поглощения в эмиссию. Не легко в пределах мультиплета разделить линии на эмиссионные и линии поглощения. Многочисленные и в высшей степени разнообразные аномалии в поведении эмиссионных линий Fe I могут быть согласованы, по крайней мере для большинства случаев, с гипотезой физического экранирования при допущении, что главная роль в этом феномене принадлежит поглощающим атомам Fe I.

RADIAL VELOCITIES OF 107 B8—A0 STARS

V. A. ALBITZKY

The observations of radial velocities of B8—A0 stars were produced in 1932—1937 with one-prism spectrograph and short camera giving a dispersion of 75 A/mm at $H\gamma$. When reducing the observations the systematic error as described in our previous paper (I) has been taken into account. From the comparison of the radial velocities of 7 stars in common with two catalogues the systematic correction to our radial velocities was deduced, viz.+ 0,44±1.51 km/sec in the sense Moore-Simeis. In table XII there are given the final radial velocities for 91 stars with mean value of p. e. equal to ±3.57 km/sec. In table XII are given observed velocities for 16 stars with variable radial velocities. Very large velocity of the star H. D. 161817 leads to the conclusion that this star belongs to the class of high-velocity stars.

After completing in 1932 the observations of radial velocities with a dispersion of 36 A/mm at H_γ on account of exhaustion of stars with undetermined velocities in the practical limits of brightness and position acessible to our reflector it was resolved to use for the observations of radial velocities in bulk the short focus camera with a dispersion of 75A/mm at H_γ.

Considering that so small a dispersion furnishes radial velocities of somewhat reduced precision, it was resolved to observe the stars of spectra. subdivisions B8-A0, as these spectra contain generally few lines of the worst quality and their velocities cannot be, generally speaking, determined with good precision.

It is true that the small resolving power of such a dispersion obliterates the weak metallic lines which can sometimes give good precision even for these stars; but the advantage of the greater light-gathering power is self-evident for this class of observations.

For this catalogue were observed the stars in the limits of brightness $6^m.6—7^m.3$ vis. and, as before, between declinations 0° and +40°.

OBSERVATIONS

The observations were produced in the period between May 1932 and the end of 1935, and from March to November 1937. In 1936 were obtained only few spectrograms as the spectrograph was dismounted to observe the solar eclipse. In total were secured negatives: 233 for stars with known velocities and 518 for programme ones.

THE CAMERA

In the paper of ours, «Radial Velocities of 114 stars» (1) the optical properties of the short camera were described in detail. In this paper are given some complementary details of the computations which disclosed the importance of account of the error depending on the curvature of the camera field.

WAVE LENGTHS

The wave-lengths for the iron-arc comparison spectrum were taken from «Transactions of the International Astronomical Union», Vol. I, p.41. The wave-lengths used for stellar lines were firstly taken: for B-stars from «Publications of the Domininon Astrophysical Observatory, Victoria; Vol. V, Nr. 1. All these wave-lengths were reduced to the I. A. U. system with the help of the corresponding table from H. Kayser's «Tabelle der Hauptlinienspektren aller Elemente», S. VI.

On the basis of these wave-lengths have been constructed the reduction tables with which were performed the reductions of all the measurements.

Before the final computations of this catalogue the wave-lengths of the lines of the A-F stars were reduced to those recommended by I. A. U. (Trans. IV, p. 188) and the corresponding corrections were introduced into all the velocities from different lines. The wave-lengths for the B-stars remained unchanged.

The data for the lines used in this catalogue are given in table II, columns II_1 and II_2. In II_3 are given the factors for converting the displacements of lines (in $0^r.001$) into velocities in kilometers per second.

MEASUREMENTS

The measurements of the spectrograms have been performed with the comparator by V. Messer, by three measurers with the numbers of spectrograms measured as follows:

V. A. Albitzky (A)	Const.	vel.	stars	232	Progr.	stars	607	All	839
L. A. Albitzky (L)	»	»	»	198	»	»	513	»	711
P. Th. Shajn (S)	»	»	»	47	»	»	96	»	143
				477			1 216		1 693

Every spectrogram was measured, as a rule, by two different measurers. The comparison between measurements of the spectrograms of constant velocity stars by different measurers revealed the personal differences as follows:

		Stars	Number of measurements	Personal differences	
Disregarding the spectral types . . .	A — L	36	187	—0.36	±0.81
	A — S	14	45	+1.97	∓1.95
B2 — A2 stars only	A — L	24	138	+0.10	±0.97
	A — S	9	29	+3.68	∓3.17

As it is seen, the differences are smaller than their probable errors, at least for the principal measurers, and they were neglected. All the measurements have been considered to be of equal weight and only when computing the final velocities of stars the results of different measurements of spectrograms were combined with weights proportional to the numbers of lines measured.

COMPUTATIONS OF OBSERVATIONS

In order to have the possibility of reductions of the observed radial velocities to the system of Moore's catalogue there were observed simulta-

TABLE I

1	2	3	4	5	6	7	8	9	10	11	12
H. D.	α (1900.0)	δ (1900.0)	vis.	H. Sp	km/sec	km/sec		km/sec	km/sec	km/sec	km/sec
	h m		m								
14 252	2 13.2	+28°11′	5.23	A2	+ 3.8 ±0.5	— 1.7 ± 2.3	10	+ 5.5	+5.78	+ 2.3 ±2.07	+ 1.5
28 375	4 23.4	+ 1 9	5.50	B8	+ 24.1 0.9	+ 0.8 3.6	10	+23.5	+8.16	+12.3 3.07	+11.8
33 254	5 3.8	+ 9 42	5.42	A2	+ 38.8 1.0	+21.4 2.2	6	+17.4	+5.56	+26.5 2.13	+11.3
38 899	5 43.9	+12 37	4.92	B9	+ 23.8 0.5	+ 3.3 5.8	8	+20.5	+8.46	+13.4 4.46	+10.4
46 300	6 27.5	+ 7 24	4.50	A0p	+ 11.6 0.4	— 0.2 2.0	11	+11.8	+7.56	+11.5 1.59	+ 0.1
76 756	8 53.0	+12 15	4.27	A3	— 13,5 0.5	—24.9 13.0	4	+11.4	+4.47	— —	—
77 350	8 56.9	+24 51	5.45	A0	— 16.3 1.0	—26.3 3.6	11	+10.0	+7.24	—16.0 2.72	— 0.3
87 737	10 1.9	+17 15	3.58	A0p	+ 2.2 0.2	— 3.7 2.1	14	+ 5.9	+6.95	+ 7.4 2.15	— 5.2
87 887	10 2.9	+ 0 7	4.50	A0	+ 5.3 0.9	— 2.4 0.8	13	+ 7.7	+7.62	+ 9.5 1.38	— 4.2
95 608	10 57.0	+20 43	4.42	A0	— 12.4 0.5	—12.2 2.2	14	— 0.2	+5.93	— 5.1 2.13	— 7.3
97 633	11 9.0	+15 59	3.41	A0	+ 7.8 0,4	— 1.6 3.0	14	+ 9.4	+6.36	+ 6.5 3.15	+ 1.3
104 180	11 54.8	+ 4 13	5.24	A0	— 2.0 1.1	—11.5 3.3	16	+ 9.5	+7.49	— 3.1 4.31	+ 1.1
108 662	12 23.9	+25 28	5.38	A0p	— 1.6 0.8	— 8.7 1.7	17	+ 7.1	+6.93	— 4.3 1.85	+ 2.7
114 378—9	13 5.1	+18 4	4.47	F5	— 17,6 0.2	—26.2 2.5	10	+ 8.6	+4.84	— —	—
118 022	13 29.1	+ 4 10	4.93	A2p	— 10.9 0.5	—20.3 2.3	16	+ 9.4	+6.34	—14.4 2.53	+ 3.5
120 136	13 42.5	+17 57	4.51	F5	— 16.2 0.3	—21.9 2.8	16	+ 5.7	+5.07	— —	—
124 850	14 10.8	— 5 31	4.16	F5	+ 11.5 0.2	— 5.8 1.4	11	+17.3	+6.67	— —	—
126 661	14 21.8	+19 41	5.36	A5	— 27.7 0.7	—34.1 3.5	7	+ 6.4	+6.59	— —	—
128 167	14 30.3	+30 11	4.48	F0	+ 0.2 0.1	— 7.2 1.8	16	+ 7.4	+4.24	— —	—
141 795	15 45.8	+ 4 47	3.75	A2	— 9.9 0.5	— 9.9 1.4	16	0.0	+5.14	— 8.4 1.38	— 1.5
142 860	15 51.8	+15 59	3.86	F5	+ 6.5 0.5	+ 2.6 0.6	14	+ 3.9	+5.17	— —	—
151 956	16 45.5	+ 7 25	5.46	A0	— 2.1 0.6	—10.3 1.8	18	+ 8.2	+7.07	— 5.5 1.86	+ 3.4
164 136	17 54.7	+30 12	4.48	F0	— 22.0 0.3	—28.1 0.7	15	+ 6.1	+5.60	— —	—
164 353	17 55.6	+ 2 56	3.92	B5p	— 4.3 0.5	— 5.6 1.3	19	+ 1.3	+7.43	+ 0.2 1.76	— 4.5
166 182	18 4.4	+20 48	4.32	B3	— 13.3 0.5	—18.9 1.3	24	+ 5.6	+5.91	—14.7 1.06	+ 1.4
171 301	18 29.0	+30 29	5.37	B8	— 12.2 0.5	— 5.9 4.6	10	— 6.3	+7.57	— 1.1 4.88	—11.1
173 667	18 41.4	+20 27	4.26	F5	+ 23.6 0.3	+17.6 —	2	+ 6.0	+3.81	— —	—
179 761	19 8.7	+ 2 7	5.10	B8	— 5.8 0.5	—11.9 3.2	14	+ 6.1	+6.94	— 4.5 2.90	— 1.3
190 229	19 58.9	+15 45	5.47	A0	— 22.5 0.9	—26.6 2.2	24	+ 4.1	+8.97	—21.3 2.17	— 1.2
195 295	20 25.3	+30 2	4.09	F5p	— 18.8 0.3	—17.7 1.4	12	— 1.1	+5.74	— —	—
195 810	20 23.4	+10 58	3.98	B5	— 18.5 0.6	—28.3 3.0	8	+ 9.8	+8.42	—22.6 3.22	+ 4.1
196 867	20 35.0	+15 34	3.86	B8	— 7.2 1.9	—10.1 8.6	6	+ 2.9	+7.39	— 4.1 8.38	— 3.1
197 461	20 38.8	+14 43	4.53	A5	+ 9.9 0.3	+ 5.9 1.9	15	+ 4.0	+5.54	— —	—
206 826	21 39.6	+28 18	4.73	F5	+ 18.4 0.2	+17.3 2.5	8	+ 1.1	+5.17	— —	—
214 994	22 37.0	+28 48	4.85	A0	+ 6 6 0.5	+ 9.9 1.1	22	— 3.3	+8.23	+14.6 1.31	— 8.0
215 648	22 41.6	+11 40	4.31	F5	— 5.2 0.3	— 1.4 1.2	10	— 3.8	+3.97	— —	—
220 825	23 21.8	+ 0 42	4.94	A2p	— 3.3 0.6	— 9.5 2.0	16	+ 6.2	+6.42	— 6.6 2.02	+ 3.3
								+5.94	+6.54		+ 34,0± 0.75

neously with programme stars 37 stars with well determined radial velocities adopted in Moore's catalogue. The data for these stars are given in table I. The columns I_1—I_5 are self-explanatory: in I_6 are given the velocities from Moore's catalogue; I_7—I_9 are the results of our observations as follows: observed radial velocity, number of measurements of spectrograms, reduction to Moore's catalogue.

The mean value of the last for all the stars is $+5.94 \pm 0.58$ km/sec. The necessity of ascertaining the origin of this very considerable error forced to undertake the investigation of the short camera which was described in the paper «Radial velocities of 114 stars».

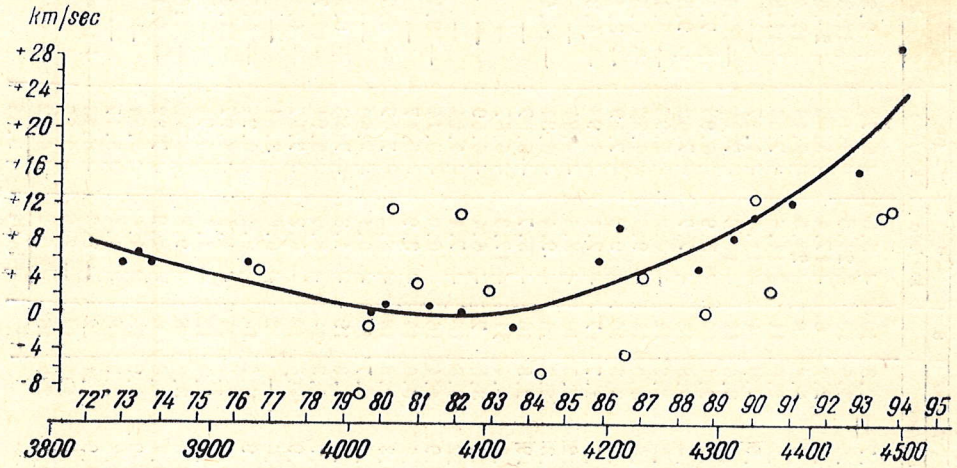

Fig. 1. Corrections to normal readings in dependence on wave-length

The determined corrections according to wave-lengths or to readings of the normal dispersion are given in the above mentioned paper; in this paper they are represented by dots and the corresponding curve on the Fig. 1.

It must be remembered that these corrections were determined by laboratory method with an iron arc spectrum. To reserve the possibility of adjustement of the corrections to the real conditions of observations was worked out the following method of testing the different systems of corrections to measured lines without much labour of recalculations in each case. For each measured line were computed the quantities $\sigma_\lambda = \Sigma \frac{1}{n}$, where n is the number of measured lines in those spectrograms, where the given line λ had been measured, and the summing up was performed for all measurements of this line. The quantities σ_λ were multiplied by the corresponding corrections from the curve, Fig. 1 (Table II_5). The sum of these products for all lines divided by the number of measured spectrograms for the star gives the final correction to the velocity of this star.

In I_{10} are given the values of the computed corrections to the observed velocities of Moore's stars; their mean value differs from the observed one, in I_9, only by 0.6 km/sec.

Excluding the star α Cancri with very discordant measurements (which was done after) we get for the computed and observed corrections the values +6,46 km/sec and +6,49 km/sec.

To verify these results the corrections for each measured line were computed, for all Moore's stars on the whole. To this end the quantities σ_λ were summed up for each line separately, but for all the stars; the so computed sums were divided by the number of measurements of all spectrograms in the

TABLE II

1	2	3	4	5	6	7	8
				km/sec	km/sec	km/sec	km/sec
3933.66 A	Ca II	1.85	0.0930	+ 3.33	+0.310	+ 3.33	+0.310
3964.73	He I	1.93	.0033	+ 2.12	+ .007	+ 2.12	.097
3995.00	N II	1.98	.0009	+ 1.19	+ .001	+ 1.19	.001
4005.33	Fe I	2.00	.0229	+ 0.94	+ .022	+ 0.94	.022
4009.27	He I	2.00	.0090	+ 0.80	+ .007	+ 0.80	.007
4026.19	He I	2.03	.0259	+ 0.41	+ .011	+ 0.41	.011
4030.61	Fe I Ti I Mn I	2.04	.0108	+ 0.21	+ .002	+ 0.21	.002
4032.93	Fe I Mn I	2.04	.0009	+ 0.20	.000	+ 0.20	.000
4045.74	Fe I	2.06	.0352	0.00	.000	0.00	.000
4063.54	Fe I	2.10	.0292	— 0.21	— .006	— 0.21	— .006
4069.79	O II	2.10	.0006	— 0.21	.000	— 0.21	.000
4071.69	Fe I	2.11	.0207	— 0.21	— .005	— 0.21	— .005
4077.64	La II Y I Sr II	2.12	.0374	— 0.21	— .008	— 0.21	— .008
4101.74	Hδ	2.16	.1303	0.00	.000	0.00	.000
4118.65	Fe I	2.19	.0040	+ 0.33	+ .001	+ 0.27	+ .001
4120.81	He I	2.19	.0068	+ 0.33	+ .002	+ 0.27	.002
4128.05	Si II	2.21	.0063	+ 0.62	+ .004	+ 0.50	.003
4130.88	Si II	2.21	.0043	+ 0.62	+ .003	+ 0.50	.002
4132.14	V I Fe I	2.21	.0057	+ 0.66	+ .004	+ 0.54	.003
4143.68	Fe I	2.23	.0263	+ 1.11	+ .029	+ 0.92	.024
4143.76	He I	2.23	.0126	+ 1.11	+ .014	+ 0.92	.012
4153.30	O II	2.25	.0008	+ 1.54	+ .001	+ 1.29	.001
4168.97	He I	2.28	.0015	+ 2.00	+ .003	+ 1.69	.003
4198.60	Fe I	2.33	.0197	+ 3.26	+ .064	+ 2.80	.055
4202.03	Fe I	2.34	.0030	+ 3.28	+ .010	+ 2.82	.008
4215.64	Fe I Sr II	2.36	.0289	+ 4.01	+ .116	+ 3.46	.100
4226.91	Fe I Ca I	2.38	.0274	+ 4.52	+ .124	+ 3.95	.108
4233.28	Fe I Fe II	2.39	.0257	+ 4.90	+ .126	+ 4.28	.110
4235.90	Fe I Y II	2.39	.0012	+ 5.02	+ .006	+ 4.40	.005
4250.48	Fe I	2.42	.0056	+ 5.81	+ .032	+ 5.16	.029
4260.42	Fe I	2.44	.0154	+ 6.34	+ .098	+ 5.60	.086
4267.16	C II	2.45	.0036	+ 6.88	+ .025	+ 6.11	.022
4271.55	Fe I	2.46	.0154	+ 6.89	+ .106	+ 6.12	.094
4282.62	Fe I Ti I	2.48	.0006	+ 7.69	+ .005	+ 6.83	.004
4289.93	Cr I Ti II Fe I	2.49	.0230	+ 8.22	+ .189	+ 7.35	.169
4307.89	Ti II Fe I	2.52	.0073	+ 9.07	+ .066	+ 8.08	.059
4314.79	Sc II Ti II Fe I	2.53	.0067	+ 9.61	+ .064	+ 8.59	.058
4325.67	Fe I Se II	2.55	.0236	+10.20	+ .241	+ 9.12	.215
4340.47	Hγ	2.58	.1362	+11.09	+1.510	+ 9.93	1.352
4351.84	Cr I Fe II Mg I	2.60	.0160	+11.96	+ .191	+10.74	.172
4387.93	He I	2.66	.0111	+14.87	+ .165	+13.48	.150
4395.04	Ti II	2.68	.0030	+15.17	+ .045	+13.74	.041
4404.75	Fe I	2.69	.0007	+15.60	+ .011	+14.11	.010
4415.12	Fe I Sc II	2.71	.0026	+16.41	+ .043	+14.87	.039
4437.55	He I	2.75	.0010	+18.31	+ .018	+16.66	.017
4443.58	Fe I Ti II	2.76	.0095	+18.90	+ .180	+17.21	.163
4468.64	Ti II	2.81	.0025	+21.21	+ .053	+19.40	.049
4471.48	He I	2.81	.0190	+21.49	+ .408	+19.65	.373
4481.31	Mg II Ti I	2.83	.1000	+22.48	+2.248	+20.60	+2.060
					+ 6.55		+ 5.94

whole, viz. $N = 477$. These quantities $\frac{\Sigma\sigma_\lambda}{N}$ are given in II_4; by multiplying them by corresponding corrections from II_5 we obtained those parts of the systematic reductions of our velocities to Moore's catalogue which are due to different lines — II_6. The sum of these parts gives the same general reduction, viz. +6.55 km/sec.

TABLE III

1	2	3	4	1	2	3	4
			km/sec				km/sec
3933.7 A	Ca II	286	+ 4.6 ± 1.0	4215.6 A	Sr II	166	— 4.3 ± 1.5
4005.3	Fe I	145	— 8.8 1.7	4233.3	Fe II Fe I	118	+ 3.8 2.1
4009.3	He I	34	— 1.5 8.1	4289.9	Cr I Ti II	142	0.0 1.8
4026.2	He I	82	+11.3 2.9	4340.5	Hγ	461	+12.4 1.0
4045.7	Fe I	207	+ 3.4 1.4	4351.8	Fe II Mg I	97	+ 2.5 1.7
4077.6	Sr II	205	+10.8 1.3	4471.5	He I	66	+10.4 3.4
4101.7	Hδ	435	+ 2.7 1.0	4481.3	Mg II	278	+11.6 1.5
4143.8	He I	43	— 6.3 3.8				

An attempt has been made to deduce this correction by comparing the star velocities determined from different lines immediately with the catalogue velocities of the stars. For this purpose were selected some 15 lines the most frequently measured; the data for these lines are given in table III (in III_3 — the numbers of measurements used). The computed corrections are given in III_4 and represented by circles in the curve, Fig. 1. Evidently that the dispersion of different values of the corrections so determined corresponds by no means to their p. e.'s (III_4). It was necessary to admit that the star wave-lengths as given by our short camera do not fit in the I. A. U. system. But still the corrections so found seemed to indicate that the curve of corrections must be somewhat lowered in its violet part comparatively to the curve determined by laboratory method. This displacement was realized so as to reduce the observed velocities of Moore's stars in the whole precisely to the system of Moore's catalogue; it is represented in Fig. 1 («Radial Velocities of 114 Stars») by the branch B and the corresponding numerical data are given in II_7 and II_8 (like II_5 and II_6). This operation was effected very easily after two trials with the quantities $\frac{\Sigma\sigma_\lambda}{N}$ from II_4. However finally as in the case of «114 Stars» the laboratory data for the correction in question were employed.

DETERMINATION OF THE WAVE-LENGTH CORRECTIONS AND THE TEMPERATURE CORRECTION

During the observations of this catalogue the focussing of the camera did not remain unchanged, but as shifting of the plate-holder has never surpassed narrow limits (13.0 to 13.15 mm), it was thought possible to use the same method of computations of observations as in the case of «114 Stars».

In the essential the computations consisted in: 1) Introducing into all the measurements of Moore's stars the corrections from II_5 (i. e. laboratory data). 2) Determining by successive approximations from the reductions to Moore's catalogue of the radial velocities of these stars: a) the coefficients

of a linear formula for the temperature correction by least squares solution, and b) the corrections to the wave-lengths—as resudual terms.

As the first correction depends on spectral type and this the more, the less is the dispersion of the spectrograph, all M o o r e's stars were divided into two groups: B3 to A2 — 24 stars and A5 to F5 — 12 stars. Both these groups were computed separately.

All the spectrograms were divided into 10 subgroups according to temperature of the spectrograph, thus:

Subgroups	Limits of temperature			Mean temperature	Subgroups	Limits of temperature			Mean temperature
	°		°	°		°		°	°
1	— 2.0	to	+ 1.0	— 0.5	6	+13.1	to	+16.0	+14.5
2	+ 1.1		+ 4.0	+ 2.5	7	+16.1		+19.0	+17.5
3	+ 4.1		+ 7.0	+ 5.5	8	+19.1		+22.0	+20.5
4	+ 7.1		+10.0	+ 8.5	9	+22.1		+25.0	+23.5
5	+10.1		+13.0	+11.5	10	+25.1		+28.0	+26.5

The observed quantities with which the computations have been started were the differences $v_{\text{Moore}} - (v_{\text{Sim}} + \delta_\lambda)$, where δ_λ means the corrections from II_5; these differences were adopted with equal weights independently on their having been measured by one, two or more measurers. This was admitted only for the sake of abbreviation of the computations. Some selectivity amongst measurers might have been expected only for a few weak lines, but not for the whole temperature subgroups; but thorough inspection of the measurements did not leave any place for doubt in this respect.

These differences were distributed amongst different temperature subgroups for which were computed weighted means with weights equal to the corresponding numbers of spectrograms with the line in question measured.

$$v_{\text{Moore}} - (v_{\text{Sim}} + \delta_\lambda) = \Delta v = xt + y + \Delta v_\lambda = \Delta v_t + \Delta v_\lambda,$$

where: x and y — the temperature coefficients, Δv_λ — the correction of the velocity from the line with the wave-length λ, and t — the mean temperature for the given subgroups.

A. First group of M o o r e's stars

In this group from 307 values of Δv 14 were discarded on account of very great disagreements, 11 of them having been of weight 1, and 3 — of weight 2.

In Table IV are given 293 values of Δv distributed according to the lines measured and temperature subgroups, in Table V are given the corresponding weights. At the beginning it was supposed that $\Sigma \Delta v_\lambda = 0$ where the summation is performed for all the lines measured, for each temperature subgroup separately. Mean values of the columns in Table IV furnished the right-hand terms of observational equations $tx + y = \Delta v$. After the solution of these equations the temperature corrections were introduced in all the lines of Table IV.

The weighted means (the weights from V) of the residuals from each line of the table furnished the corrections Δv_λ for all the lines measured. Considering the inaccuracy of the supposition $\Sigma \Delta v_\lambda = 0$, the weighting was not performed at first approximation to the values of Δv_λ.

After introducing the computed values of Δv_λ into Δv's (Table IV) the unknowns x, y and Δv_λ were determined in the second approximation with all the means weighted. The small values of the differences between the

TABLE IV

λ	km/sec								
	1	2	3	4	5	6	7	8	9
3933.66	+ 7.2	+ 3.7	— 3.1	— 2.1	+ 6.3	+ 1.0	+ 0.2	+ 2.2	— 1.2
3964.73	—	—	—	—	—	—	+ 0.7	+13.4	+ 3.4
3995.00	—	—	—	—	—	—	—	—22.3	—27.6
4005.33	—21.2	—13.4	—	—	— 2.7	—13.0	— 9.3	—10.4	+ 7.7
4009.27	—	—	—	—	—	—	— 5.8	— 7.1	— 1.3
4026.19	+36.8	+14.4	—	—	+25.6	+47.9	+22.2	+ 9.8	+ 9.1
4030.61	—14.2	—14.4	— 1.1	+ 3.9	—	—17.4	+ 6.0	—32.4	—13.9
4032.93	—	—	—	—	+ 6.3	—	—	—	—
4045.74	+17.1	+ 0.3	+11.5	+ 4.9	+ 8.3	+ 0.6	— 1.3	— 8.0	— 4.2
4063.54	+30.0	— 2.3	+26.2	+21.3	+ 5.3	+ 2.3	— 5.8	+ 6.4	+16.1
4069.79	—	—	—	—	—	—	+17.8	—	— 4.4
4071.69	+24.4	— 7.8	—	+ 0.4	—33.3	—12.3	— 8.1	— 2.3	+17.4
4077.64	+31.6	+ 6.0	+ 7.6	+17.6	+28.3	+ 3.7	+12.6	+11.1	+14.8
4101.74	+14.7	0.0	+ 6.8	+ 2.1	+10.3	+ 4.1	+ 5.6	+ 0.9	+ 0.3
4118.65	—32.3	+41.9	—	—	—30.8	—	— 2.0	+ 6.5	—
4120.81	—	—	+18.3	—	—	—20.0	— 1.8	+ 3.6	+ 8.4
4128.05	+18.6	—	—	+ 6.6	+27.6	— 4.7	+ 3.5	—10.6	+ 7.0
4130.88	+ 7.0	—	—	—18.8	—	—	+ 4.0	+ 6.0	—13.6
4132.14	—	— 7.9	+ 3.4	+ 7.1	—	— 5.3	— 4.8	— 8.2	—26.7
4143.68	+40.3	—17.0	+ 1.2	— 3.5	+12.1	+ 9.4	+15.7	+ 7.5	+ 7.8
4143.76	—	+36.7	+31.5	—	—	— 4.3	+ 6.4	—22.5	—19.8
4153.30	—	—	—	—	—	—	—25.9	—20.4	—43.1
4168.97	—	—	+ 1.6	—	—	—	—26.4	—	—26.1
4198.60	+18.9	+14.3	—13.7	+17.8	— 6.8	—3.3	+12.9	+14.7	+ 6.9
4202.03	+ 7.4	—	—21.8	—	— 8.7	—	—23.0	—	—39.1
4215.64	+ 8.9	— 6.6	—15.0	— 5.9	—16.1	+ 6.1	— 8.4	—16.0	—16.7
4226.91	+19.2	+16.8	—	+ 0.1	+24.8	+17.6	— 5.4	+ 9.6	—13.0
4233.28	+22.7	+ 9.0	— 0.6	— 8.4	— 0.2	— 5.4	+ 1.6	—13.1	+ 0.5
4235.90	—	—	—	—	+15.6	—	— 8.7	+31.3	—
4250.48	—	—	—	—	+ 3.5	—44.0	— 0.7	—19.3	—10.3
4260.42	—16.1	—41.1	—	+ 2.3	—	—19.0	—15.2	—18.5	—30.8
4267.16	—	—	—	—	—	—	+15.5	+ 3.2	+ 1.9
4271.55	— 7.2	—15.4	—	—22.3	+20.9	+ 0.5	—10.4	+ 2.3	+ 8.3
4282.62	—	—	—	—	—	—	—19.6	—	—
4289.93	+ 4.0	—	+11.4	+ 5.8	—11.6	— 3.6	— 3.2	— 9.2	— 4.1
4307.89	+ 4.3	—	+ 2.5	+21.1	—	—	—37.1	—	—
4314.79	+24.6	—21.8	—	—27.7	—13.6	—27.6		— 7.4	— 3.4
4325.67	+ 9.8	—40.3	—	— 6.8	—13.8	—10.7	— 4.6	—12.9	— 7.9
4340.47	+ 6.0	+ 3.5	+ 5.2	+ 3.6	— 2.9	+ 4.6	— 3.2	— 3.1	+ 1.8
4351.84	—18.1	—15.2	—44.5	—17.8	—26.9	—15.7	+ 9.2	—15.5	— 6.2
4387.93	—	+23.9	— 0.8	—	—	+ 5.4	+ 0.5	— 2.0	+ 6.2
4395.04	+15.0	—18.2	+24.5	—	—	—	—20.7	+ 3.5	—
4404.75	—	—	—	—	—	—	—	—	—
4415.12	—44.2	+ 0.4	—	—20.6	—	—29.2	—	—27.9	—12.8
4437.55	—	—	—	—	—	—	—	—	—18.7
4443.58	—	—17.2	—	—	—	—15.5	— 4.5	—16.6	—22.1
4468.64	—16.0	—35.3	—	—	—	—11.4	—27.9	+ 0.3	—14.7
4471.48	+ 3.8	+39.3	+27.6	—	—	+10.1	— 8.8	—15.5	—20.5
4481.31	+10.4	—15.2	— 1.7	—12.1	— 9.8	— 3.4	— 8.3	—16.7	—21.6
Δv_t	+6.99	—2.60	+3.48	—0.71	+0.21	—4.77	—3.94	—5.00	—7.31 1st appr.
	+9.85	—4.81	+1.06	—1.83	—1.30	—3.02	—2.71	—5.94	—6.37 2nd appr.
	2	2	1	2	2	2	4	5	5

TABLE V

λ	1	2	3	4	5	6	7	8	9
3933.66	10	10	5	18	12	9	20	26	27
3964.73							3	2	6
3995.00							1	2	
4005.33	2	3			1	4	5	9	2
4009.27							6	4	10
4026.19	2	1			2	2	10	8	19
4030.61	2	1	1	2		5	4	3	2
4032.93					1				
4045.74	3	4	3	7	6	5	8	9	2
4063.54	3	4	1	5	3	6	8	11	4
4069.79							1		1
4071.69	2	4		2	1	3	2	7	3
4077.64	4	5	4	7	3	7	8	14	7
4101.74	11	11	8	18	15	9	24	29	33
4118.65	1	1			1		2	2	
4120.81			1			1	7	3	7
4128.05	2			3	1	1	3	2	4
4130.88	1			1			1	1	5
4132.14		1	1	1		3	2	2	1
4143.68	4	4	2	5	2	4	7	9	3
4143.76		1	1			1	8	6	9
4153.30							1	1	2
4168.97			1				1		4
4198.60	3	3	1	3	2	3	6	6	6
4202.03			3		2		1		1

λ	1	2	3	4	5	6	7	8	9
4215.64	3	4	3	6	5	7	9	11	5
4226.91	1	2		1	4	3	4	7	2
4233.28	7	6	2	9	4	9	8	9	5
4235.90					1		2	3	
4250.48					2	2	3	1	1
4260.42	1	3		2		2	3	2	1
4267.16							2	4	6
4271.55	2	3		1	3	3	3	6	2
4282.62							2		
4289.93	1		3	3	4	2	7	8	6
4307.89	3		1	1			2		
4314.79	1	1		1	2	2		4	2
4325.67	2	2		3	2	6	5	7	2
4340.47	11	10	2	19	13	11	24	31	35
4351.84	1	1	1	5	1	2	4	8	5
4387.93		1	1			6	7	5	9
4395.04	1	1	1				3	1	
4404.75									
4415.12	1	1		1		1		1	1
4437.55									2
4443.58		2				4	6	2	4
4468.64	1	2				1	1	1	1
4471.48	2	1				2	8	6	18
4481.31	10	11	7	15	15	11	19	26	28

TABLE VI

λ	km/sec 1	2	3	4
3933.66	+ 4.1	+ 4.1	±0.80	± 9.32
3964.73	+10.6	+10.2	2.32	7.38
3995.00	−19.2	−20.0	1.56	2.70
4005.33	− 6.8	− 6.9	2.36	12.02
4009.27	+ 2.2	+ 1.7	2.06	9.20
4026.19	+21.1	+20.8	2.61	17.30
4030.61	− 8.6	− 8.7	3.30	14.70
4032.93	+ 7.8	+ 7.9	—	—
4045.74	+ 1.8	+ 1.7	1.38	9.45
4063.54	+ 8.8	+ 8.7	2.55	18.20
4069.79	+12.4	+12.0	8.40	11.75
4071.69	+ 1.2	+ 1.2	5.71	18.20
4077.64	+15.5	+15.5	1.87	14.69
4101.74	+ 7.0	+ 6.8	0.85	10.76
4118.65	+ 1.0	+ 1.0	8.72	23.10
4120.81	+ 8.1	+ 7.8	3.07	13.35
4128.05	+ 8.8	+ 9.0	2.42	9.70
4130.88	− 3.5	− 3.9	3.80	11.40
4132.14	− 3.0	− 3.1	1.69	5.85
4143.68	+10.7	+10.8	3.17	20.27
4143.76	− 2.6	− 2.8	5.15	26.30
4153.30	−27.1	−27.5	5.20	10.41
4168.97	−16.7	−16.5	3.71	9.35
4198.60	+12.1	+12.5	1.89	10.89
4202.03	−16.4	−16.3	4.25	12.00

λ	km/sec 1	2	3	4
4215.64	− 6.0	− 6.0	±1.84	±13.18
4226.91	+12.6	+12.5	2.77	13.60
4233.28	+ 1.7	+ 1.6	2.05	15.83
4235.90	+19.9	+19.7	9.20	22.50
4250.48	− 8.7	−11.1	6.10	18.30
4260.42	−18.6	−18.6	3.60	13.45
4267.16	+10.8	+10.4	2.07	7.15
4271.55	+ 1.7	+ 1.7	3.78	18.20
4282.62	−15.3	−15.5	—	—
4289.93	+ 0.1	0.0	1.34	7.85
4307.89	− 6.0	− 5.9	7.81	20.80
4314.79	− 8.0	− 8.1	4.40	15.80
4325.67	− 6.2	− 6.2	2.66	14.40
4340.47	+ 3.8	+ 3.9	0.75	9.52
4351.84	− 8.8	− 8.9	3.18	16.80
4387.93	+ 8.9	+ 8.0	1.56	8.45
4395.04	− 3.8	− 3.8	6.67	17.87
4404.75	—	—	—	—
4415.12	−20.8	−20.8	4.15	10.15
4437.55	−11.6	−12.1	—	—
4443.58	− 9.6	− 9.7	2.43	10.45
4468.64	−18.5	−18.5	4.43	11.75
4471.48	− 6.5	− 6.8	3.35	20.70
4481.31	− 8.6	− 8.6	1.70	19.46

TABLE VII

km/sec

λ	4	5	6	7	8	9	10
3933.66				+ 7.7	+ 3.5	+ 2.7	—16.8
3964.73							
3995.00			+54.8				
4005.33	+2.6	—11.4	+12.6	—11.4	— 9.5	—12.0	—22.9
4009.27							
4026.19							
4030.61	+ 8.0	+10.4	+30.4	+ 7.9	— 5.4	—10.8	—32.1
4032.93	+11.8	+10.7			—34.5		
4045.74	+ 8.6	+ 5.3	+31.9	+11.5	+ 3.6	+ 1.8	— 2.4
4063.54	+11.6	+13.8	+26.1	+ 8.3	+ 1.2	+ 6.2	+ 2.7
4069.79							
4071.69	+ 5.4	+15.7	+16.6	+ 1.9	+ 6.2	+ 6.7	+ 8.0
4077.64	+12.1	+ 2.2	+15.6	+21.8	+ 8.9	— 0.6	+18.2
4101.74	— 3.4	— 4.1	—19.1	— 2.3	— 2.0	— 6.1	—10.9
4118.65	—12.2	—14.1	+ 5.5	+ 2.6	+ 0.7	—20.9	
4120.81							
4128.05							
4130.88							
4132.14	—32.7					+19.8	
4143.68	+25.1	+11.0	+10.8	+10.4	+13.2	+ 6.0	+ 4.9
4143.76							
4153.30							
4168.97							
4198.60	+ 1.9	— 2.2	+ 3.9	+ 5.4	+ 6.0	— 4.1	— 8.8
4202.03	+13.9			— 0.1	— 5.3	+15.2	
4215.64	—10.8	—22.0	+13.9	— 7.9	— 3.8	—25.7	— 3.5
4226.91	+ 7.4	+ 8.3	+25.3	+15.7	+10.1	+ 8.5	+ 9.6
4233.28	—25.7	— 6.6		— 2.2	— 5.2	— 8.1	—12.8
4235.90				— 6.6			
4250.48	+15.7	— 5.4	— 4.6	— 1.0	—14.9	— 8.2	—30.3
4260.42	—10.3	+ 7.8	— 9.4	—22.8	— 5.0	—30.4	— 2.8
4267.16							
4271.55	+ 0.9	— 4.5		— 5.0	— 3.5	+ 2.9	—15.3
4282.62					—24.1	—23.2	
4289.93	+ 0.5	—25.9	+14.5	+ 6.4	— 3.5	—11.2	—21.6
4307.89	—18.8	—44.2	+ 0.3	—36.4	—30.9	—38.9	—31.7
4314.79		+12.1	+42.9	+ 7.5	+10.3	+15.7	+16.4
4325.67	+ 2.9	— 9.9	+39.5	+ 1.8	+ 0.5	+ 2.7	— 0.4
4340.47	— 0.9	— 2.3	+18.0	+ 6.7	— 0.6	— 9.6	— 9.0
4351.84	— 8.1	—23.2	— 0.6	+15.2	—12.7	—19.1	—11.3
4387.93							
4395.04		—22.9		—15.5	—19.5	— 4.4	—17.4
4404.75	+ 6.4				+ 4.9	—13.1	
4415.12	—66.7	—13.7		—60.6	—34.2	—16.2	+ 1.4
4437.55							
4443.58	—26.7		+18.9	— 0.1	+ 9.9	+ 2.2	+ 3.9
4468.64				—53.2	—48.1	—29.2	—54.4
4471.48							
4481.31	—22.6	—18.8	+12.6	— 6.3	—14.4	—33.0	—32.2
Δv_t	— 3.39	— 6.64	+12.28	— 3.01	— 4.76	— 8.95	—10.51
	2.0	1.5	1.0	3.0	7.0	2.5	2.0

values of x, y, and Δv_λ found in the first and second approximations signified the completion of successive approximations.

The last three lines in Table IV contain the values of Δv_t in both approximations and the weights of them, which are proportional to the sums of weights from Table V. In VI_1 and VI_2 are given the values of Δv_λ in both approximations; VI_3 and VI_4 — probable errors of the result (r) and of one observation of weight unity (r_o).

To illustrate the precision of the measurements in general from the mean value of $r_o's$ équal to ± 13.66 km/sec for two measurers was calculated the p. e. of the measurement of a line by one measurer, viz. ± 19.2 km/sec. Mean value of the p. e.'s of Δv_λ is ± 2.84 km/sec, or ± 0.04 A approximately.

The temperature coefficients turned out to be:

1st approx. $x = -0.46 \pm 0.08$ km/sec $y = +3.81 \pm 1.07$ km/sec

2nd » $x = -0.42 \pm 0.09$ » $y = +3.26 \pm 1.56$ »

In table I_{11} are given the final values of the observed radial velocities of the stars of I group after introduction of the corrections $\delta_\lambda + \Delta v_\lambda + \Delta v_t$; in I_{12} are given the reductions of these velocities to Moore's catalogue. Their mean value is $+0.34 \pm 0.75$ km/sec, i. e. it is well within its p. e.

TABLE VIII

λ	4	5	6	7	8	9	10	λ	4	5	6	7	8	9	10
3933.66				1	6	3	6	4215.64	6	4	3	10	18	7	5
3964.73								4226.91	8	6	3	10	24	8	6
3995.00			1					4233.28	1	1		3	8	5	3
4005.33	5	4	2	10	23	8	6	4235.90				1			
4009.27								4250.48	1	3	1	3	10	3	2
4026.19								4260.42	6	5	4	10	17	4	4
4030.61	4	1	2	4	11	3	5	4267.16							
4032.93	1	1			2			4271.55	5	3		6	18	6	3
4045.74	7	6	4	10	23	8	6	4282.62					1	1	
4063.54	8	6	4	10	22	6	6	4289.93	6	3	2	6	22	8	6
4069.79								4307.89	5	3	3	6	9	2	1
4071.69	7	5	4	9	18	5	6	4314.79		1	1	3	11	4	3
4077.64	7	5	2	8	22	8	6	4325.67	6	5	3	9	20	7	6
4101.74	8	6	4	10	23	8	6	4340.47	8	6	4	10	24	8	6
4118.65	5	1	1	2	4	1		4351.84	5	4	2	3	18	7	5
4120.81								4387.93							
4128.05								4395.04		1		2	4	4	3
4130.88								4404.75	1				2	1	
4132.14	1					1		4415.12	1	1		1	5	2	1
4143.68	8	5	4	9	23	8	6	4437.55							
4143.76								4443.58	2		1	3	7	5	4
4153.30								4468.64				2	4	2	1
4168.97								4471.48							
4198.60	6	5	3	8	15	6	4	4481.31	7	5	4	9	20	8	5
4202.03	1			2	5	1									

B. Second group of Moore's stars

On account of the small number of observations the subgroups 1, 2 and 3 were rejected at all; among other subgroups were distributed all observed values of Δv_λ, on whole 198. Data for these values are given in Tables VII and VIII (like the stars of the 1 group).

The order of successive approximations was somewhat changed comparatively with the previous group. Into the data of Table VII were introduced temperature corrections with the coefficients x and y from the pre-

TABLES IX—X

λ	km/sec					km/sec
	1	2	3	4		
3933.66	+ 2.7	±3.85	±15.4	—	—	+ 7.4
3964.73	—	—	—	—	—	+12.3
3995.00	+51.7	—	—	—	—	—18.8
4005.33	— 5.0	1.58	12.0	— 9.4	±1.62	— 6.0
4009.27	—	—	—	—	—	+ 2.5
4026.19	—	—	—	—	—	+21.2
4030.61	+ 1.0	3.75	20.7	—	—	— 8.5
4032.93	— 8.4	11·85	23.7			+ 8.1
4045.74	+11.1	1.75	14.0	+11.2	1.43	+ 1.7
4063.54	+11.6	1.23	9.7	+11.6	1.72	+ 8.5
4069.79	—	—	—	—	—	+11.8
4071.69	+11.6	1.08	7.9	+19.7	2.13	+ 1.0
4077.64	+13.4	2.08	15.8	+23.4	1.62	+15.3
4101.74	+ 2.1	1.18	9.5	+ 0.5	1.26	+ 6.8
4118.65	— 3.0	3.32	12.4	—	—	+ 1.3
4120.81	—	—	—	—	—	+ 8.1
4128.05	—	—	—	—	—	+ 9.6
4130.88	—	—	—	—	—	— 3.1
4132.14	— 3.0	—	—	—	—	— 2.4
4143.68	+16.8	1.24	9.8	+17.7	1.37	+11.9
4143.76	—	—	—	—	—	— 1.7
4153.30	—	—	—	—	—	—26.0
4168.97	—	—	—	—	—	—14.5
4198.60	+ 6.1	1.52	10.2	—	—	+15.8
4202.03	+ 5.1	3.03	9.1	—	—	—13.0
4215.64	— 4.0	2.45	17.8	—18.5	2.35	— 2.0
4226.91	+15.5	1.26	10.2	+ 6.3	1.62	+17.0
4233.28	— 2.0	1.51	6.9	—	—	+ 6.5
4235.90	— 2.4	—	—	—	—	+24.7
4250.48	— 5.7	2.33	11.2	—	—	— 5.3
4260.42	— 5.8	3.13	22.0	+ 8.5	4.07	—12.3
4267.16	—	—	—	—	—	+17.3
4271.55	+ 1.6	1.20	7.7	— 4.1	2.04	+ 8.6
4282.62	—17.5	—	—	—	—	— 7.8
4289.93	— 0.8	2.70	19.7	—19.3	2.90	+ 8.2
4307.89	—24.8	2.98	16.1	—33.9	4.50	— 3.2
4314.79	+18.8	2.23	10.7	+13.9	2.90	+ 1.5
4325.67	+ 7.7	2.17	16.2	— 0.9	1.69	+ 4.0
4340.47	+ 4.1	2.00	15.1	+ 3.9	1.34	+15.0
4351.84	— 6.7	2.27	15.0	—	—	+ 3.1
4387.93	—	—	—	—	—	+22.9
4395.04	— 8.4	2.62	9.7	—	—	+11.4
4404.75	+ 5,3	3.45	6.9	—	—	—
4415.12	—26.1	6.78	22.4	—	—	— 4.4
4437.55	—	—	—	—	—	+ 6.2
4443.58	+ 8.3	3.07	14.4	—	—	+ 9.2
4468.64	—39.9	4.46	13.4	—	—	+ 2.7
4471.48	—	—	—	—	—	+14.7
4481.31	—12.2	3.48	26.5	—	—	+13.9

vious group. The absence of considerable changes in Δv_λ (all < 0.2 km/sec) between two approximations permitted to be satisfied with one aproximation to the temperature coefficients which turned out to be

$$x = -0.44 \pm 0.23 \text{ km/sec} \quad y = +3.55 \pm 4.60 \text{ km/sec}$$

The values of Δv_λ and their p. e.'s are given in Table IX, col. 1—3. For this group all the computations were performed with the weights from the table VIII.

FINAL RESULTS FOR OBSERVED STARS

As it is seen the values of x, y for both groups coincide in the limits of their p. e.'s.; the corrections differ for both groups as it must be expected. For our work more useful are those values of Δv_λ which have been determined from the first group of Moore's stars; so the values of x and y must be taken as determined from the same group.

In Table X are given those values of corrections $\delta_\lambda + \Delta v_\lambda$ which have been introduced into measurements of the spectrograms of programme stars, and in Table XI — the temperature corrections used.

The rather large disagreement between the values of x for this catalogue and for «114 Stars» is to be explained by the focussing of the camera having been partially corrected in the course of observations for this catalogue while in that of «114 Stars» it remained absolutely constant.

The comparison of thecorrections Δv_λ determined for the above mentioned catalogues is given in table IX for 16 common lines (the line λ 4415.12 was rejected on account of poor precision in both cases). In the «114 stars» the spectral types are A5 — F4, i. e. practically the same as in this case. The mean of the absolute values of differences in Δv_λ for these two catalogues is 6,9 km/sec, i. e. 0.1 A. The reliability of the determined corrections Δv_λ may be corroborated by the fact that the systematic error of our velocities is quite small (see below).

So all the radial velocities observed for this work were corrected for $\delta_\lambda + (xt + y) + \Delta v_\lambda$, where δ_λ as determined independently by laboratory method may be thought of as an absolute correction and $xt + y + \Delta v_\lambda$ as a well grounded interpolation formula for the reduction of the observed velocities to the system of Moore's catalogue. For the future the corrections δ_λ are to be determined by laboratory method for different temperatures; so simultaneous observations of stars with known velocities may be dispensed with. All this on condition that the focussing of the camera will be absolutely constant.

TABLE XI

$t°$	$xt+y$	$t°$	$xt+y$	$t°$	$xt+y$	$t°$	$xt+y$
—2.0	+4.1	+6.0	+0.7	+14.0	—2.6	+22.0	—6.0
—1.0	+3.7	+7.0	+0.3	+15.0	—3.0	+23.0	—6.4
0.0	+3.3	+8.0	—0.1	+16.0	—3.5	+24.0	—6.8
+1.0	+2.8	+9.0	—0.5	+17.0	—3.9	+25.0	—7.2
+2.0	+2.4	+10.0	—0.9	+18.0	—4.3	+26.0	—7.7
+3.0	+2.0	+11.0	—1.4	+19.0	—4.7	+27.0	—8.1
+4.0	+1.6	+12.0	—1.8	+20.0	—5.1	+28.0	—8.5
+5.0	+1.2	+13.0	—2.2	+21.0	—5.6		

In Table XII are given the final values of the observed radial velocities for 107 stars. For 16 of these stars the radial velocities have been admitted to be variable which makes 14% of the total number of the stars observed. This percentage is smaller than that usually accepted, viz. about 25—30%; but with so small dispersion as ours one must be more careful in announcing the variability of a radial velocity. The data of the Table XII are self-explanatory; the magnitudes are visual and the spectral types

TABLE XII

1	2	3	4	5	6 km/sec	7 km/sec	8	9
	h m	° ′						
1 223	0 11.5	+36 5	6.95	A0	— 1.3	±2.7	5	βGC 105, br
4 269	0 40.0	+23 3	7.26	B8	+18.0	2.7	4	
6 612	1 1.8	+37 31	7.02	B9	— 5.2	2.2	4	
10 894	1 41.8	+10 21	6.97	B9	+10.5	5.3	5	
11 079	1 43.8	+26 0	6.73	B8	+13.3	3.0	5	
16 694	2 35.5	+18 23	6.89	B9	+19.9	3.8	6	βGC 1374 A
17 330	2 41.8	+29 17	7.19	B9	— 1.3	2.3	3	βGC 1422, br
22 860	3 35.2	+28 32	6.89	B9	+10.9	2.6	7	
26 256	4 4.1	+ 6 28	6.74	B9	+14.9	3.1	7	
30 466	4 42.9	+29 24	7.21	A0p	+17.2	3.1	4	
34 364	5 11.8	+33 39	6.11	B9	+13.4	5.9	5	
34 719	5 14.4	+19 30	6.81	A0p	+16.9	1.9	5	
48 864	6 40.4	+18 57	6.83	B9	Var.	—	5	Range + 53.0 — — 4.6 km/sec
49 406	6 43.2	+22 25	7.10	B9	+45.6	4.7	5	
66 925	8 0.6	+ 2 28	6.77	A0	— 6.5	4.2	5	
68 903	8 9.4	+16 23	7.18	B8	— 4.0	2.9	5	D.D.O. + 3.4 ± 1.6 km/sec
74 815	8 41.1	+ 8 50	6.94	B9	+25.4	4.3	5	
75 390	8 44.6	+ 6 56	6.76	B9	—10.0	5.9	5	
77 986	9 0.6	+16 15	7.27	B9	+ 1.1	4.9	6	
83 434	9 33.3	+20 45	6.80	B9	+31.3	2.5	5	
89 363	10 13.6	+18 13	6.62	A0	+16.8	3.1	4	
97 938	11 10.8	+13 9	6.73	A0	Var.	—	5	Range + 46.0 — — 44.4 km/sec D.D.O. + 11.2 ± 3.0 km/sec
102 056	11 39.6	+29 13	6.98	A0	—13.2	3.8	5	
105 262	12 2.1	+13 33	7.00	B9	+40.2	4.6	5	
105 388	12 3.0	+31 37	7.24	A0	— 5.1	1.5	5	D.D.O. — 8.5 ± 1.5 km/sec
106 224	12 8.2	+22 36	7.42	A2	Var.	—	5	Range + 8.5 — — 60.6 km/sec
115 301	13 11.2	+21 55	7.18	B9	Var.	—	5	Range + 24.3 — — 23.6 km/sec
115 709	13 13.8	+ 4 13	6.56	A0	— 6.9	5.0	5	
120 448	13 44.4	+ 6 50	6.75	A0	+ 1.4	5.3	4	
124 586	14 9.4	+31 40	7.25	A0	—16.1	2.4	5	
127 067	14 24.2	+28 44	6.95	A0	—16.5	6.5	6	βGC 6887, br.
128 481	14 32.0	+13 18	6.90	A0	— 6.7	3.7	5	
128 661	14 33.1	+36 22	6.97	A0	Var.	—	5	Range + 49.7 — + 14.7 km/sec
130 256	14 42.0	+ 1 32	6.59	A0	Var.	—	6	βGC 7002, br. Range + + 25.8 — — 10.0 km/sec
134 854	15 7.0	+10 36	6.78	A0	—13.3	3.9	5	
135 679	15 11.3	+26 1	6.67	A0	— 4.3	2.2	5	
139 268	15 32.1	+15 15	6.86	A0	Var.	—	5	Range + 29.7 — — 45.6 km/sec
139 609	15 34.0	+12 36	7.14	B9	+ 5.8	5.2	5	
140 101	15 36.8	+37 21	6.97	A0	—13.2	4.6	5	
141 070	15 42.0	+10 6	6.97	A2	—28.0	2.0	5	
141 458	15 44.1	+13 1	6.80	A0	Var.	—	5	Range + 21.9 — — 32.0 km/sec
144 359	16 0.4	+34 27	7.02	A0	Var.	—	8	Range + 63.6 — — 79.9 km/sec.
145 774	16 7.6	— 1 28	7.46	B8	+30.3	1.9	6	
146 010	16 8.9	+21 49	6.58	A2	—11.2	4.4	5	
150 361	16 35.5	+29 25	7.21	A0	—24.9	2.6	5	

TABLE XII (*Continued*)

1	2	3	4	5	6 km/sec	7 km/sec	8	9
	h m	° ′						
150 379	16 35.6	+ 4 24	6.86	A0	— 33.5	±7.0	5	βGC 7711, f.Moore — 30 ± 1 km/sec.
150 525	16 36.5	+ 5 4	6.75	A0	+ 2.3	3.4	5	
154 888	17 3.1	+35 27	7.19	A0	— 18.7	1.3	5	
156 377	17 12.1	+18 8	6.92	B9	+ 1.6	4.1	6	
156 547	17 13.1	+26 0	7.06	B9	+ 0.3	3.0	5	
161 270	17 39.5	+ 2 37	6.25	A0	Var.	—	5	βGC 8136, br. Range + 0.9 — — 46.2 km/sec.
161 289	17 39.6	+ 2 37	6.64	A0	— 37.7	2.6	6	βGC 8136, f.
161 464	17 40.6	+33 17	7.04	B8	— 12.3	2.4	5	
161 542	17 41.0	+ 5 57	7.22	A0	— 29.5	1.7	8	} Open cluster NGCI 4665
161 572	17.41.2	+ 5 44	7.46	B8	— 19.3	4.1	6	
161 573	17 41.2	+ 5 35	6.66	B8	— 7.2	2.7	5	
161 603	17 41.4	+ 5 42	7.19	B9	— 7.7	3.7	7	} Open cluster NGCI 4665
161 677	17 41.8	+ 5 49	6.93	B8	— 26.4	5.1	5	
161 817	17 42.6	+25 48	6.87	A0	—360.7	3.8	5	
161 921	17 43.2	+18 56	6.66	A0	— 22.6	3.0	6	
162 028	17 43.8	+ 5 44	7.35	B9	— 6.5	5.4	8	Open cluster NGCI 4665
165 475	18 1.1	+12 0	7.05	A0	Var.	—	8	βGC 8348, br. Range +41.5 — — 38.4 km/sec.
168 131	18 13.2	+11 51	7.02	B8	— 3.3	3.2	5	
168 431	18 14.5	+12 9	6.93	B8	— 6.4	2.7	5	D.D.O. — 7.9 ± 3.0 km/sec
168 440	18 14.6	+12 30	7.34	B8	— 7.6	2.2	5	
172 650	18 36.3	+26 2	6.74	B9	— 11.7	4.4	5	
173 000	18 38.1	+15 6	6.84	A0	— 5.6	5.3	5	
173 171	18 38.9	+19 22	7.12	B9	— 24.6	3.7	7	βGC 8755, br.
173 921	18 42.9	+16 48	6.66	B8	— 3.3	3.1	5	
173 952	18 43.1	+13 20	7.09	B9	+ 3.1	4.5	5	
177 595	19 0.3	+27 10	7.05	B9	— 18.4	1.3	5	
177 599	19 0.3	+15 25	6.84	A0	— 9.0	1.2	5	
178 512	19 3.8	+12 57	6.97	B8	— 2.1	2.0	5	
179 309	19 7.0	+23 19	6.84	B9	— 18.3	6.2	6	
179 782	19 8.8	+36 16	6.80	A0	— 11.5	2.3	6	
180 316	19 11.0	+27 46	6.69	B8	Var.	—	5	Range + 20.6 — — 40.4 km/sec.
180 613	19 12.1	+31 4	6.75	B8	+ 8.7	2.8	5	
184 940	19 31.7	+34 28	6.98	B9	Var.	—	6	Range + 31.0 — — 60.8 km/sec.
185 755	19 35.6	+30 11	7.11	B9	— 18.4	3.0	5	
186 179	19 37.8	+27 9	6.74	B8	— 24.2	5.8	5	βGC 9535
191 295	20 4.1	+11 58	7.02	B9	+ 9.7	5.1	5	
191 855	20 6.9	+30 29	6.72	B9	— 9.2	3.6	6	
192 022	20 7.7	+26 36	7.10	B8	— 10.7	1.5	5	
192 684	20 11.0	+32 33	6.71	B9	— 16.5	5.4	5	
192 913	20 12.3	+27 29	6.69	A0p	+ 2.0	4.6	5	Moore — 15 ± 2 km/sec.
192 954	20 12.6	+15 33	7.34	B9	+ 16.0	2.6	5	
193 325	20 14.6	+20 9	7.35	B9	— 38.9	2.4	5	
195 102	20 24.2	+33 33	6.88	B9	— 9.1	3.3	5	
196 120	20 30.2	+34 20	6.62	B8	— 28.1	4.3	4	βGC 10338, br.
197 562	20 39.4	+23 26	6.78	A0	— 26.2	2.9	5	

TABLE XII (*Continued*)

1	2	3	4	5	6 km/sec	7 km/sec	8	9
	h m	° ′						
198 184	20 43.5	+25 49	7.00	B9	— 2.3	±5.0	5	
200 930	21 1.4	+20 33	6.66	B9	+ 9.7	3.0	6	
201 671	21 6.0	+22 3	6.94	A0	— 6.8	2.2	5	βGC 10795, br.
202 198	21 9.2	+33 18	7.09	B8	— 6.4	4.2	5	
205 746	21 32.3	+11 16	7.20	A0	+12.3	3.1	6	
206 807	21 39.5	+37 51	6.87	A0	—17.7	4.6	4	βGC 11208, f.
206 991	21 40.8	+26 31	7.18	B9	Var.	—	5	Range + 46.9 — — 44.3 km/sec.
207 469	21 44.1	+32 20	6.79	A0	— 8.3	3.7	6	
211 304	22 11.1	+11 15	7.04	B9	+ 5.6	2.6	4	
211 433	22 11.9	+22 24	6.80	A0	Var.		8	Range + 45 — 14 km/sec
211 733	22 14.1	+15 45	6.91	A0	—29.1	6.6	5	D.D.O. — 24.1 ± 1.0 km/sec.
215 955	22 43.8	+30 24	7.26	B9	+ 8.5	3.3	6	
218 154	23 0.6	+24 7	7.01	A0	Var.	—	7	Range + 48.2 — — 71.4 km/sec.
218 155	23 0.6	+14 25	6.81	A0	+11.9	3.3	7	
218 428	23 2.9	+29 31	7.25	B9	+ 5.1	1.1	8	D.D.O. + 0.1 ± 1.6 km/sec
218 767	23 5.5	+31 57	6.89	B9	+ 0.1	6.0	8	βGC 12201 A + B D.D.O — 5.2 ± 5.3 km/sec.
219 361	23 10.1	+27 32	6.95	A0	+ 2.6	3.3	6	

are those of H.D.; in the column 8 are given the numbers of spectrograms measured. In the remarks βGCs ignifies Burnham's General catalogue of Double Stars, etc.; Moore — J. H. Moore, General Catalogue of the Radial Velocities of Stars, etc.; D.D.O. — Publications of the David Dunlap Observatory, University of Toronto, Vol. I, Nr. 3. (2). For 91 stars with adopted constant velocities the mean value of p. e's is ±3.57 km/sec and the number of spectrograms per star is 5.3. For the catalogue D.D.O. corresponding data are ±2.85 km/sec and 5.8 (for the stars B8 — A0). The lower precision of the present catalogue may be explained by the small dispersion of our spectrograph: 75A/mm instead of 33—66 A/mm for D.D.O.

SYSTEMATIC CORRECTION

Amongst the observed stars there are two stars in common with Moore's catalogue and seven stars — with that of D.D.O. Using the table of reduction of D.D.O. velocities to Moore's catalogue the reductions of our velocities to the same are as follows:

	Moore-Simeis		Moore-Simeis
H. D. 68903	+ 7.8 km/sec	H. D. 192913	— 17.0 km/sec
105388	— 3.0	211733	+ 5.4
150379	+ 3.5	218428	— 4.6
168431	— 1.1	218767	— 4.9

Velocity of the H.D. 97938 was adopted by us to be variable.

Excluding the star H.D. 192913 with a very large deviation the systematic correction to our velocities turns out to be

Moore — Simeis + 0,44 ± 1,51 km/sec (7 stars)

The distribution of the observed stars on the celestial sphere is far from being uniform: angular distances from the solar apex for 80% of them are less than 90°, and $^2/_3$ of them are situated west of it.

But taking into account the parallactic motion and the effect of galactic rotation, the K-term may be determined and so some information about the systematic error of our velocities may be gained. To this end the necessary data have been used as follows:

1) The solar apex and solar motion after Smart and Green (3) $\alpha_0 = 267°.0$, $\delta_0 = +32°.0$; $U = 19.5$ km/sec.

2) The galactic centre according to Shapley $G_1 = 327°$, $g_1 = 0°$.

3) The constant of galactic rotation $A = 0.017$ km/sec.

4) The distances of stars according to Trumpler's mean absolute magnitudes, viz.

B8	$M = -0^m.2$	A0	$M = +0^m.9$
B9	$+0.3$	A2	$+1,7$

To calculate the distances from absolute magnitudes the galactic absorbtion ought to be taken into account. For our stars the mean distance is $r \approx 200$ parsecs, for which the total visual absorbtion is $0^m.1$, according to P. C. Keenan (4), with the corresponding correction to the K-term about 0.7 km/sec. We have neglected it.

From the whole of stars with adopted constant radial velocities were excluded 6 stars belonging to galactic cluster NGCI 4665 and a star with high velocity — HD 161817. The remaining 84 stars were used to determine the K-term from the equation:

$$\rho = U\cos\lambda + rA\sin 2(G - G_1)\cos^2 g + K + \rho' + \varepsilon,$$

where ρ and ρ' — observed and peculiar radial velocities, ε — accidental error of the observed ρ. With the usual assumption concerning the accidental nature of ρ, the K-term is deduced from the formula:

$$K = \frac{1}{N}\sum[\rho - U\cos\lambda - rA\sin 2(G - G_1)\cos^2 g],$$

where N is the number of stars used.

In Table XIII are given the values of $K + \rho' + \varepsilon$ and $\rho' + \varepsilon$ for the stars used. The value of the K-term turned out to be

$$K = +3.10 \pm 1.06 \text{ km/sec.}$$

The p. e. of one observed value of the K-term is ± 9.73 km/sec.

In the paper by Smart and Green (3) there are given values of the K-term for the whole spectral classes only:

B0-B9	$K = +4.68$	km/sec
A0-A9	» $+0.03$	»

Taking into account the spectral classification of the observed stars (B8—17%, B9—42%, A0—39%, A2—2%) it may be concluded that our value of the K-term differs from that of Smart and Green less than our p. e.

It is true that the selection of stars with respect to magnitudes is not identical in both cases: in the paper by Smart and Green are used the stars of Schlesinger's catalogue, all of them brighter than $6^m.5$, whereas in our case they are fainter than this limit. There has been expressed an opinion

TABLE XIII

HD	$K+\rho'+\varepsilon$	$\rho'+\varepsilon$	HD	$K+\rho'+\varepsilon$	$\rho'+\varepsilon$	HD	$K+\rho'+\varepsilon$	$\rho'+\varepsilon$	HD	$K+\rho'+\varepsilon$	$\rho'+\varepsilon$
1223	+ 7.5	+ 4.4	105388	+ 1.2	— 1.9	161921	— 8.6	—11.7	192954	+24.6	+21.5
4269	+23.1	+20.0	115709	+ 0.7	— 2.4	168131	+ 7.1	+ 4.0	193325	—29.4	—32.5
6612	+ 3.0	— 0.1	120448	+11.3	+ 8.2	168431	+ 4.0	+ 0.9	195102	+ 3.5	+ 0.4
10894	+ 7.6	+ 4.5	124586	— 3.4	— 6.5	168440	+ 2.4	— 0.7	196120	—15.7	—18.8
11079	+15.9	+12.8	127067	— 3.5	— 6.6	172650	+ 1.1	— 2.0	197562	—16.7	—19.8
16694	+16.3	+13.2	128481	+ 5.7	+ 2.6	173000	+ 6.6	+ 3.5	198184	+ 8.4	+ 5.3
17330	— 1.0	— 4.1	134854	0.0	— 3.1	173171	—13.1	—16.2	200930	+19.3	+16.2
22860	+ 7.3	+ 4.2	135679	+10.0	+ 6.9	173921	+ 7.7	+ 4.6	201671	+ 3.5	+ 0.4
26256	+ 0.2	— 2.9	139609	—19.4	—22.5	173952	+13.6	+10.5	202198	+ 5.3	+ 2.2
30466	+10.1	+ 7.0	140101	+ 1.4	— 1.7	177595	— 6.2	— 9.3	205746	+19.5	+16.4
34364	+ 6.8	+ 3.7	141070	—14.5	—17.6	177599	+ 2.6	— 0.5	206807	— 4.9	— 8.0
34719	+ 3.8	+ 0.7	145774	+42.3	+39.2	178512	+ 7.2	+ 4.1	207469	+ 3.4	+ 0.3
49406	+31.5	+28.4	146010	+ 4.7	+ 1.6	179309	— 6.6	— 9.7	211304	+11.8	+ 8.7
66925	—25.2	—28.3	150361	—10.3	—13.4	179782	+ 2.9	— 0.2	211733	—21.6	—24.7
68903	—19.6	—22.7	150379	—20.3	—23.4	180613	+21.7	+18.6	215955	+18.9	+15.8
74815	+ 9.8	+ 6.7	150525	—15.5	—18.6	185755	— 6.1	— 9.2	218155	+17.7	+14.6
75390	—25.7	—28.8	154888	— 3.6	— 6.7	186179	—12.8	—15.9	218428	+14.9	+11.8
77986	—11.1	—14.2	156377	+14.4	+11.3	191295	+18.2	+15.1	218767	+10.3	+ 7.2
83434	+23.4	+20.3	156547	+13.7	+10.6	191855	+ 3.2	+ 0.1	219361	+11.2	+ 8.1
89363	+11.9	+ 8.8	161289	—25.2	—28.3	192022	— 0.1	— 3.2			
102056	— 9.0	—12.1	161464	+ 1.3	— 1.8	192684	— 3.9	— 7.0			
105262	+43.6	+40.5				192913	+14.6	+11.5			

that the value of the K-term decreases with apparent brightness of stars as far as 0.0 km/sec (5), (6). But more recent investigations (7), (8) do not corroborate this opinion pointing out the most probable value of the K-term of the order 3.6 to 4.2 km/sec (for O — B7 stars) (9). The same results seem to be received from the simultaneous determinations of the K-term and $\overline{rA}$ for different intensities of the Ca II interstellar lines (10). The resulting decrease of the K-term with eightfold increment of $\overline{rA}$ is in its p. e.'s.

There are very few determinations of the K-term for spectral subdivisions B8-B9; in one of the most recent works (8) these stars are excluded from discussion, although just these stars are very interesting because of the rapid decline of the value of the K-term for these spectral subdivisions. For the stars B8-B9 there is a determination of the K-term by Lindblad (11), viz. $K = +2.8$ km/sec with simultaneous determination of the motion of the Sun $U = 21.8$ km/sec which differs from that of Smart and Green.

SOME STATISTICAL CHARACTERISTICS OF THE OBSERVED RADIAL VELOCITIES

Allowing the distribution of $\rho' + \varepsilon$ to be Gaussian from the formula $hr = 0.4769$ with $r = \pm 9.73$ km/sec we obtain the value of the module- $h = 0.4902$, using which from the relation $\overline{|\rho' + \varepsilon|} = \frac{1}{h\sqrt{\pi}}$ the mean of absolute values of $\rho' + \varepsilon$ turns out to be $\overline{|\rho' + \varepsilon|} = 11.5$ km/sec. Direct computation from the Table XIII gives for this quantity 10.89 km/sec. This disagreement may be explained by the distribution of $\rho' + \varepsilon$ not being strictly Gaussian.

That this is the case may be seen from the following table:

$\lvert\rho' + \varepsilon\rvert$ (km/sec)	Number of stars		$\lvert\rho' + \varepsilon\rvert$ (km/sec)	Number of stars	
	Comp.	Observ.		Comp.	Observ.
0.0— 5.0	23	30	25.1—30.0	4	4
5.1—10.0	20	17	30.1—35.0	2	1
10.1—15.0	16	12	35.1—40.0	1	1
15.1—20.0	11	12	40.1—45.0	0	1
20.1—25.0	7	6		84	84

As has been pointed out above the mean value of the p. e.'s of our velocities is ± 3.57 km/sec. The mean random radial velocity for the observed stars — $\overline{|\rho'|}$ is to be calculated from the relation

$$9.73^2 = \alpha^2 + 3.57^2;\ \overline{|\rho'|} = 1.183\ \alpha;\ \overline{|\rho'|} = 10.71 \text{ km/sec}$$

For the sake of comparison following results may be cited: Gyllenberg has given for this quantity the values (12):

B0 stars	7.0 km/sec
A0 »	11.7 »
F0 »	14.4 »

From these data the values of $\overline{|\rho'|}$ may be computed as a weighted mean for spectral classes of our stars; it is $\overline{|\rho'|} = 11.35$ which differs quite little from ours.

GALACTIC CLUSTER NGC I 4665

Radial velocities are observed for 6 stars of this cluster, the mean of which is -16.1 ± 3.4 km/sec. With the normal absolute magnitudes of stars the distance to this cluster turns out to be 253 parsecs, which is very near to the mean of two estimates based on two assumptions for the absolute magnitude of the fifth star in this cluster (13), viz. 200 and 300 parsecs. Correcting the observed radial velocities for the parallactic motion (-17.4 km/sec) and galactic rotation ($+3.2$ km/sec) the «peculiar» radial velocity of the cluster is obtained, viz.—1.9 ± 3.4 km/sec. The mean random radial velocity of stars of this cluster is 9.0 km/sec. Considering the small number of the observed stars in this cluster only a rough approximation may be gained to the mean space-velocity of the stars in question, viz. $S = 18.0$ km/sec and to the mean tangential velocity $\overline{T} = 14.1$ km/sec.

HIGH VELOCITY STAR HD 161817

This star is an outstanding representative of its class not only because of great velocity, but also on account of its early spectral type. No data has been found in the literature about the parallax and proper motion of this star. Allowing for the parallactic motion (-19.3 km/sec) and the effect of galactic rotation ($+2.1$ km/sec), the radial velocity of this star refered to the centroid of near stars is -344 ± 3.8 km/sec. As the data for parallax and proper motion are lacking, only a rough approximation to the space-velocity may be computed by supposing the direction of the last to coincide with observed radial velocity, namely, $G = 197°$, $g = -24°$; $V = 344$ km/sec. So the direction of motion seems to be usual for high velocity stars.

REFERENCES

1. V. A. Albitzky. Radial velocities of 114 stars; Pulkovo Obs. Bull. (in press)
2. David Dunlap Observatory, Publications, Vol. I, No 3, 73 1939
3. W. M. Smart and H. E. Green. M. N. **96**, 471, 1936
4. P. C. Keenan. Ap. J. **91**, 515, 1940
5. Victoria Obs. Publications, Vol. V, 225, 1936
6. Handbuch der Astrophysik, Bd. VII, 604
7. W. M. Smart; M. N. **100**, 376, 1940
8. A. Ali. M. N. **101**, 324, 1941
9. P. S. Lall. M. N. **99**, 42, 1938
10. E. v. d. Pahlen. Lehrbuch der Stellarstatistik, 862
11. B. Lindblad. M. N. **90**, 803, 1930
12. E. v. d. Pahlen. L. c., 753
13. H. Shapley. Star Clusters. Harvard Monographs. No. 3

РАДИАЛЬНЫЕ СКОРОСТИ 107 B8-A0 ЗВЕЗД

В. А. АЛЬБИЦКИЙ

В статье изложены обработка и окончательные результаты наблюдений радиальных скоростей для 107 звезд спектральных типов B8-A0, в пределах яркости 6.6—7.3 виз. вел. со склонениями от 0° до +40°. Наблюдения производились с короткой камерой однопризмового спектрографа Симеизской обсерватории, дающей дисперсию 75 A на mm у $H\gamma$.

Метод обработки измерений спектрограмм аналогичен методу, изложенному в нашей работе «Радиальные скорости 114 звезд», с той разницей, что в то время как в последней работе коэффициенты температурной поправки были выведены графически, в настоящей работе было применено решение условных уравнений по способу наименьших квадратов. Поправки же длин волн звездных линий получены как остаточные члены.

Примененные при редукции наблюдений программных звезд поправки были определены по опорным звездам спектральных типов B3-A0. Температурная поправка имеет вид:

$$\Delta v_t = \underset{(\pm 0.09)}{-0.42} \cdot t + \underset{(\pm 1.56)}{3.26} \text{ km/sec},$$

а поправки длин волн звездных линий Δv_λ приведены в таблице VI_2 и их вероятные ошибки — в VII_3. Значительное отличие коэффициента при t в Δv_t от такового же в предыдущей работе («114 звезд») объясняется тем, что при наблюдениях для настоящей работы фокусировка камеры подверглась частичной корректировке, в то время как в предыдущей работе она оставалась неизменной. Среднее значение вероятных ошибок для Δv_t равно ± 2.84 km/sec $\sim \pm 0.04$ A.

Окончательные значения полученных радиальных скоростей приведены в таблице XII вместе с их вероятными ошибками; для 16 звезд с переменными радиальными скоростями приведены наблюденные пределы их изменений. Среднее значение вероятной ошибки окончательной скорости равно 5.57 km/sec. при среднем числе спектрограмм 5.3. Систематическое приведение к системе каталога Moore'a определенных радиальных скоростей получено из сравнений с определенными ранее в иных местах радиальными скоростями 7 звезд, а именно: Moore — Симеиз $+0.44 \pm 1.51$ km/sec. В настоящей работе впервые была наблюдена радиальная скорость «быстрой» звезды HD 161817, равная —360 km/sec, точно так же впервые были определены радиальные скорости для 6 звезд открытого звездного скопления NGC I 4665.

A LIST OF RADIAL VELOCITIES OF 131 STARS FAINTER THAN 6.75

G. SHAJN

In the present paper are given the results of observations of radial velocities of 131 stars fainter than 6.75. A thorough investigation of the system of wave-lengths brought out a dependence of the corrections to the radial velocities for individual lines upon wave-lengths, an effect connected with the shape of the focal curve of the short camera used. A serious systematic error of seasonal character arising from the smallest deviation from the true focus turned out to be the most characteristic feature of our observations. The account for the systematic error in question allowed at last to reduce the preliminary value of the mean arithmetic and algebraic difference Moore-Simeis for 29 standard stars from ± 4.2 and $+3.2$ to ± 2.1 and $+0.3$ respectively. A fair elimination of the systematic error is tested by the very small value of the K-term. The velocity of solar motion and the K-term as derived from our small observational material turned out to be $V_{\odot} = 15.2 \pm 0.5$, $K = -0.6 \pm 0.3$.

The probable error of a spectrogram and a star is ± 6.2 and ± 2.5 respectively. The probable error as derived from the comparison of few common stars observed at Simeis and the David Dunlap Observatory turns out to be about ± 3.0 km/sec.

Among the observed stars there are found three doubtless and two suspected new spectroscopic binaries.

INTRODUCTION

The present list includes 131 stars mainly of type B3-A0 fainter than 6.75 and 29 standard and other brighter stars. While the first list of 343 stars (1) was observed with a long camera, we used in the present work a short one (f=290 mm) giving a dispersion 75 A per mm at H_{γ}. We hoped that since at least for the half of the whole number of the stars of type B3-A0 the spectral lines are wide and nebulous the two-fold reduction of the dispersion as compared with the long camera (f = 560) would not affect considerably the accuracy.

The short camera much concedes the long one especially with regard to the focal curve. In the case of the long camera the spectrum may be obtained in the best focus within 3900—4600, the deviations being within ± 0.05 mm. The focal curve of the short camera is represented on Fig. 1. The ordinates are the focus settings. The difference in the focus for 4200—4600 reaches about 0.30 mm. Even for 4400 the bad focus becomes perceptible. The inclination was selected such as to bring in the best focus the portion of the spectrum from 3950 to 4350. When rotating the camera by 180 with-

out change of the inclination one obtains in fair focus the region from 4500 to 4850.

The procedure of measurements of the spectrograms and the method of reduction is the same as described in detail in the preceding paper. The interpolation formula was obtained in the usual manner from the measurements of iron spectra on ten plates. The constants are as follows

$$X^r = 148.2558 - \frac{[5.1013530]}{\lambda + \Delta\lambda - 2169.234}$$

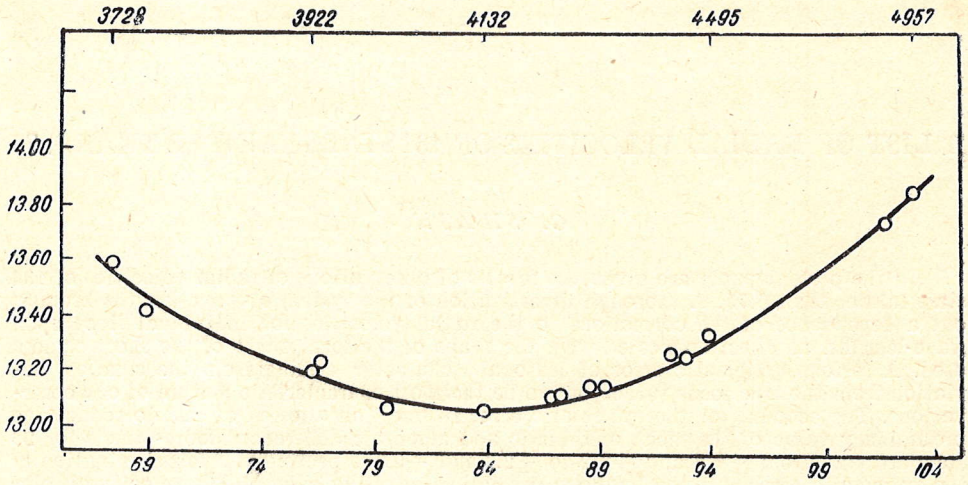

Fig. 1. The focal curve of the short camera. The abscissae are micrometer readings (bottom) and wave-length (top). The ordinates are focal settings in mm.

Below are given the micrometer readings for iron lines

λ (I. A.)	Computed	O — C ($\Delta x \cdot 0^r.001$)		Δ λ (Smoothed)
3865.53	73.805	—2		
3922.91	76.243	+1	3850	—0.07 A
3977.75	78.428	—2	3900	—5
4021.87	80.090	+2	3950	—3
4076.64	82.048	—3	4000	—1
4101.49	83.102	0	4050	0
4118.55	83.472	0	4100	0
4191.44	85.807	+1	4150	+1
4210.34	86.385	0	4200	+1
4233.61	87.083	+1	4250	+1
4282.41	88.495	0	4300	0
4315.09	89.405	—2	4350	—1
4337.05	90.001	—1	4400	—2
4375.93	91.027	+2	4450	—4
4427.31	92.329	+1	4500	—6
4447.79	92.829	0		
4494.57	93.946	+1		

STELLAR WAVE-LENGTHS

For the stellar wave-lengths of B8-A0 types we have used the values given in the Transactions of I. A. U. IV, 188, 1932. The effect of blends is by no means negligible, partly in connection with the fact that many stars classified in the HDC as A0 are really of somewhat later type (A2,

A3). Although the dispersion used is about twice as small as that given in I. A. U, it seemed best to use the published values.

The measurements of our spectrograms brought out a peculiarity which called attention at once: namely the radial velocities of the lines to the red from 4315 appeared to be systematically different from those in the violet portion of the spectrum. To bring the former in agreement with the other part of the spectrum a considerable positive correction is afforded, especially for the lines 4471 and 4481. This shows that in the case of the short camera there is an urgent need to investigate the wave-lengths of individual

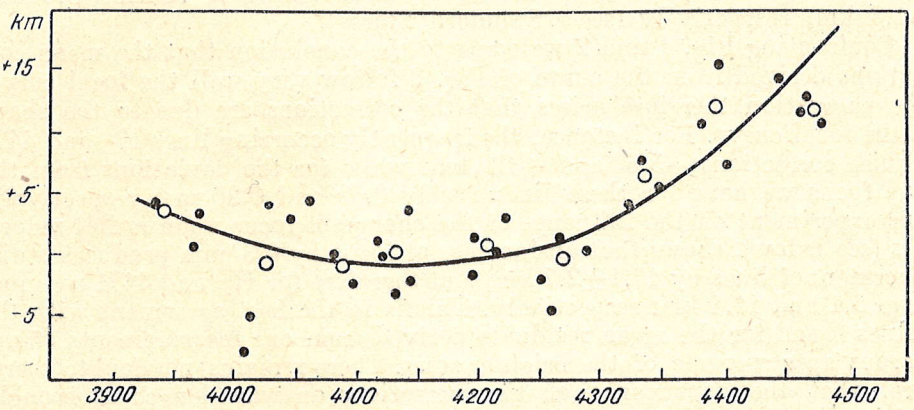

Fig. 2. The dots and the open circles are the residuals for the individual lines (velocity of the standard star minus velocity of a line).

lines. The deviations in question might be connected partly with the blends and especially with the peculiarity of the focal curve. The adopted procedure was the same as in the course of the investigation of the same question in our preceding work (2). Nearly for all good spectrograms of the brighter stars the deviations for the individual lines from the stars velocity have been computed. However the accuracy of measurements is low and only when the number of spectrograms is sufficiently high one can obtain a trustworthy systematic correction for individual lines. For seldom occurring lines the accuracy of the derived corrections is about ± 1.5 km.

The systematic residuals for the individual lines (velocity of the star minus velocity of the line in question) are plotted in Fig. 2. It is true, the dispersion is considerable, but we think that for many lines the residuals are real. Besides, there is manifested a dependence of the residuals upon the wave-length. It is evident that the measured velocity of the star requires in the mean a positive correction, especially if the radial velocity, as this occurs not seldom for A type stars, is based mainly on the lines H_γ and 4481.

In our preceding analogous investigation relating to the long camera we have found that the correction for many lines reaches several kilometers, sometimes 10 and more. Though we have now used the corrected wave-lengths, but because of the difference in dispersion many individual lines again need corrections. The last circumstance causing a dispersion of dots in Fig. 2 obscures the dependence of the residuals on wave-length. It is of importance to emphasize the last point. For this purpose in order to smooth the dispersion of dots on Fig. 2 (mostly due to real systematic corrections for individual lines) we combined the latter in groups, and plotted on the same Fig. 2 the corresponding mean values of the residuals (open circles). At last, apart from some exceptions (the maximum one is 4383, for which

the correction turns out to be —21 km), we may in general neglect the individual corrections for the lines as they are brought out in the dispersion of dots in Fig. 2 and use only the corrections depending on wave-lengths. Using the curve drawn in Fig. 2 a table of corrections was derived. Basing upon the latter, all the observational material was re-discussed anew. In so doing we obtained a considerable improvement with respect to the accidental as well as to the systematic error. Namely the preliminary values found for the mean arithmetical and algebraic residuals (M o o r e-Simeis) for 29 stars with well known velocities were 4.2 and +3.2 km, while after the corrections in question were added, these residuals became 3.6 and +1.3 km, respectively (see «Standard Stars»).

Confronting Fig. 1 and 2 we come to the conclusion that the mean corrections derived from the curve of Fig. 2 follow very well the focal curve. The suggestion therefore arises that the corrections are due to the shape of the focal curve. For instance, the frequently occurring lines H_γ and 4471 require corrections +5.5 and +12 km, while for the deviations from the true focus we have for these lines nearly 0.09 and 0.20 mm respectively. Our experiment on the influence of the change of focus upon radial velocities (see below), shows that an increase of focus by 0.3 mm produces a displacement of lines by 17.1±2.7 km, and therefore for H_γ and 4471 we must have 5.1 and 11.4 km. respectively. This is in the best agreement with the values found for the mean residuals derived from our measurements of numerous spectrograms of the brighter stars. There remains no doubt, therefore, that the dependence of the corrections on wave-length as brought out in Fig. 2 is a pure effect of the shape of the focal curve (Fig. 1). The effect in question is very considerable and the error in focus by 0.1 mm corresponds to an error in the radial velocities equal to about 6 km. If the focus is not frequently controlled or controlled not accurately enough, the above mentioned sensitivity of the measured radial velocities to the change of focus may produce a sensible systematic error and a general decrease of the accuracy of observations.

SYSTEMATIC ERROR

In the chapter on the systematic error in the preceding catalogue of 343 stars (3) serious attention was paid to the question of the effect of temperature, of the focus a. o. Especially it was suggested that the deviation from true focus influences the results. In addition, a seasonal change of the systematic error was suggested there. From two accordant sets of observations it was found there that the displacement of the focus near its normal setting from —0.2 to +0.4 mm makes the velocity more positive by +7.8±1.2 km. The suggestion was made that this is probably due to the uneven distribution of light within the spectral lines, mainly the iron emission ones of the comparison spectrum. This effect of focus setting was previously found for the long camera ($f = 560$), and therefore it must be expected to be still greater for the short camera of the same spectrograph ($f = 290$). In fact, the measurements of an analogous series of solar spectra taken with the short camera brought out a considerable positive displacement of the spectral lines with the increasing focus (the focus increases with decreasing temperature).

When reducing two sets of observations taken with the long and short camera to the same value of displacement of the focus we find:

Increase of focus	Change in the radial velocity	
	Camera 560	Camera 290
by 0.3 mm	+3.9±0.7	+17.1±2.7

TABLE I

Name	α_{1900}	δ_{1900}	Magn	Spectrum H. D.	Spectrum Rev.	R. V. Moore	R. V. Simeis′	M—S′	R. V. Simeis″	M—S″	R. V. Simeis°	M—S°	n
	h m	° ′											
γ Pegasi	0 8.1	+14 38	2.9	B2	B2ss	+ 5.0	— 0.6	+ 5.6	+ 0.5	+ 4.5	+ 5.2	—0.2	9
θ Andromedae	0 11.9	38 8	4.4	A2	A1n	+ 0.7	— 3.1	+ 3.8	— 1.1	+ 1.8	0.0	+0.7	8
Boss 526	2 13.2	28 11	5.3	A2	A3s	+ 3.8	— 3.6	+ 7.4	— 2.0	+ 5.8	+ 3.3	+0.5	2
68 Tauri	4 19.7	17 42	4.2	A2	A3s	+35.2	+34.8	+ 0.4	+36.4	— 1.2	+33.5	+1.7	3
11 Orionis	4 58.9	15 16	4.7	B9		+17.0	+ 9.2	+ 7.8	+12.2	+ 4.8	+12.4	+4.6	2
Boss 1226	5 3.8	9 42	5.4	A2	A7s	+38.8	+32.1	+ 6.7	+34.5	+ 4.3	+37.9	+0.9	13
β Orionis	5 9.7	— 8 19	0.3	B8p	cB8	+23.6	+18.0	+ 5.6	+20.4	+ 3.2	+21.9	+1.7	7
13 Monocerotis	6 27.5	+ 7 24	4.5	A0p		+11.6	+ 8.8	+ 2.8	+12.0	— 0.4	+12.8	—1.2	7
η Leonis	10 1.9	17 15	3.6	A0p	A2s	+ 2.2	— 3.4	+ 5.6	+ 1.9	+ 0.3	+ 2.8	—0.6	12
χ Leonis	10 59.9	7 53	4.7	F0	F5	+ 6.1	— 5.6	+11.7	— 4.9	+11.0	— 3.6	+9.7	8
θ Leonis	11 9.0	15 59	3.4	A0	A2s	+ 7.8	+ 4.1	+ 3.7	+ 6.6	+ 1.2	+ 8.2	—0.4	12
σ Bootis	14 30.3	30 11	4.5	F0	F0s	+ 0.2	— 5.2	+ 5.4	— 4.8	+ 5.0	— 2.5	+2.7	13
ε Serpentis	15 45.8	4 47	3.8	A2	A6s	— 9.9	—11.4	+ 1.5	—10.1	+ 0.2	—10.5	+0.6	20
ω Herculis	16 20.8	14 16	4.5	A0p	A2s	— 5.3	— 9.4	+ 4.1	— 9.0	+ 3.7	—10.2	+4.9	12
47 Herculis	16 45.5	7 25	5.5	A0		— 2.1	— 6.3	+ 4.2	— 6.0	+ 3.9	— 3.8	+1,7	6
59 Herculis	16 57.9	33 43	5.3	A2	A3s	—12.2	—13.8	+ 1.6	—13.4	+ 1.2	—12.4	+0.2	8
67 Ophiuchi	17 55.6	2 56	3.9	B5p	B8s	— 4.3	— 6.9	+ 2.6	— 3.5	— 0.8	— 4.6	+0.3	25
72 Ophiuchi	18 2.6	9 33	3.7	A3	A5s	—24.5	—24.8	+ 0.3	—23.5	— 1.0	—23.4	—1.1	10
102 Herculis	18 4.4	20 48	4.3	B3	B2sk	—13.3	—19.1	+ 5.8	—16.9	+ 3.6	—15.7	+2.4	29
101 Herculis	18 4.6	20 2	5.2	A3	A4s	—15.8	—18.7	+ 2.9	—17.6	+ 1.8	—17.1	+1.3	24
Boss 4702	18 29.0	30 29	5.4	B8	B9s	—12.2	—15.1	+ 2.9	—11.5	— 0.7	—11.9	—0.3	4
110 Herculis	18 41.4	20 27	4.3	F5	F4	+23.6	+30.0	— 6.4	+33.6	—10.0	+29.5	—5.9	6
Boss 4942	19 18.7	26 4	4.9	B5	B8s	—12.8	—14.6	+ 1.8	— 9.7	— 3.1	—10.0	—2.8	6
15 Vulpeculae	19 57.0	27 29	4.7	A5		—22.3	—16.9	— 5.4	—16.4	— 5.9	—13.7	—8.6	4
41 Cygni	20 25.3	30 2	4.1	F5p	F6	—18.8	—15.9	— 2.9	—13.9	— 4.9	—18.6	—0.2	8
H. D. 196724	20 34.1	20 51	4.8	A0	B9s	—17.1	—25.8	+ 8.7	—28.1	+11.0	—19.1	+2.0	7
δ Delphini	20 38.8	14 43	4.5	A5		+ 9.9	+ 5.5	+ 4.4	+ 6.6	+ 3.3	+11.3	—1.4	5
o Pegasi	22 37.0	28 48	4.9	A0	A2s	+ 6.6	+ 6.4	+ 0.2	+ 9.8	— 3.2	+ 8.6	—2.0	11
χ Piscium	23 21.8	0 42	4.9	A2p	A3p	— 3.3	— 2.2	— 1.1	— 0.2	— 3.1	— 2.4	—0.9	6

This shows, how carefully the focus must be controlled. It is probably necessary to control the focus every night by the modified H a r t m a n n's method when by mere inspection of a spectrogram the focus may be determined with accuracy of about 0.05 mm. Unfortunately no sufficient attention was paid to this point. In fact, the focus was controlled once or twice per two months, sometimes more often. However, no large variations in focus setting were found (mostly 13.05, the limits being 13.00—13.15). It is true, the focus was not controlled at the extreme temperatures. But it seemed to be probable that the focus underwent to uncontrolled slow

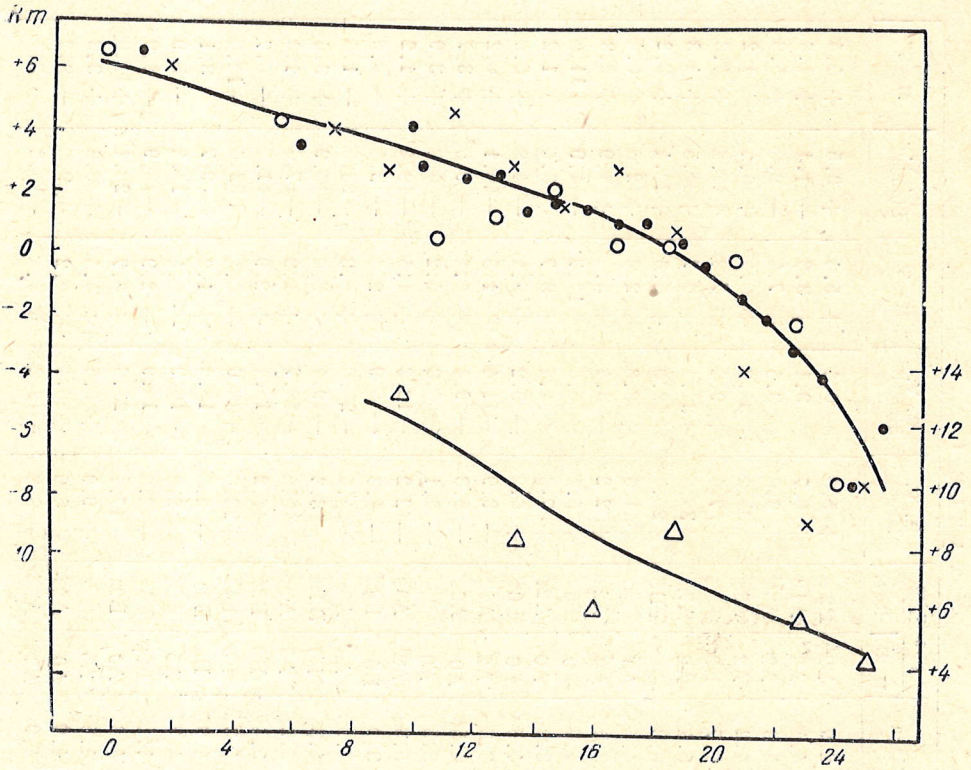

Fig. 3. The corrections to the radial velocities in dependence on the temperature. The circles, crosses and dots relate to the observations of 1932—33, 1934—37 and 1932—37 respectively. The lower curve relates to the second half of 1938.

changes. It was striking that the great deviations in the observed radial velocities occurred mostly in the coldest and warmest nights. This was especially brought out when searching for the seasonal systematic error as it was suggested in our preceding study (4).

Our observations of B8-A0 stars were rather unevenly distributed over a period of about six years (1932—1938). The majority of observations has been made in 1932—33. In 1934 the observations were less numerous, and in 1935—36 only sporadic. Some observations were made for control in 1937—38. Having in view the inevitability of a systematic error, especially in our case, we obtained also for control during the course of observations more than 300 spectrograms of 33 stars with well known velocities, in the mean about one spectrogram per observation night (Table 1). A detailed discussion of the measured radial velocities of all these stars leads to the following conclusions:

1) The period from May 1932 to the end of August 1933 may be considered as homogeneous with respect to the dependence of the systematic error on temperature. The results are represented in Fig. 3 (circles are the corrections to radial velocities corresponding to a temperature interval of 2°). A dependence of these corrections upon the temperature is clearly manifested, the total amplitude for the temperature interval from 0 to 25° reaching about 14.5 km.

2) To bring the observations of 1934 (March — July) in agreement with the preliminary reduction curve for 1932—33 the following constant corrections are to be previously added: March —2, April —1, May +1 and June — July +2 km.

3) In 1935—36 the observations are so few that the systematic error could not be controlled. However in March 1936 a large systematic error was manifested. Namely at this time one of the prisms of total inner reflection on the way of the light beam from the iron arc was readjusted and this caused a very uneven illumination of the collimator. Since the beginning of this unfortunate circumstance could not be fixed, we decided to reject all the spectrograms taken during March 1936. As to the few observations of 1937 a constant correction —1.3 km is needed to bring them in agreement with the preliminary reduction curve of 1932—33. The so reduced observations of 1934—37 (crosses) are plotted in Fig. 3.

4) Finally the observations of the second half of 1938 outstand too much to be considered together with those of the preceding years. The measured radial velocities are too negative (in the mean by 10 km). Adding this correction we find the reduction curve for the temperature effect in 1938 to be more or less similar to that for other years. However, notwithstanding the small number of observations of the brighter stars (at all 27 spectrograms) and the sensible dispersion (triangles) we preferred to use a separate reduction curve for the second half of 1938 (Fig. 3 below).

Considering the observations of 1932—1937 together we derived the final values for the corrections (the dots in Fig. 3). The latter also correspond to a temperature interval of 2°; however these intervals overlap one another, say 10—12°, 11—13°...

A peculiarity of the reduction curve must be noted, namely the rapid increase of the negative corrections for the higher temperatures. We have also an independent proof of the fact that at higher temperatures the change of corrections as brought out in Fig. 3 is really more rapid. Namely, when comparing the radial velocities of faint stars obtained at different temperatures we find the following values for Δv km per 1°:

28°.0—24.5	+0°.99 km	23°.5—16.5	+0.45 km
25 .5—21.5	+0.71	<18.5	+0.30

The reduction curve cannot be considered as a pure temperature curve since, as it was mentioned above, the change of focus was partly controlled (the majority of spectrograms were taken at the focus 13.05—13.10 and a small portion at 13.00 and 13.15). For this reason we have here but a smoothed curve partly of irregular character. We do not think that there exists a pure temperature reduction curve at all. For instance, at the same focus setting and nearly within the same range of temperatures as in the preceding years, the velocities of the brighter stars observed in the second half of 1938 turn out to be too negative, approximately by —10 km. This is partly confirmed when comparing 65 spectrograms of faint stars obtained in 1938 with those of the preceding years: the former became more negative in average by —6 km and if excluding few spectrograms even by —8 km.

The spectrogram rests in our plate-holder in such a manner that we cannot be sure that during a long period of time the position of the plate at the given focus setting is accurately the same. This may be the cause of the difference in the systematic error in different years.

Our observations have been taken in overwhelming majority within the temperature interval from 0 to 26°, and the corresponding corrections, as it is seen from Fig. 3, change nearly from +8.5 to —8.5. We have registered during the course of our observations a change of the focus setting from 13.00 to 13.15. Afterwards we have recognized that for the above temperature interval the focus changes within ±0.15 mm approximately. Confronting this with the corresponding change in the corrections for the radial velocities (15 km) we find that this third way also indicates that the focus or temperature effect is nearly of the same order as given by the two other independent methods considered above. It is true we have obtained here a somewhat smaller value for $\Delta v/\Delta t$, but this is in agreement with the fact that in the last case we are dealing with a smoother temperature or focus effect.

It is of importance to note that the account for the systematic error due to error in focus for the spectrogram as a whole as well as for the individual spectral lines considered in detail above and in the «Standard stars» (p. 51) reduces the mean arithmetical residual (M o o r e—Simeis) from 4.2 to 2.1 km and the mean systematic one from +3.2 to +0.3 km.

The question now arises on the cause of the effect in question. Certainly, the error in the radial velocities as caused by poor focus is trivial. This may be connected, for instance, with uneven illumination of the collimator objective. In our preceding paper (5) serious attention was called to this point, especially in connection with the astigmatism of the main mirror. Now we have tried to fix more precisely the cause in question. In order to judge on the effect of uneven illumination of the collimator we have obtained two series of spectrograms of the sky: A) the light of sky illuminates the whole objective and Fe only its upper half, B) the light of the sky illuminates the whole objective and Fe only its lower half. When measuring both series the micrometer reading for the Fe line 4337.05 was adjusted in both cases to 90.000. The results of immediate comparison are represented in Fig. 4. The dots (sky) and the crosses (Fe) give the difference of the mean micrometer readings (series A minus series B). The reality of Fig. 4 cannot be disputed. On the other hand, the same spectrograms have been reduced in the usual manner using our reduction table for the stars. The computed radial velocities for individual lines in the sky spectrum are plotted in Fig. 5 (the dots and the crosses relate to the series B and A respectively). We have measured eight good lines to the violet from Hγ. It is worth of attention that the radial velocities within this region may be expressed to some extent by a sine curve. Besides, it may be noted that the mean radial velocity for the series A is equal to +12.2 km while for B we have —11.5 km. Unfortunately the few lines in the solar spectrum to the red from Hγ are blends and overexposed on our plates, and we were not able to measure them for the investigation of the effect in question for this portion of the spectrum. In any case it is evident that the uneven illumination of the collimator highly influences the radial velocities. But in practice the deviations from uniformity in the illumination are probably but small, apart from some rare exceptional cases. We are not able to investigate the effect in question which occurs in reality, but beyond doubt it may reach several kilometers.

The peculiar character of Figures 4 and 5 is probably connected with the shape of the focal curve as well as with the uneven illumination of

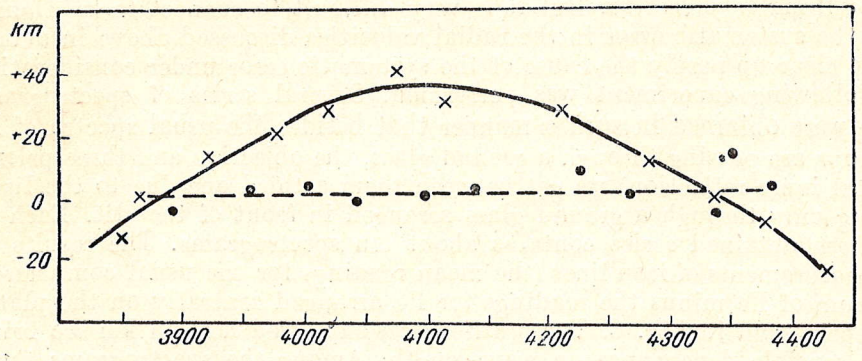

Fig. 4. The effect of the uneven illumination of the collimator. The dots (sky) and the crosses (Fe) give the differences of the micrometer readings (series A minus series B).

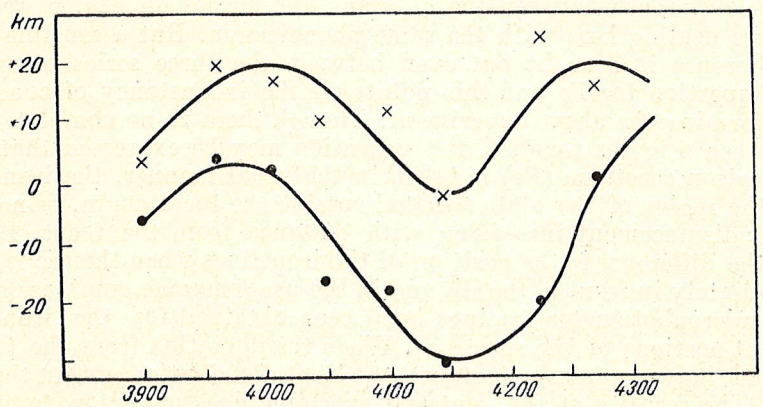

Fig. 5. The radial velocities of individual lines of the sky spectrum (the crosses and the dots relate respectively to the cases when Fe illuminates only the upper and lower half of the collimator objective).

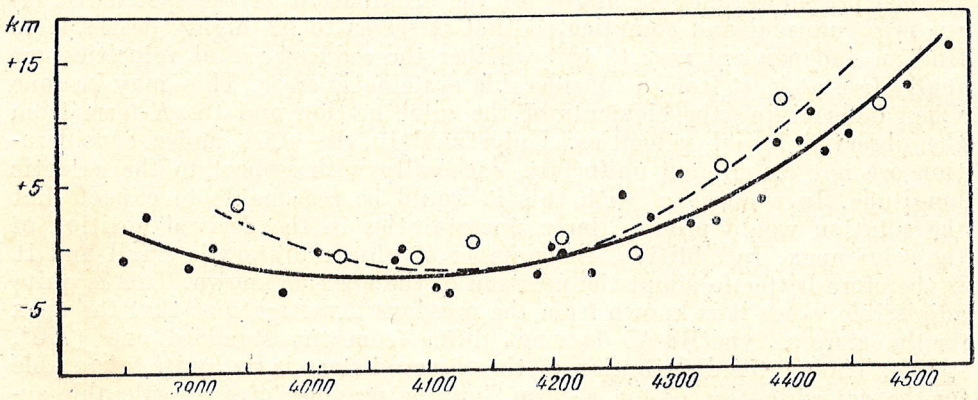

Fig. 6. The dots are the mean readings for the usual comparison spectrum of Fe minus the readings for Fe arranged centrally. The open circles are the residuals for the groups of stellar lines.

the collimator objective. But it is very difficult to connect these figures with the systematic error in the radial velocities discussed above in detail.

To clear up partly the cause of the systematic error under consideration the following experiment was performed. Several series of spectrograms of Fe were obtained in such a manner that besides the usual spectra of Fe (the rays are passing through a ground glass, the objective and three prisms of total inner reflection) we get between them a third one due to the light passing only through a ground glass arranged in front of the slit. Each of the three obtained series contains about ten spectrograms. The results of the measurements of iron lines (the mean readings for the usual comparison spectrum of Fe minus the readings for Fe arranged centrally on the plate) are represented in Fig. 6. These differences expressed here in km/sec bring out a sensible dependence on wave-length. Among the spectrograms there are normally exposed and overexposed ones, but one could discern no evident difference in the effect under consideration. The same experiment was performed still earlier by V. A. Albitzky (his paper is now in press).

A close similarity of Figures 6 and 1 is to be emphasized. In spite of the systematic difference between the dots and the circles on Fig. 6 we think that we are dealing here with the same phenomenon. But a sensible systematic difference is brought out even between the three series of spectrograms in question for Fe and this points on the inconstancy of conditions when performing the above experiment. Though there is no complete agreement between Figures 6 and 1, the suggestion may be expressed that when the comparison spectrum (Fe) is taken in the usual manner, the iron lines, lying in the region of the plate situated outside the focal curve, bring out a systematic displacement increasing with distance from the focus. But the cause of the difference in the position of the iron lines when the arc is arranged immediately in front of the slit and in the usual manner remains obscure.

Some microphotometer tracings have been obtained for the iron lines in different portions of the spectrum. When the deviation from the focus is sensible one may see an asymmetry in the light distribution within the spectral line. The scarcity of the material available does not allow to connect this asymmetry with the systematic error in the observed radial velocities.

The above experiments throw much light on the phenomenon under consideration. However, we are not able at present to fix a more intrinsic cause. One may conclude only that the systematic error in the radial velocities is, beyond doubt, due to the deviation from the true focus.

The procedure adopted above for the elimination of the systematic error is so unusual and complicated that it seems to be highly desirable to find an independent way to test whether the reduced radial velocities are really free at least from a considerable systematic error. This may be done when determining the elements of the solar motion and the K-term from the observed radial velocities. Unfortunately the stars under consideration are not distributed uniformly, especially with respect to the galactic longitude. In connection with this it would be reasonable to expect that the solution would produce large uncertainties in the derived position of the solar apex. In addition, the number of observed stars is small and it is therefore better to adopt the position of the apex as known. This is quite admissible since it is known from the previous investigations that the apex for the stars of type B8-A5 does not differ from the standard one (270°, +30°). Though the distribution of the observed stars is not quite favourable for the determination of the K-term, but the presence of a considerable systematic error will be brought out in the usual solution as a spurious K-term.

All the stars have been divided in 22 groups, each of which included a more or less equal number of stars. But the areas are unequal: in the summer

hours we have usually $0^h.5$ and in the winter ones 1—3 hours. The least squares solution of equations $V_\odot$ Cos $D+K=V$ gave $V_\odot = 15.2$ km/sec $\pm$ 0.44 (m. s. e) and $K = -0.6$ km/sec $\pm$ 0.30 (m. s. e.).

As it is well known the brighter stars of the type B8-A5 do not manifest the presense of the K-term, and for this reason the obtained small value for K may be interpreted as an indication of our radial velocities being free at least from any appreciable systematic error. This proof is of purely kinematic character. It is worthy of attention that the obtained va-velocity of the sun $V_\odot = 15.0$ km/sec is much smaller than the standard value 20.0. However, it is known that also the brighter stars of this class give a smaller velocity *.

STANDARD STARS

The list of 29 brighter stars mostly of type B8-A3 which serve as standard ones in the present work is given in Table 1. The derived velocities for them are based on more than 300 spectrograms. This large observational material was discussed to derive the systematic deviations for individual spectral lines selected for the measurements of radial velocities, and, on the other hand, to control the systematic error as a whole. In the sixth column are given the R. V. from Moore's General Catalogue.

The results of our immediate measurements without any correction and the differences M—S′ are given in the seventh and eighth column. The mean algebraic M—S′ amounts to +3.2 km, while the mean arithmetical of residuals M—S′ is 4.2 km. It was shown (p. 48) that the individual spectral lines are affected by a systematic error depending on wave-lengths. Using the new corrected system of wave-lengths (Fig. 2.) we obtained the columns 9(S″) and 10 (M — S″). The systematic error now turns out to be only +1.3 km, while the mean arithmetical is 3.6 km. Though the mean algebraic M— S″ = +1.3 is not large, the residuals for individual stars are rather great.

After reduction to the new corrected system of wave-lengths the radial velocities were again discussed from the standpoint of the influence of the systematic error considered in detail on p. 44. In such way have been obtained the final values of the radial velocities S^0, which are given together with the differences M —S^0 in columns 11 and 12. The algebraic mean of the residuals M — S^0 equal to +0.3 km/sec may be considered as the remaining systematic error of our list since the radial velocities of all program stars were reduced in the same manner. But the reality of this small value remains still doubtful. After accounting for the systematic errors the mean arithmetical of residuals M—S^0 has been also sensibly diminished and became equal to $\pm$2.1 km.

The probable error for a spectrogram of a program star is $\pm$6.2 km/sec. Having in view the low dispersion used and the spectral class of the stars (mostly B8-A0) this does not seem to be surprising. The probable error of a star is about $\pm$2.5 km/sec.

We have only very few faint stars in common with other catalogues published after our observations and reductions were completed. For 10 stars in common (see notes in Table II) with «The radial velocities of 500 stars» (6) the mean deviation is $\pm$4.7 km (if excluding H. D. 133330, $\pm$3.9 km). The systematic difference in the last case is only +0.2 km. If we admit the accuracy of Simeis and Toronto observations to be equal (the

* Strömberg, Aph. J. **57**, 79, 1923, $V_\odot$=12.8. Wilson, A. J. **36**, 138, 1926. $V_\odot$=16.4. Campbell and Moore, L. O. Bull. **16**, 1928, $_\odot$=18.6. Lindblad, M. N. **99**, 503, 1930, $V_\odot$=16.6. Nordström, Lund Medd, N 79, $V_\odot$=16.1.

TABLE II

H. D.	α_{1900}	δ_{1900}	vsim	Spectrum H. D.	Spectrum Rev.	R. V.	p. s. e	n	Notes
	h m	° ′							
4902	0 46.0	+40 43	7.22	A0	B9n	+ 4.2	±3.5	7	
5032	47.2	56 41	7.09	B9	B9n	— 9.3	3.3	7	
5083	47.6	49 7	7.17	B8	B8n	+ 6.0	1.5	8	
5397	50.7	34 41	6.80	A0	A2n	+ 7.0	3.0	8	
5638	53.0	46 31	6.75	A0	B5s	—12.9			1
5764	54.2	47 29	7.00	B8	B5s	— 9.8	2.5	5	
5854	55.0	37 15	7.00	A0	A3s	+ 7.2	2.3	6	
8317	1 17.4	44 48	7.27	B9	A1s	+ 4.2	2.5	5	
8452	18.6	36 22	7.08	B9	A2n	+14.1	1.7	7	
8908	22.7	36 34	7.26	B9	B8s	—21.5	1.0	6	
9223	25.7	38 15	7.15	B8	B8n	+10.7	3.1	7	
18439	2 52.8	54 48	7.10	A0	A3s	— 4.3	2.6	6	
18881	57.1	38 1	7.01	A0	A0n	+14.3	1.4	7	
18950	57.8	37 43	6.91	B9	B9s	— 4.9	1.7	8	
21062	3 18.8	28 18	6.99	A0	A3s	+ 4.0	1.9	5	2
21590	24.0	16 25	7.02	A0p	A0s	+ 3.2	1.4	6	
24434	48.1	21 38	7.07	B8	B3s	+13.8	2.5	5	
24899	52.4	23 48	7.07	B9	A0s	+ 7.8	5.4	5	
27770	4 17.9	34 5	6.95	B9	B9n	+10.6	1.5	7	
β Ori (comp)	5 9.7	— 8 19	6.6	B5	—	+16.9	1.5	11	
50634	6 49.0	+21 41	6.81	B9	A0	— 3.8	2.8	5	
59430	7 24.8	20 44	7.06	A0	A3s	— 2.9	2.7	7	
71262	8 21.3	7 58	6.78	A0	A1n	+15.5	1.3	6	
95190	10 54.4	10 28	7.04	A2	A5s	— 3.8	0.8	7	
95651	57.3	9 43	7.08	A0	A3n	— 8.5	1.8	7	
98547	11 15.2	17 52	6.87	A0	A3n	—12.1	2.1	5	
103152	47.6	16 00	6.73	A2	A5s	— 9.8	1.3	6	
106999	12 13.2	27 52	7.40	A2	A5s	— 9.7	2.0	4	3
107276	14.9	29 1	6.53	A2	—	0.0	0.1	4	4
107513	16.4	25 34	7.10	A3	F0s	— 1.2	1.3	6	5
107935	19.1	26 23	6.65	A3	A5n	— 0.4	0.8	7	6
108486	22.7	26 27	6.57	A3	A3s	— 0.4	1.4	7	7
108561	23.2	4 57	6.76	A0	A0s	+16.3	4.2	6	
108651	23.8	26 27	6.69	A3	A5s	+ 2.5	1.8	5	8
110326	36.2	30 59	6.88	A2	A2s	— 8.6	0.6		9
113365	58.1	23 10	6.87	A0	A0n	—11.6	0.6	5	
115983	13 15.6	5 22	6.90	A3	A3n	—19.2	1.0	5	
116542	19,2	1 55	7.08	A2	A5s	—16.2	1.3	6	
121109	48.4	13 15	7.12	A3	A3s	—17.6	1.1	5	
121626	51.5	29 10	7.11	A0	A2	—10.0	1.8	5	10
121907	53.3	16 54	7.26	A0	A3s	+23,0	1.4	6	
125798	14 16.7	36 51	7.18	A0	A3s	— 4.7	0.3	4	
127043	24.1	28 44	7.45	A0	A0	—20.7	2.1	6	
127067	24.2	28 44	6.95	A0	A0s	—12.0	1.8	9	
130767	44.9	19 56	6.89	B9	B9	—13.8	3.0	6	
131265	47.5	20 43	6.88	A0	A2s	— 1.7	0.4	5	
133330	58.8	28 40	6.90	A0	A3	+ 1.8	5.6	6	11
136754	15 17.3	24 42	7.16	A0	A0s	—15.4	1.5	5	
137182	19.5	10 54	7.19	A0	A2	—19.3	2.0	7	
142742	51.1	34 40	6.95	A2	A3s	—10.8	1.3	10	
142864	51.8	— 6 1	7.01	A0	A3n	—24.8	1.3	6	
142930	52.2	+ 3 41	7.01	A0	A2	—13.8	2.4	8	
143992	58.4	22 30	6.94	A2	A3s	—35.0	1.4	7	
144271	59.9	— 3 15	6.88	A0	A2s	—29.0	2.3	7	
150781	16 38.1	+21 46	7.06	A0	A0s	—24.0	2.9	6	
152155	46.6	15 58	7.24	A0	A2s	—22.6	4.4	7	
152210	46.9	— 2 38	6.96	A0	A3	+ 1.5	3.6	6	
153809	56.5	+16 45	7.24	A0	A1s	— 0.2	1.7	5	
154015	57.8	9 58	6.94	A2	A5s	—10.0	2.3	8	
156987	17 15.5	28 7	7.02	A0	A1s	—10.8	3.0	5	
157151	16.5	21 39	6.95	B9	A0s	— 7.9	2.4	9	
157255	17.1	32 47	6.83	A0	A2s	—28.1	4.1	8	12

TABLE II (*Continued*)

H. D.	α_{1900}	δ_{1900}	m_{vis}	Spectrum H. D.	Spectrum Rev.	R. V.	p. s. e	n	Notes
	h m	° ′							
157297	17 17.3	+ 11 47	7.08	A0	A2	+ 9.5	±4.0	6	
157495	18.5	9 34	7.07	A2	A3s	— 4.6	1.8	5	
158263	23.2	11 31	6.83	A	A5s	—26.6	2.1	5	
162428	45.9	24 29	7.01	A0	—	—14.2	3.5	6	
162651	47.0	1 8	7.13	A0	A0	—29.0	3.4	7	
162936	48.5	32 2	7.04	A0	A2	—26.3	3.2	8	13
163590	51.8	32 28	7.20	A0	A2n	—10.2	2.3	5	14
163973	53.8	14 32	7.29	A0	A2	— 0.2	3.3	6	
164212	55.0	43 26	6.88	B9	B9	—34.0	3.8	6	
164967	58.6	8 25	6.98	A0	A0s	—12.3	3.4	6	
168852	18 16.8	20 53	7.38	B9	A0s	—19.1	2.3	7	
169169	18.3	14 57	7.34	A2	A5	—10.0	3.1	7	15
169491	19.8	15 36	7.40	B9	B5n	—22.0	2.4	5	16
169617	20.4	38 18	6.83	A0	A1s	—13.2	1.3	5	
169952	22.0	38 23	7.12	A0p	A0n	— 9.1	1.9	8	
170314	23.6	24 37	6.82	B9	A0n	—26.1	4.4	8	17
170699	25.7	4 27	6.80	A2	A3n	—38.9	2.0	8	
174485	45.6	11 24	7.06	A0	A2n	—35.7	4.6	6	
175334	49.8	13 16	7.01	B9	B9n	—16.9	3.9	8	
175427	50.2	20 29	6.83	A0	A0n	—19.5	2.3	6	
175428	50.2	15 13	7.02	B9	B8n	—14.2	3.1	6	
175579	50.9	13 5	6.88	A0	A0n	—19.3	3.6	6	
175785	51.9	30 11	7.31	A0	A0	—23.0	4.4	5	18
176803	56.9	20 1	7.25	B8	B8	—16.7	3.4	9	
182010	19 17.6	17 34	6.84	A0	B5n	—37.7	2.9	10	
182616	20.4	30 51	7.20	B8	B5s	—15.6	2.3	7	
182991	22.3	11 52	6.85	A0	A0	+ 2.3	2.0	6	
183363	24.1	36 19	7.23	A0	A0	—11.1	3.7	8	
183363	24.1	36 19	7.23	A0	A0	—12.8	4.5	6	
183728	25.8	16 30	7.05	A0	A2s	—18.6	3.8	9	
187731	46.4	16 37	7.01	B8	B8n	—19.3	4.0	11	
188383	49.8	26 20	6.81	A0	A3s	— 5.8	3.4	6	
189474	55.1	35 13	6.78	A0	A1s	+ 4.6	1.5	7	
189598	55.7	12 49	7.7	F2	A5s	—45.8	1.0	4	
189689	56.2	32 31	7.21	B9	B8	+ 0.8	2.2	6	
189692	56.2	13 6	7.10	A0	B9n	— 4.5	2.6	7	
189756	56.5	14 16	7.03	A0	A2	+ 4.7	1.3	6	
190167	58.6	28 14	6.79	B9	A0s	—12.1	4.0	7	
194495	20 20.8	21 10	7.09	B9	B7	+ 7.5			19
194885	23.0	39 10	7.16	A0	A0	—16.0	1.5	6	
195053	23.9	19 47	6.82	A0	A2n	—33.7	3.5	6	
195340	25.6	19 20	6.71	B8	B5s	— 7.2	0.1	11	
195341	25.6	19 6	6.99	B9	B8n	— 8.7	4.1	6	
195358	25.7	19 5	6.59	B9	B9s	— 2.4	0.7	6	20
195612	27.3	16 39	7.12	B9	B9	— 7.6	2.3	6	
197245	37.4	23 49	6.79	A0	B9s	+ 6.7	2.9	7	
198436	45.3	39 25	7.32	A0	A0n	—21.1	2.2	6	
198527	45.8	27 0	7.04	B9	B9	— 6.9	2.4	7	
199234	50.8	36 42	7.24	A0	B9n	—26.0	2.4	7	
199837	54.6	31 15	7.17	B9	B9	—13.5	2.1	7	
205201	21 28.6	32 20	7.17	B9	B9n	— 2.0	3.0	6	
209260	56.9	38 47	7.08	A0	A0s	—14.8	2.0	6	
209469	58.6	42 20	7.06	B9	B9	—13.5	4.2	7	21
209484	58.7	29 44	7.01	B9	B9s	— 9.3	1.8	5	22
209636	59.8	54 24	6.98	B9	B9	—11.7	2.9	6	
212734	22 21.4	25 24	7.11	A0	A2n	— 4.5	2.4	6	
213871	29.4	46 3	7.22	A0	A0	—10.0	3.3	5	
216308	46.8	14 34	6.89	A0	A3n	—10.5	2.7	6	
216321	46.9	48 12	6.88	B9	B8n	—16.3	4.7	6	
216369	47.3	40 47	6.84	A0	B9	—18.1	2.5	10	
220501	23 19.1	29 8	7.02	A0	B8s	+ 1.5	3.2	7	

TABLE II (*Coutinued*)

H. D.	α_{1900}	δ_{1900}	m_{vis}	Spectrum H. D.	Spectrum Rev.	R. V.	p. s. e	n	Notes
	h m	° ′							
220582	23 19.8	+ 24 57	7.21	B9	B8n	+ 4.7	±1.6	7	
220750	21.2	38 48	6.78	A0	A0n	— 4.4	2.0	7	
221237	25.2	58 1	7.06	A0	B9	— 3.5	1.4	5	23
224155	50.5	7 40	6.74	A0	A0	— 1.8	1.7	6	
224166	50.6	45 48	6.84	A0	B9	—17.2	1.4	5	24
224235	51.1	32 55	6.96	B9	B9	+12.6	2.0	8	
225001	57.4	15 43	7.19	A0	A2s	—11.0	1.5	6	
225023	57.6	35 16	7.32	A0	A2	— 2.5	2.1	8	

N o t e s

1	5638	Sp. Bin.	K = 64.3	P = 10.418
2	21062	D.D.O.1 N°3	+ 6.4 ± 1.6	
3	106999	L0B N°494	— 6.7 ± 1.5	
4	107276	» »	— 1.3 ± 1.4	
5	107513	» »	+ 0.4 ± 1.5	
6	107935	» »	— 0.8 ± 1.5	
7	108486	» »	— 0.6 ± 1.5	
8	108651	» »	— 0.4 ± 1.5	
9	110326	Sp. Bin	K = 40.7	P = 2.7045
10	121626	D.D.O. 1 N°3	— 8.8 ± 3.6	
11	133330	» »	+ 15.4 ± 6.1	
12	157255	Suggested Sp. Bin. Range about 50 km.		
13	162936	D.D.O.1 N°3	— 16.9 ± 1.6	
14	163590	» »	— 17.1 ± 2.5	
15	169169	» »	— 15.8 ± 5.4	
16	169491	» »	— 15.8 ± 1.3	
17	170314	Possibly Sp. Bin. Range about 50 km.		
18	175785	D.D.O.1 N°3	— 25.8 ± 5.4	
19	194495	Sp. Bin.	K = 82.2	P = 4.9052
20	195358	Probably c—star, Fe II 4233 is sufficiently strong		
21	209469	D.D.O.1 N°3	— 12.7 var. ?	
22	209484	» »	— 2.0 var. ?	
23	221237	» »	— 5.0 ± 3.6	
24	224166	» »	— 20.8 ± 1.8	

dispersions used are nearly the same), the probable error of the radial velocities may be computed independently by the formula

$$r'_0 = \frac{\pm 0.67}{\sqrt{2}} \sqrt{\frac{\Sigma \Delta^2}{n-1}}$$

where Δ is the difference Toronto-Simeis. This gives ±3.0 km or ±2.4 if excluding H. D. 133330. This is in good agreement with the error mentioned above.

We have also in our catalogue a number of stars belonging to the Coma Berenices cluster. These stars were partly observed with the long camera and their radial velocities were already published by us several years ago (7). Now we can compare them with Trumpler's radial velocities (8) (published simultaneously with my paper). The agreement seems to be very good. The mean residual for 6 stars in common is only ±1.6 km and the mean systematic difference Lick-Simeis is —1.1 km. However it is to be emphasized that the accuracy for these stars can by no means be considered as typical of the radial velocities of our list.

The results of observations of the program stars are given in Table II, in which the headings of various columns are self-explanatory. The pro-

bable error of the mean velocity is computed by the formula

$$\text{p. e.} = 0.845 \frac{\Sigma v \sqrt{p}}{\sqrt{\Sigma p}}$$

In our list are indicated only few spectroscopic binaries. At the small dispersion used the detection of binary character of the stars with range less than 30—40 km is mostly uncertain. We preferred to consider them as stars with constant velocity. But doubtless several of them are spectroscopic binaries. The observations have been carried out in overwhelming majority by the author (95 per cent), but the measurements have been made by Mrs. P. Shajn and M. Glushenko.

All the spectrograms of the stars of the list under consideration were lost during the war, and thus any additional measurements for control are rendered impossible.

REFERENCES

1. V. A. Albitzky and G. A. Shajn. Publ. Pulk. Observ. XLIII, 1933
2. L., c., p. 13—19
3. L., c., p. 22—27
4. L. c., p. 26
5. L. c., p. 22—23
6. Publ. D. Dunlap. Observ. Toronto 1, № 3, 1939
7. Bull. Pulk. Observ. XVI, 2, № 131, 1939
8. Lick Observ. Bull. № 494, 1938

РАДИАЛЬНЫЕ СКОРОСТИ 131 ЗВЕЗДЫ СЛАБЕЕ 6.75

Г. ШАЙН

В настоящей работе даны результаты наблюдений 131 звезды слабее 6.75. Тщательное исследование системы длин волн выявило зависимость поправок к радиальным скоростям для индивидуальных спектральных линий от длины волны, — эффект, тесно связанный с формой фокальной кривой короткой камеры, которой мы пользовались.

Наиболее характерной особенностью наших наблюдений является наличие серьезной систематической ошибки сезонного температурного характера, происходящей от малейшего отклонения пластинки от истинного фокуса. Учет выявленной систематической ошибки позволил снизить в конце концов предварительное значение среднеарифметического и среднегеометрического для разности Мур-Симеиз от ± 4.2 и 3.2 для 29 стандартных звезд до ± 2.1 и $+0.3$ соответственно. Удовлетворительный учет доказывается тем, что вычисленное значение члена K оказалось очень малым. Именно, скорость солнечного движения и значение члена K, выведенные из нашего небольшого наблюдательного материала, оказались равными

$$V_\odot = 15.2 \pm 0.5 \text{ км/сек} \quad K = -0.6 \pm 0.3 \text{ км/сек}$$

Вероятная ошибка спектрограммы и звезды равна соответственно ± 6.2 и ± 2.5 км/сек. Вероятная ошибка, полученная из сравнения небольшого числа общих звезд, наблюденных в Симеизе и на обсерватории Давид Данлап в Канаде, оказалась равной около ± 3.0

Среди наблюденных нами звезд найдены 3 несомненные и две подозреваемые новые спектрально-двойные звезды.

THE SPECTRUM OF γ CASSIOPEIAE IN 1940 AND 1941

V. HASE

The paper contains the description of spectral changes in 1940 and 1941. There are two periods Sept. 7-10 and Oct. 6-Nov. 20 1940 when the sharp absorption cores of H are weakened till almost complete disappearance and the spectrum is dominated by the broad lines of the reversing layer. Between these periods the shell lines appear again.

Besides H and He there are measured in the spectrum 171 faint lines. A number of them are surely identified with Ar II.

The radial velocity curve for the metastable helium lines is strongly shifted to greater negative velocities relatively to the curve corresponding to the diffuse series lines and the H curve, showing that the S-P lines originate in a higher and more rapidly moving layer of the shell than the H lines.

γ Cassiopeiae was under systematic observation at the Simeis Observatory from August 1940 to September 1941 when the work was interrupted by the war. During this period the spectrum underwent to quite uncommon variations hitherto unobserved in this star and suggestive of partial dissipation and new formation of the outer shell before its disappearance in 1941. From September 7 to Sept. 10 and from Oct. 6 to Nov. 20 the hydrogen cores characteristic of the shell spectrum became weakened till almost complete disappearance and the lines looked wide and diffuse. In the intervals between these periods of diffuse lines the spectrum returned to its usual shell type. Such phenomenon being on our knowledge never observed in γ Cassiopeiae, we found it useful to give a detailed description of the spectral changes of the star.

THE 1940 SPECTRUM

The observations of 1940 cover the period from Aug. 5 to Nov. 20. The spectrograms were secured with the single prism spectrograph attached to the 40 inch reflector giving a dispersion of about 36 A at Hγ. The emulsions used are: Eastman Process, Imperial 1200, Eastman 2F, Ilford Hypersensitive Panchromatic and Astra III. The total number of spectrograms is 77; generally 4—6 spectrograms during one night were taken.

The 1940 spectrum shows prominent lines of H and He, those of other elements being faint and difficult for measurement. The Balmer lines seen as far as H_{13} are of composite structure resulting from the superposition of the sharp and strong shell spectrum on the broad and diffuse lines of the

reversing layer. With the exception of H_α consisting of a strong and broad emission line, all Balmer lines show as their most outstanding feature a deep and sharp absorption core flanked by faint and generally narrow emission lines, the violet component being stronger and sharper than the red one; the emission lines are followed by faint and narrow absorption lines which look as separate components when seen with a magnification of 15-20 times, but which prove to be only dips on the shallow absorption wings, too weak to be detected by the eye and revealed only on microphotometer tracings. Moreover there are spectrograms on which second still fainter absorption components can be suspected. Generally the violet absorption component is stronger than the red one.

Helium is represented by the series: $2^3P - n^3D$ (3819, 4026, 4471, 5876), $2^3P^0 - n^3S$ (3867, 4121), $2^3S - 3^3P^0$ (3889), $2^1S - n^1P^0$ (3965, 5016), $2^1P^0 - n^1D$ (4009, 4144, 4388, 4922). The diffuse triplet lines differ in character: 3819 appears broad and diffuse, 4026 is narrow and sharp with wide wings, 4471 is sharp and strong sometimes equal to or slightly less intense than H_γ and 5876 is sharp, strong and narrow with faint emission components detected not always and traces of an absorption component. The $2^3P^0 - n^3S$ and $2^1P^0 - n^1D$ lines are always faint and diffuse and seen not everywhere.

The metastable line 3889 blended with H_ζ is the most prominent line in the whole spectrum and looks sharp and strong; structural details similar to those of the H lines and apparently relating to H_ζ are faint, the absorption components being weak and narrow and the emission lines observable not everywhere. The metastable singlet lines 3965 and 5016 are sharp and of moderate intensity; 3965 seems to be sometimes accompanied by faint violet emission.

Such was the general character of the hydrogen and helium lines on the spectrograms taken on Aug. 5, 20, 23, 26, 29 and Sept. 4 although the diffuse triplet lines were slightly varying in shape and intensity.

But on the next observation night, Sept. 7, the spectrum appeared quite different. The Balmer lines H_γ-H_{13} became diffuse and the structural details less distinctly seen as before; the central absorption cores looked much fainter as well as the emission lines, and the absorption components were broader than before. The H_β absorption is strong and seems to be less affected by the general change of the spectrum. H_α remains strong in emission.

The He lines behave in a different manner: while the diffuse series lines are broadened, the metastable ones — 3889 and 5016 remain sharp and strong; 3965 is faintened, but as sharp as before.

On the next observation night — Sept.10 the change in question is progressing, the H lines appearing still more diffuse and the broad underlying absorption becoming still shallower. H_γ is much more diffuse than on Sept. 7. The emission components are very faint, the violet one — broad and the red somewhat narrower. H_β is strikingly different from the previous days; for the first time it looks like a strong double emission line, while the central absorption dividing both components is hardly seen. The H_α emission is very strong.

The He lines behave nearly as on Sept. 7, only 4026 and 4471 appear more diffuse. 5876 is much fainter than previously and has two rather doubtful emission components. The metastable line 5016, strong on Sept. 7, is faint, as well as 3965, and only 3889 remains apparently unaltered.

On Sept. 13 the spectrum again returns to the stage of narrow lines. The central absorption cores of the hydrogen lines become sharp and narrow and much stronger than they were during the diffuse lines stage. The violet

emission lines are rather broad, the red ones very narrow. As before, the violet emission lines are stronger than the red ones. The lines of He: 3819, 4026 and 4471 are narrow, 4026 has faint wings and 4471 is nearly as strong as H_γ. 3965 and 3889 are sharp and strong.

Contours of H_δ and H_γ for Sept. 4, 7, 10 and 13 are given on Fig. 1. The intensity is expressed in units of the continuous background. The inspection

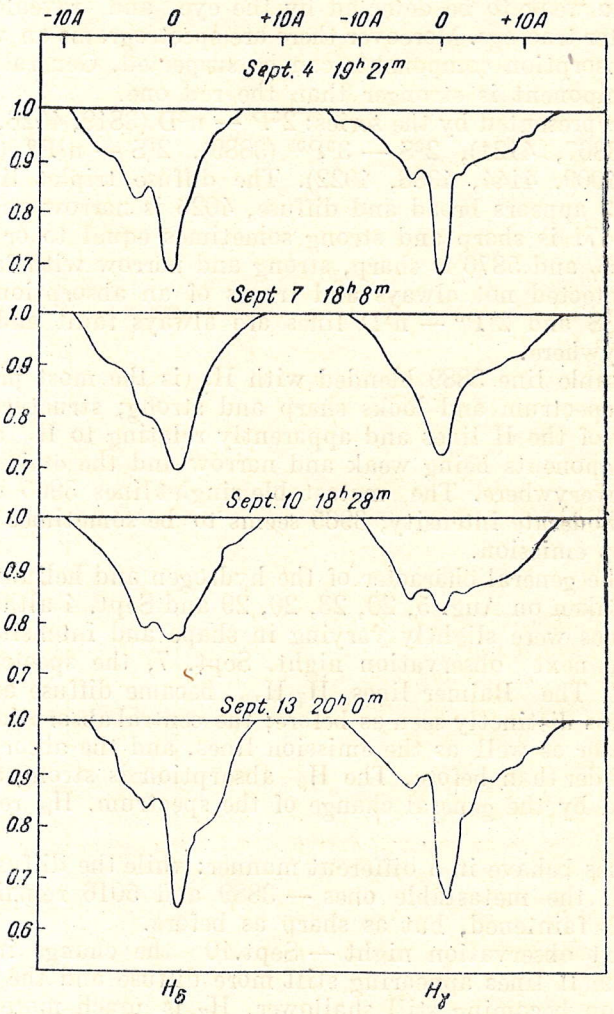

Fig. 1. Contours of H_δ and H_γ

of these contours makes the impression of the shell becoming more transparent on Sept. 7 and 10 and allowing a deeper insight into the spectrum of the reversing layer.

The main variations in the following days are the further narrowing and strengthening of the hydrogen cores on Sept. 15 and, beginning with Sept. 21, the general weakening of the emission lines at H_γ — H_{13}, which appear in reverse relation of strength, the red component becoming now the brighter. The absorption components are weak and somewhat diffuse, the violet ones being broader. H_δ has two violet absorption components. The emission H_α remains strong as before and H_β looks different almost

on every plate. Although this phenomenon is seen also on previous dates one cannot affirm its reality, as H_β lies in the region of lowered sensitivity of the plates.

From Oct. 6 begins a new stage of diffuse lines, which lasts till Nov. 20, when the lines again become sharp.

Oct. 6. The Balmer lines, except H_γ are diffuse, the higher members above H_9 cannot be measured at all. H_ε and H_δ are broad and diffuse, the absorption components looking like wings. The emission lines are vanishingly faint. H_γ is less diffuse, and faint emission components can be measured, the red one being the brighter. The diffuse series helium lines are fainter and worse defined than before. 3965 is much faintened but not diffuse, and only 3889 appears as sharp as before.

Oct. 12. All lines are still more faint and diffuse except 3889. The cores of the Balmer limes are hardly more intense, than the absorption components. H_γ has two emission components, the red one being the stronger. H_β is badly seen. The helium lines, except 3889, are faint and diffuse, 3965 is barely recognizable.

Oct. 15. The Balmer lines are also diffuse as on Oct. 12, but the central cores are somewhat stronger and the structure rather better defined than on Oct. 6. The core of H_γ is well defined, two emission components are seen, the violet one being the stronger, H_β looks so faint that the measurements are absolutely uncertain. H_α is notably weakened. 3964 is sharp and well defined, 3889 — strong and sharp, 3819 — diffuse, 4026 — narrow, sharp, with wings, 4471 — rather sharp, but somewhat broader than usually.

Oct. 21. The H lines are still more diffuse. The central cores of H_ε and H_δ are not seen. H_γ makes the impression of three absorption lines divided by doubtful emission. H_β shows one distinct broad emission line and a faint absorption. H_α is brighter than on Oct. 15. The helium lines are faint and diffuse, 3889 is somewhat faintened.

Nov. 14. All lines are faint and diffuse. H_δ and H_γ appear as double absorption lines of a new structure: a faint violet emission, followed by a narrow and rather sharp absorption core, flanked by very faint red emission. Then follows a second absorption line somewhat fainter than the first one and worse defined. Its red emission component is stronger than the violet one. H_β looks quite different on three plates. H_α is much fainter than during August and September. 3889 is fainter, but sharp and well defined as always. 3965 is vanishing and the $2^3P^0 - n^3D$ lines are faint and diffuse.

Nov. 20. All lines of H are again sharp and rather narrow, but distinctly fainter than they were before the last period of diffuse lines. Emission lines are not seen at all, except H_α much faintened.

The unusual appearance of the spectrum of γ Cassiopeiae in 1940 was reported also by other observers: Struve and Swings (1) announced that toward the end of the period covered by their observations between Sept. 20 and Oct. 23 the deep and sharp absorption cores disappeared in all lines between H_3 and H_ε. On the other hand, Merrill (2) observed anew the sharp and narrow hydrogen cores from Nov. 21. The Simeis observations show that in 1940 the diffuse and sharp line stages were varying alternately in the spectrum of γ Cassiopeiae, and that the shell of the star must have been in an unstable state. In agreement with our estimates, Merrill also states that the absorption cores are gradually faintening. *

* The conditions of war time caused that the Observatory could not receive in due time the paper by Struve and Swings (Ap. J.94, 2,1941). Only when this paper was ready for press we received the McDonald Observatory Contribution No 37. The authors give no data for the interval between Aug. 30 and Oct. 20, 1940, where the changes described in this paper took place.

TABLE I

Measured wave-length	Intensity	Number of plates	Character	Identification
3734.37	0—1	11		H_{13}
3750.15	1—2	15		H_{12}
3764.12	1	4	n	?
3770.63	2	27		H_{11}
3775.94	0	1	n	Ti II 6.06
3796.00	2	2	d	Si III 6.11
3797.90	2	31		H_{10}
3807.21	1	2	n	(Si III 6.56)
3813.98	0	3	n	Fe II 4.12
3816.84	2—1	5	n	O III 6.75
3819.63	2—3	36	d	He I 9.61, He I 9.75
3821.76	1	3	n	O II 1.68
3824.62	1	3	n	Fe II 4.91
3830.20	1	1		N II 9.80, Ar II 0.43, O II 0.45
3835.39	2—4	35		H_9
3841.07	0	3	n	?
3842.97	1	3	n	Ca III 2.55, O II 2.82
3845.77	1	3	n	Ar II 5.42
3849.11	1	4	s	?
3850.64	1	2	n	Ar II 0.57
3857.34	0	5	d	O II 7.17
3865.38	0	1	s	?
3867.52	0	3	s	He I 7.46, He I 7.62
3868.66	1	2	n	(Ca III 8.42), Ar II 8.53, C II 8.84
3869.49	1	2	n	?
3880.85	0—1	3	s	(Fe II 0.78)
3882.70	1	1	d	O II 2.19, O II 2.45, O II 3.15
3885.06	0	2	d	P II 5.17
3885.61	0—1	3	s	Ca III 5.29, C III 5.86
3888.85	10	61	s	He I 8.65, $H\zeta$
3893.41	0	1	n	O II 3.53
3894.98	1	3	n	P III 5.03, Ar II 5.26
3896.21	0—1	1	n	O II 6.30
3902.06	0	1	n	S III 1.55 (S II 1.99)
3911.63	1	1	n	Ar II 1.58, O II 1.95
3919.10	1	1	n	C II 8.98, N II 9.00, O II 9.28
3923.49	0—1	7	n	P III 2.72, S II 3.48
3925.87	0	3	n	Ar II 5.71
3926.57	0	4	n	He I 6.53
3927.84	0	2	s	?
3933.63	1	6	s	(S II 3.29), (P III 3.38), Ca II 3.68
3935.84	0	1	n	(He I 5.91), Fe II 5.94
3937.31	1	3	s	S III 7.24
3940.85	1	1	s	?
3947.67	0	1	n	O I 7.33, O I 7.51, C II 7.60, O I 7.61
3851.86	1	1	n	P III 1.51 (O III 1.82)
3952.68	0	4	s	Ar II 2.74
3954.72	1	1	s	O II 4.37
3956.03	1	2	s	N II 5.85
3957.27	1	3	n	P III 7.64
3958.57	0—1	3	n	Ar II 8.39
3961.36	1	2	s	S III 1.55, O III 1.59
3964.75	3—5	53	s	He I 4.73
3970.08	4—5	61		$H\varepsilon$
3974.94	1	1	n	Ar II 4.76, Fe III 5.13
3981.94	1	2	n	?
3983.84	0	2	n	(O II 2.73), S III 3.76
3984.48	1	4	n	Ca III 4.71
3990.28	0	1	n	?
3995.10	1	2	n	Ar II 4.81, N II 5.00
3996.50	1	4	d	Al II 5.86, Al II 6.16, Al II 6.38
3997.45	1	3	d	P III 7.47

TABLE I *(Continued)*

Measured wave-length	Intensity	Number of plates	Character	Identification
4003.18	1	2	s	Ca III 3.35, Fe III 3.41
4004.59	0	1	n	?
4005.20	1	1	n	?
4007.26	1	2	w	?
4009.42	1	8	d	He 1 9.27
4012.07	0	3	n	?
4024.09	1	5	n	(He I 3.99)
4026.09	2—4	55	s. w.	He I 6.19, He I 6.36
4028.49	1	1	n	Ti II 8.35, S II 8.79
4032.08	0	2	s	S II 2.81, Fe II 2.95
4033.80	0	2	n	P II 3.68, Ar II 3.83
4036.54	0	3	n	P 11 6.23
4038.87	0	1		Ca III 8.53, Ar II 8.82
4043.23	0	2	n	Ar II 2.91
4043.86	1	1	n	N II 3.54
4044.61	0	3	n	(Fe III 4.05), P II 4.49
4058.25	1	1	s	?
4062.26	2	1	d	P II 2.08
4063.02	1—2	2	n	O II 2.90
4069.07	1	1	n	C III 8.94, Ca III 9.01
4069.88	1	2	d	O II 9.64, O II 9.90
4070.81	1	2	n	C III 0.43
4074.74	1	2	b	C II 4.89
4079.41	0	1	n	Ar II 9.60
4087.47	0	2	b. d.	O II 7.16 (N II 7.35)
4089.30	1	3	n	(Si IV 8.86), P III 9.25, O II 9.28
4091.61	1	1	n	P II 1.53
4101.75	4—5	61		Hδ
4120.79	0—1	12	b. d.	He I 0.81, Fe III 0.97, He I 0.98
4122.24	1	2	b. d.	Fe III 1.31, C III 2-05, Fe III 2.06
4127.49	1	1	n	P II 7.49
4128.55	0	1	n	Si II 8.05, Fe II 8.74
4131.06	0	1	n	P II 0.77, Si II 0.88
4131.72	0	1	n	Ar II 1.73
4132.71	0	1	n	O II 2.82
4143.84	0—1	10	b. d.	(O II 3.52), He I 3.77 (O II 3.77)
4151.94	1	2	n	N I 1.46
4153.01	2—0	3	n	S II 3.10, O II 3.31
4156.11	0	1	n	Ar II 6.11
4176.93	0	1	n	Fe III 6.79
4185.11	0	1	n	O II 5.45
4187.30	1	1	d	C III 7.05
4188.10	1	2	n	P III 8.07
4189.08	1	2	s	P III 9,08, Fe III 9.10
4214.68	0	1	n	N I 4.73
4224.87	1	2	s	P II 4.43
4250.04	1	2	s	(P IV 9.57), Fe III 9,95
4254.11	2	2	b. d.	S III 3.59. Fe III 3.62, O II 3.98
4256.63	1	3	n	Ca III 6.69
4284.88	1	1	n	S III 4.99
4288.67	0	1		P II 8 52, O II 8.83
4303.59	1	1	n	Fe II 3.17, O II 3.82
4305.30	1	2	s	Fe III 4.81, N I 5.46
4307.75	1	1		Ti II 7.91 (P III 7.94)
4312.72	1	1	n	Ti II 2.88
4313.49	1	1	s	O II 3.43, C II 3.50
4314.67	1	1	n	Fe II 4.29, Ti II 4.98
4319.16	1	1	s	S II 8.63, O II 9,65
4340.48	5—7	61		Hγ
4352.62	0—1	1	n	Ar II 2.23, Fe III 2.70
4357.79	1	1	n	(O II 7.25), Fe II 7.57 (N I 8.27)
4369.14	0	1	n	(O I 8.30), O II 9.28 (Fe II 9.40)

TABLE I *(Continued)*

Measured wave-length	Intensity	Number of plates	Character	Identification
4370.27	1—2	1	n	(Ar II 0.76)
4371.87	1	1	n	Ar II 1.36, C II 1.59, O II 1.65
4377.03	1	1	n	C II 6.78
4378.20	1	2	s	O II 8.40
4380.35	1	1	n	(Ar II 9.74), (C III 9.97)
4383.60	1—2	1	s	(C III 3.24), Ar II 3.79
4387.94	0—1	27	b. d.	He I 7.93, (C III 8.24)
4395.75	1	1	n	(Ti II 5.04), Fe III 5.78, O II 5.95
4413.74	0	2	n	Fe II 3.60, Ca III 3.74, P II 4.29
4415.96	1—0	3	d	?
4416.98	0	1	s	O II 6.97, Fe II 6.82 (P II 7.31)
4419.42	0	4	d	Fe III 9.59
4426.47	0	1		Ar II 6.01
4427.32	1	1	n	N II 7 21, N II 7.97
4430.86	1	1	n	Fe III 0.95, Ar II 1.02
4434.07	1	1	s	Ar II 3.83
4444.01	2	1	n	Ti II 3.81, P III 3.87
4449.06	1	1	s	O II 8.21, Ar II 8.88
4467.99	1	1	d	O II 7.55, O II 7.88, P II 7.98
4468.82	1	3	n	Ti II 8.50
4471.46	4—8	55	s	He I 1.48, He I 1.69
4482.39	0	1	n	Ar II 1.83
4487.33	1	1	n	(O II 7.72), (O II 8.09), (N II 8.15)
4491.71	1	1	n	O II 1.25, Ar II 1.33, Fe II 1.40
4496.10	1	2	d	?
4521.68	1	2	n	Fe II 0.22, Fe II 2.64
4528.92	1	3	n	Al III 8.91, Al III 9.18
4530.58	1	2	d	N II 0.37, Ar II 0.57, P II 0.78
4534.04	1—2	2	n	S II 3.39, P II 3.81, Ti II 3.97, Fe II 4.17
4536.44	0	1	n	S IV 5.69
4537.50	1	1	n	Ar II 7.67
4552.50	0—1	2	b. d.	S II 2.37, N II 2.50, Si III 2.60
4572.90	1	1	n	(Ar II 2.92)
4575.15	2	2	d	Si III 4.75, P III 4.90
4598.63	1	1	s	Fe II 8.53, Ar II 8.77
4608.20	1—2	3	b. d.	N II 7.17, Ar II 9.60
4629.78	2	1	b	P II 8.71, Fe II 9.34, Ti II 9.34
4631.29	1	1	n	N II 0.55, Si IV 1.38
4639.77	1	1	d	O II 8.86, Al II 0.36, Al II 0.38
4649.56	2 - 3	23	b. d.	C III 7.40, O II 9.15, C III 0.16, O II 0.85, C III 1.35
4655.37	1	2	s	(N II 4.57), (S II 6.75)
4659.08	1	2	n	(P II 8.11), (C IV 8.64)
4678.14	1	2	n	N II 7.93
4709.51	1	1	n	Fe II 8.97 (N II 9.45), O II 0.04
4713.46	1	2		He I 3.14, He I 3.37
4861.34	3—5	46		Hβ
4921.49	2—3	33	b. d.	He I 1.93
4942.24	2	2	s	O II 1.12, O II 3.06
4955.36	1—2	2	s	P II 4.33, O II 5.78
4969.80	2	1	s	P II 9.65
5005.10	2	1	n	N II 5.14
5015.71	5	20	s	He I 5.68
5048.14	0	1		He I 7.74
5087.17	1	1	n	Fe III 6.78
5094.24	0	1	d	(Fe II 3.47), (Fe II 3.64), (Al II 3.65)
5100.82	1	2	d	(Al II 0.34), (Fe II 0.70), Fe III 0.7, Fe II 0.84
5127.66	0	1	s	Fe III 7.32
5135.58	1	1	d	S II 5.85
5156.79	1	2	s	Fe III 5.97, S II 7.04
5194.47	1	1	d	Fe III 3.90, Fe III 4.43

TABLE I *(Continued)*

Measured wave-length	Intensity	Number of plates	Character	Identification
5234.62	1	2	n	Fe II 4.62, Fe III 5.30
5242.77	0	1	d	Fe III 3.26
5321.17	0	1	d	S II 0.70, N II 0.93
5329.90	2	1	d	O I 8.93, O I 9.59, O I 0.66
5436.89	1	1	d	O I 5.16, O I 5.78, O I 6.83
5577.86	0	1	b. d.	N II 6.76, N II 9.56
5875.68	4—6	11	s	He I 5.62, He I 5.93
5891.02	2	4	s	C II 9.97, C II 1.65
6562.82		14		Hα
6676.70	3	5	s	He I 8.15

A preliminary account of the peculiar changes in the shell spectrum of γ Cassiopeiae was given in another publication. (3)

IDENTIFICATION OF FAINT ABSORPTION LINES

Besides the H and He lines there are measured in the 1940 spectrum of γ Cassiopeiae a number of extremely faint lines, seen only on the best spectrograms. Table I contains the wave-lengths of those of them, whose reality is ascertained by measurement on several plates. From lines, which remained unidentified we give the wave-lengths of such lines only which were measured by other observers in B stars.

The lines are in the majority sharp and narrow, the diffuse ones being mostly blends. The measured wave-lengths were corrected for radial velocity using the constant value of —6.8 km/sec. as given in Moore's General Catalogue of Radial Velocities.

The table contains the list of 197 lines identified with 27 elements. In column 1 is given the measured wave-length, except for the Balmer lines, for which laboratory wave-lengths are given. Column 2 contains the intensity estimates on an arbitrary scale ranging from 0 to 10, the estimate 0 meaning a line just barely visible. Columns 3 and 4 give the number of plates on which the line was measured and the character of the line respectively; the abbreviations n, s, b, d, w mean: narrow, sharp, broad, diffuse, with wings. Column 5 contains the identification. Doubtful cases are given in brackets.

Lines of following elements are identified: H, He I, C II, C III, (C IV), N, I, N II, O I, O II, O III, Al II, Al III, Si II, Si III, (Si IV), P II, P III, (P IV), S II, S III, (S IV), Ar II, Ca II, Ca III, Ti II, Fe II and Fe III.

From these — quite sure is the identification with H, He I, C III, N II, O I, (although the ionization potential seems to be somewhat low), O III, Si III, P II, P III, Ar II, Ca II, Ti II and Fe III.

Some of these elements deserve special attention.

Ar II. The presence of this element can be considered as safely stated. From the 33 lines found in the spectrum, 15 cannot be identified with other elements and are decidedly not blends. In order to prove this identification a spectrogram of γ Pegasi, where the presence of Ar II is ascertained by Kühlborn's detailed investigation (4), was measured. From 20 lines measured in γ Cassiopeiae — 18 were found in γ Pegasi within reasonable errors and only two could not be detected as superposed on the wings of H_δ and H_γ.

The wave-lengths were taken from the papers by Rosenthal (5) and de Bruin (6).

Ca II. Only the K line is surely measured, H disappears in the wings of H_ε. It cannot be decidedly said whether the K line is of stellar or interstellar origin.

Ti II. 10 strong lines of Ti II are found; unfortunately some of them are blends. The Ti II lines appear only on the plates taken between Aug. 20 and Sept. 7.

Fe III. From the 23 lines coinciding with wave-lengths given in the paper by Swings, Edlén and Grandjean (7) four are decidedly not blends and cannot be identified with another ion or atom, namely: 4176.79, 4419.59, 5086.78 and 5127.32 The remaining lines participate to blends, but in most cases Fe III must be the chief contributor. The presence of this ion in γ Cassiopeiae is quite sure.

The following elements are probably present in γ Cassiopeiae, but the identification is somewhat unsatisfactory for different causes: 1) The number of observed lines is insufficient: C II, N I, Al III, Si II, S II, S III; 2) the strongest lines are not identified; O II, Al II, Fe II; 3) the lines are observed mostly in blends — Ca III.

The presence of the four trebly ionized elements: C IV, Si IV, P IV and S IV is quite uncertain, no more than one or two lines being found in all cases, and the excitation potentials appearing rather high.

From other elements, possible in a B0 star, some coincidences were found for N III, Ne I, Ne II, Ar I and K II, but they were not included in the table, as being probably due to chance. Special attention was paid to the detection of lines of He II and Mg II, but the result was negative in both cases.

Table II gives the number of lines of different elements identified in the 1940 spectrum of γ Cassiopeiae.

TABLE II

Element	Number of lines		Element	Number of lines	
	Certain	Doubtful		Certain	Doubtful
H	11	—	Si III	3	1
He I	23	2	Si IV	1	1
C II	9	—	P II	17	2
C III	8	3	P III	10	2
C IV	—	1	P IV	—	1
N I	3	1	S II	10	3
N II	16	4	S III	6	—
O I	9	1	S IV	1	—
O II	41	6	Ar II	30	3
O III	2	1	Ca II	1	—
Al II	5	2	Ca III	8	1
Al III	2	—	Ti II	9	1
Si II	2	—	Fe II	20	4
			Fe III	22	1

Besides the lines, which could be more or less surely identified with known spectra, there remain 17 absorption lines which cannot be attributed to any element. In table III are given the wave-lengths of these unidentified lines, and the measurements by other observers when such data could be found.

TABLE III

γ Cassiopeiae	Baldwin γ Cas. (8.9)	Baldwin ζ Tau. (10)	Kühlborn ζ Per. γ Peg. γ Ori ζ Cas. (4)	Struve B stars (11)	Marshall Mich V (12)	Struve Dunham τ Sco. (13)	Swings Désirant (14)	Struve U. V. Spectra of B Stars (15)
3764.12	3.93	—	—	—	3.86	—	—	—
3841.07	—	—	0.98	—	—	—	—	—
3849.11	9.47	—	—	—	9.35	—	—	9.12
3865.38	—	—	—	—	5.15	—	—	—
3869.49	—	—	9,57	—		—	—	—
3927.84	7.73	7.48	7.31	—	—	—	7.93	—
3940.85	—	0.59	0.67	—	—	—	—	—
3981.94	—	—	1.76	—	—	—	—	—
3990.28	—	—	0.24	—	—	—	—	—
4004.59	—	—	4.56	—	—	—	—	—
4005.20	4.98	—	5.00	5.03	5.09	—	—	—
4007.26	—	—	—	—	7.22	—	—	—
4012.07	—	—	1.68	—	2.07	—	—	—
4058.25	—	—	8.20	—	—	—	—	—
4415.96	5.72	—	5.92	—	—	5.69	—	—
4496.10	—	5.67	—	—	—	—	—	—

THE 1941 SPECTRUM

There are few observations in 1941, these being done only on June 6, 18, 23, July 2, 11 and Sept. 12, 17. The total number of spectrograms is 25; the emulsions used are: Eastman Process, Agfa-Astro and Agfa-Astro-Panchromatisch.

The spectrum strongly differs from 1940. The presence of the shell is manifested only by the H_α emission. However, one may suggest, that just to the end of the period of observations, the shell begins to appear anew also in other frequencies. On 5 spectrograms taken on Sept. 12 there is seen a faint, but rather real violet emission component at H_β; on the same day on three spectrograms a still fainter violet emission component and perhaps also a red one are seen at H_γ. On earlier spectrograms a very faint component can be found at H_γ on July 2 and both emission components at H_β on July 11. H_δ shows no emission.

The absorption lines are very broad and diffuse, no traces of central cores being seen. Observed are only the following lines: the Balmer series from H_β to H_{13} (intensity estimates 2—3 on the 10 degree scale). From the helium lines are measured only: the diffuse triplets 3819, 4026, 4471, 5876 and singlets: 3926, 4009, 4144, 4388, 4922. The sharp series lines are observed uncertainly and from these only the triplet line 4121 (on 2 spectrogram) and the singlet line 5048 (1 spectrogram). The lines originating from the metastable levels ^3S and ^1S: 3889, 3965 and 5015 are not observed. We judge on the absence of 3889 from the appearance of H_ζ, differing in no way from the other Balmer lines.

Besides the H and He I lines there are measured in the spectrum two very broad, diffuse and faint blends with the following wave-lengths: 4641.05 ± 0.15 (5 spectrograms) and 4650.44 ± 0.21 (8 spectrograms), which can be interpreted as composite blends of O II, N II and C III, namely: 4638.86 O II, 4640.64 N III, 4641.83 O II, 4641.90 N III for the blend at 4641 and 4649.15 O II, 4650.16 C III, 4650.85 O II, 4651.35 C III for the blend at 4650. However other lines of these ions are not seen. Generally the lines of O II, C III and N III are not strong in B stars. One may suggest

that the rapid rotation of γ Cassiopeiae renders them invisible and the above mentioned lines become observable only owing to the closeness of their wave-lengths. Besides, they all belong to the strongest lines of the respective spectra and correspond to transitions of low excitation potentials. The identification of O II and C III lines is quite sure, that of N III somewhat less convincing; in 1940 N III was not found in γ Cassiopeiae.

The 1941 spectrum of γ Cassiopeiae contains a peculiar feature, which was also observed on some spectrograms of 1940.

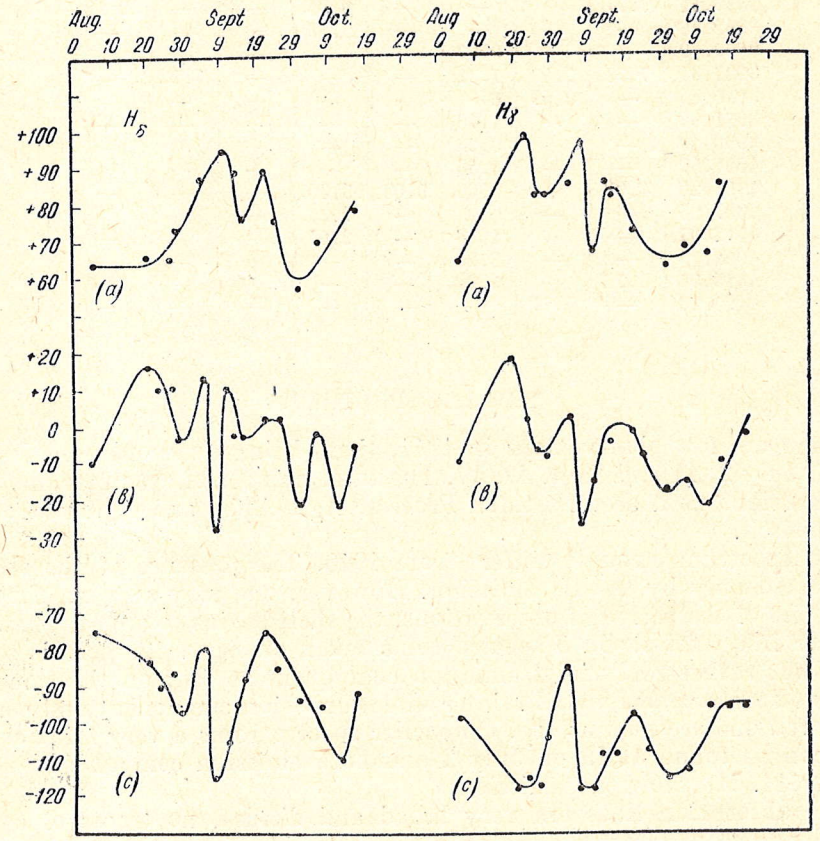

Fig. 2. Radial velocity curves for H_δ and H_γ (*a*) — red emission component, (*b*) — central absorption core, (*c*) — violet emission component.

To the red side of the helium line 4471, there is observed a diffuse broad emission which finds no adequate interpretation and whose reality may be called in question. But it is apparently too bright to be considered as a contrast effect, there being, besides, no absorption lines, which could be responsible for it, as all attempts to find the Mg II line led to negative results. The wave-length of this detail determined from 13 plates and corrected for radial velocity found from the H and He lines is 4475.60 ± 0.18. We could find no adequate identification for such a line.

This strange feature reminds the red emission companion of 4471 observed by S t r u v e (16) and G i l l (17) in the spectrum of β Lyrae in phases near the minimum. The contours of this emission given by G i l l show it located nearly at the same wave-length as in γ Cassiopeiae. H_δ and

H_γ have just similar contours in that phase. While in the β Lyrae spectrum there is no doubt in the belonging of this emission to He, the case of γ Cassiopeiae finds no explanation.

A search for a similar detail for 4026 revealed on some 5 or 6 spectrograms a faint feature, which could be perhaps considered as traces of emission. As for 5876— the spectrograms of 1941 are rather poor in this region, and on those of 1940 nothing was found.

This emission feature is distinctly stronger in 1941, and in 1940 seen mostly in the epochs of greater transparence of the shell.

It is extremely hard to reconcile such a helium emission with the formerly observed shells in γ Cassiopeiae and, on the other hand, there seem to be no reasons to reject completely this detail as an unreal one. Probably future observations will decide upon this question.

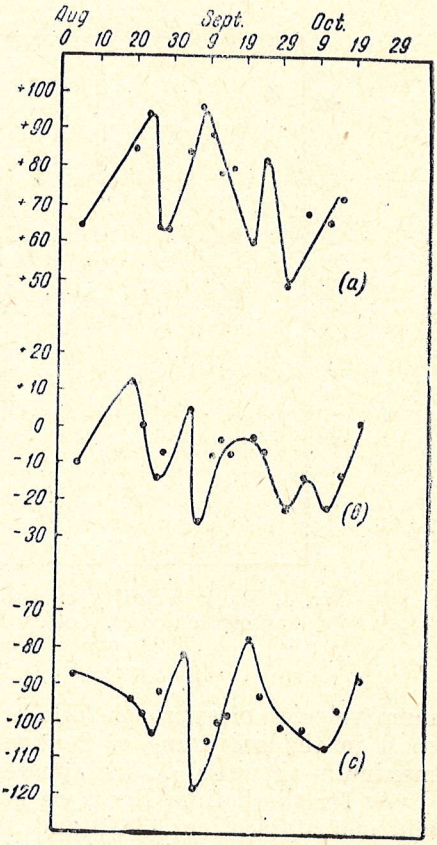

Fig. 3. Mean radial velocity curves from all Balmer lines: (*a*) — red emission component, (*b*) — central absorption core, (*c*) — violet emission component.

RADIAL VELOCITIES

In the measurement of the 1940 spectrograms settings were made on the following structural details of the H lines: the central absorption cores, the emission components and the faint absorption ones; individual curves were drawn for every detail.

The physical interpretation of the absorption components, especially of the red one, being rather difficult, we hoped that the velocity curves would throw some light on their origin. While the velocity curves of the emission lines agree in their general rate with these of the central cores, the curves drawn for the absorption components differ much from these undoubtedly relating to the shell spectrum and look moreover rather uncertain. Probably the supposed absorption components are merely some points on the broad underlying lines of the reversing layer strengthened by contrast with the neighbouring emission lines and have no individual physical significance. For that reason we do not reproduce here the curves for the absorption components. These for the emission components and central absorption cores are shown on Fig. 2 for H_δ and H_γ respectively.

The shifts of the emission lines are distinctly dependent on wave-length. The mean values corrected for the velocity as given by the central absorption cores are:

	Em. V	Em. R		Em. V	Em. R
H_ε	-78.5 ± 2.1	$+84.5 \pm 3.6$	H_γ	-98.6 ± 3.1	$+89.2 \pm 3.3$
H_δ	-83.7 ± 2.4	$+84.4 \pm 3.5$	H_β	-125.8 ± 2.9	$+124.3 \pm 9.2$

These values, if interpreted as the effect of rotational broadening of the emission lines, do not agree with theory, the change with wave-length being much greater than can be caused by rotation.

In Fig. 3 are given the mean curves for all Balmer lines: the curves for the emission lines are drawn for H_{12} — H_γ , these for the central absorption for H_{12} — H_β . All curves relating to the red emission component are rather uncertain in view of the extreme faintness of the line.

The inspection of all the curves shows that the star is subject to irregular fluctuations in radial velocity of relatively short duration. The maxi-

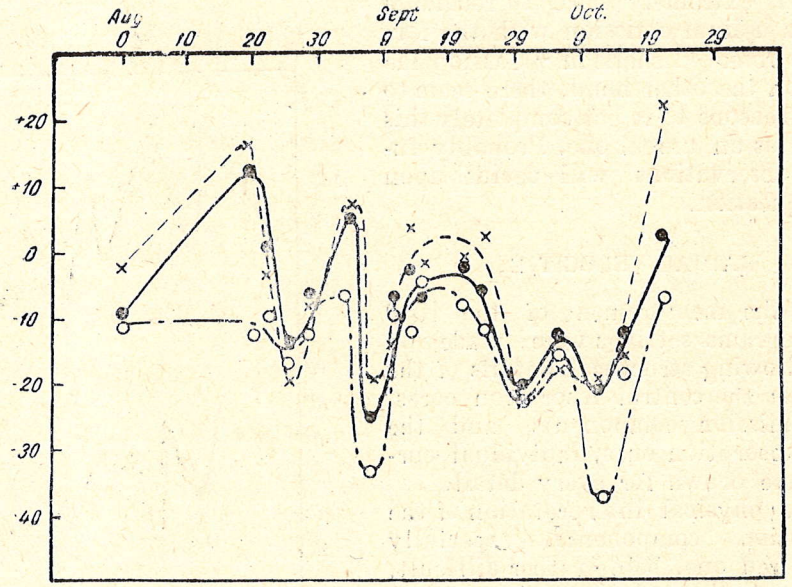

Fig. 4. Radial velocity curves for H and He. Heavy curve, dots — H absorption cores, dotted lines, crosses — He P—D lines, open circles — S—P lines.

mum velocity of approach falls just in the periods of the dissipation of the shell in the beginning of September and October. The negative velocity maximum about Aug. 25 is apparently not connected with spectral changes.

As for the helium lines, we have drawn separate curves for the diffuse and metastable lines (3889 and 3964) which are shown in Fig. 4 together with the hydrogen absorption cores curve. All three curves are similar in shape. That corresponding to the metastable lines is strongly shifted to greater negative velocities relatively to the reversing layer curve represented by the diffuse series lines of He, the difference reaching maximum in the periods of the dissipation of the shell. The hydrogen cores curve is more close to the reversing layer curve; the difference between them, although very small, appears to be real. These curves indicate clearly that the metastable helium lines originate in a higher and more rapidly moving layer of the shell than the hydrogen ones.

In 1941 the velocities were determined from the hydrogen and helium (P—D) lines. They are given in Table IV.

Although the measurement is difficult and uncertain in view of the diffuseness and great width of the lines, the agreement of separate spectrograms taken during one night is rather satisfactory. The scarcity of observations does not allow to draw a curve.

Within the limits of accuracy of radial velocity determination for a B0 star with broad lines, the velocity of γ Cassiopeiae between June 23 and Sept. 12 appears to be constant. But observations done at June 6 yield quite an outstanding figure of +110.8±4.0 (3 spectrograms), which may be called

TABLE IV

Date	R. V.	Probable error	Number of plates
1941 June 23	+ 7.8 km/sec	±1.0	2
July 2	+17.6	±1.0	4
July 11	+21.2	±1.2	5
Sept. 12	+17.7	±0.8	5

in question. Although two other spectrograms taken during the same night and rejected in view of overexposure give still higher values of positive velocity, we cannot affirm the reality of this value: the star was observed in June in very great hour angles, and instrumental causes may occasionally strongly affect the result. Between June 6 and June 23 we possess only one determination of radial velocity on June 18 —13.8, derived from one spectrogram and thus quite uncertain. The outstanding value for June 6 must be controlled.

REFERENCES

1. Struve and Swings. Harv. Ann. Card. 545, 1941
2. Merrill. Publ. of the Astr. Soc. of Pacific **53**, 125, 1941
3. Hase. Bull. of the Academy of Sciences of the Georgian SSR. Vol. III,N. I, p. 15 1942
4. Kühlborn. Veroff. d. Univ. Berlin-Babelsberg, Bd. XII, H. I, 1938
5. Rosenthal. Ann. d. Physik (5), **4**, p. 49, 1930
6. de Bruin. Z. P. **61**, p. 307, 1930
7. Swings, Edlén, Grandjean. Ap. J. **90**, p. 378, 1939
8. Baldwin. Ap. J. **87**, p. 573, 1938
9. Baldwin. Ap. J. **93**, p. 333, 1941
10. Baldwin. Ap. J. **93**, p. 420, 1941
11. Struve. Ap. J. **74**, p. 225, 1931
12. Marshall. Publ. Mich. Obs. V, p. 12
13. Struve and Dunham. Ap. J. **77**, p. 321, 1933
14. Swings and Désirant. Ap. J. **83**, p. 31, 1936
15. Struve. Ap. J. **90**, p. 699, 1939
16. Struve. Ap. J. **93**, p. 104, 1941
17. Gill. Ap. J. **93**, p. 118, 1941

СПЕКТР γ CASSIOPEIAE в 1940 и 1941 гг.

В. ГАЗЕ

Звезда наблюдалась в Симеизе с 5 августа 1940 г. по 17 сентября 1941 г.

Для спектра 1940 г. характерны глубокие и резкие линии поглощения водорода с тонкими и слабыми эмиссионными линиями с обеих сторон. Эти линии оболочки звезды накладываются на широкие и размытые линии поглощения обращающего слоя. Очень сильна метастабильная линия гелия 3889.

Наблюдения обнаруживают неустойчивое состояние оболочки. До 4 сентября спектр более или менее неизменный; 7 сентября линии

водорода и гелия резко меняются, становясь размытыми, и структурные детали пропадают. 13 сентября спектр возвращается к прежнему виду. Изменения контуров H_δ и H_γ показаны на фиг. 1. Подобная же картина наблюдается и в начале октября.

Кроме водорода и гелия, в спектре γ Cassiopeiae наблюдаются 171 слабая линия, отождествление которых дано в таблице I. Ряд слабых линий уверенно отождествляется со спектром Ar II.

В 1941 г. спектр имеет совершенно другой вид: наблюдаются только широкие и размытые линии водорода и диффузной серии гелия. Характерная для оболочки метастабильная линия гелия 3889, так же как и 3965, не наблюдается. Присутствие оболочки выражается только в эмиссионной линии H_α; под конец периода наблюдений появляются слабые эмиссионные спутники у H_β и H_γ.

В спектре 1941 г. более сильна наблюдавшаяся и в 1940 г. размытая эмиссионная деталь с красной стороны от линии гелия 4471, для которой не находится удовлетворительного объяснения.

Кривые лучевых скоростей для 1940 г. представлены на фиг. 2, 3 и 4. Скорость звезды подвержена кратковременным и неправильным изменениям, причем максимум отрицательной скорости совпадает с периодами исчезновения оболочки. Кривая скоростей, полученная по метастабильным линиям гелия 3889 и 3964 (фиг. 4), значительно смещена в сторону больших отрицательных скоростей относительно кривой, соответствующей линиям диффузной серии гелия. Относительно кривой, построенной по линиям водорода, это смещение меньше. Наблюдаемое смещение указывает на образование метастабильных линий гелия в более высоких и быстро движущихся слоях оболочки, чем линии водорода.

EFFECT OF THE CONVERGENCE LIMIT AND TAIL BANDS IN THE SPECTRA OF CARBON STARS

G. SHAJN and *V. HASE*

In this paper is treated chiefly the problem of continuous absorption in the spectra of N and R stars in connection with the existence of a convergence limit of bands in some sequences and also of the tail bands. The discussion of the observed and theoretical data leads to the conclusion that the well known gap in the continuous spectra of N and R stars as observed in the regions of the sequences +1 and 0 of the Swan system are due to the overlapping of bands of C_2 and that there are no evidences in favour of any sensible rôle of the tail bands in this phenomenon. It is shown that the identification of the convergence limit of the sequence 0 of C_2 with the unidentified band 4976 as declared by Wurm is not correct. Also Wurm's identification of the convergence limit of the sequence +1 with the unidentified band 4642 seems to be unsounded.

At present we have no data to speak about the identification of the tail bands of CN in the N and R spectra. There are no evidences in favour of that the tail bands of CN are responsible for the well known faintening of the violet region in N and R spectra.

The question on the convergence limit and the tail bands of the oxydes and hydrides in M and S spectra is practically to be dropped.

At very low temperatures when the ionization is reduced to minimum and the usual factors of opacity of the atmosphere (interaction between ions and electrons, neutral atoms and electrons) are gradually disappearing, the rôle of continuous absorption due to molecules may become important. Separate regions of molecular continua more or less wide must determine the complicated dependence of the general opacity of the stellar atmosphere on wave-length. The character of the function κ_ν must strongly influence the energy distribution in the continuous spectrum of the star.

The sources of continuous absorption for molecules may be different. One may speak in the general case on continuous molecular absorption connected with transitions when one or both of the combining states are characterised not only by discrete levels, but also by a continuous set of energy levels infinitesimally differing from one another. For instance, the continuous absorption beyond the limit of vibrational series is to some extent analogous to the continuous absorption beyond the limits of atomic series. The continuous absorption of some molecules is determined by the curve of potential energy. One may speak also on special absorption by quasi-molecules treated in astrophysics by L i n d b l a d (1).

Laboratory data concerning the continuous absorption by molecules important in astrophysics are rather scarce (2). This absorption lies mostly in the far violet or ultra-violet region. For instance, the well known and

easily received in laboratory continuous spectrum of the hydrogen molecule cannot appear in absorption in spectra of M, S and N stars in conditions of thermodynamic equilibrium.

At the moderate and small dispersion generally used in astrophysics, when the rotational structure remains indiscernable and the vibrational bands themselves of one or different sequences and systems are rather close, there can be formed depressions covering more or less wide regions of the spectrum. Such are, for instance, rather wide regions in the visual part of the late subdivisions of type M. However in this case the most outstanding band heads are well seen and it is easy to explain the depressions. But it is a difficult matter if the bands are faint. For instance, the region 4000—4400 in the spectra of Me stars shows a sort of inversion in the energy distribution in the continuous spectrum; the latter consists in that the intensity ratio 4340/4100 in the continuous spectrum does not increase but rather decreases from M2e to M8e (3). In N and R stars are well known gaps of about 100 A towards shorter wave-lengths from 4737, 5165 a. o. Depressions of the latter type rather limited in width deserve attention particularly from the point of view of possible criteria of spectral class and absolute magnitude.

In the present paper we are treating chiefly the problem of continuous absorption in connection with the existence of a convergence limit of bands of some sequences and the so called tail bands, i. e. bands which turn back about the convergence limit and proceed as a diverging sequence in opposite direction. W u r m (4) who was the first to set this problem in astrophysics emphasizes two points: 1) The identification of the convergence limit of the sequences 0 and +1 of C_2 with the unidentified bands 4976 and 4642 found by S a n f o r d and S h a n e in spectra of N and R types. 2) The importance of the rôle of the tail bands in the well known faintening of the violet region in N and R spectra and in the change in energy distribution in the continuous spectrum in general. W u r m finds it also possible to attribute a similar effect in M type spectra to the oxydes and hydrides.

As concerns the identification in question W u r m is speaking in a categoric form: «Die nach rot abschattierte Bande bei 4642 ist zweifelsohne die Konvergenzstelle der bei λ 4737 beginnenden Bandenserie $\Delta v = +1$ des Kohlenstoffmoleküls. Entsprechendes gilt für die andere der zwei stärkeren Banden bei λ 4976, welche die Konvergenzstelle für $\Delta v = 0$ darstellt» (5). This statement of W u r m is quoted in the monograph by M e r r i l l (6).

In view of the importance of this statement in both its points, especially the second one with its far going consequences we find it necessary to repiscuss the whole question, moreover that W u r m' s conclusions appear on our opinion to be unsounded.

The value of the quantum number corresponding to the convergence limit is approximately computed, as known, by the formula:

$$v'_{conv} = \frac{\omega_e' - \omega_e'' - 2(v' - v'')x_e'' \omega_e''}{2(x_e' \omega_e' - x_e'' \omega_e'')}.$$

Favourable conditions for the formation of the convergence limit and tail bands are: a small change in ω_e and a possibly greater change in $x_e \omega_e$. From the numerous band systems known these conditions are satisfied but very rarely. Until recently tail bands were found in laboratory only in three cases: CN — sequences 0 and +1 of the violet system, N_2^+ — sequences +1, +2, +3, +4 of the negative system, CaF — sequence +1 of the orange system. It was also suggested that the four bands about 4834—4997 recently found by F o x and H e r z b e r g (7) may be tail bands of C_2.

From all molecules known in stellar spectra CN and C_2 are the most suitable for the detection of the convergence limit and tail bands. We shall consider first the molecule C_2. The computed values of the convergence limit for the sequences +1 and 0 are λ 4654 (8, 7) and λ 4988 (10, 10) respectively. The effect of the tail bands may manifest itself in the formation about the convergence limit of a more or less wide separate band; besides this the tail bands can cause a continuous absorption due to the overlapping of the separate bands in addition to that of the ordinary bands in the same region. In Fig. 1 are shown for illustration the computed positions of the null lines of the ordinary and tail bands (dotted lines) for the sequence +1. It is necessary to analyse the question whether the bands at the convergence

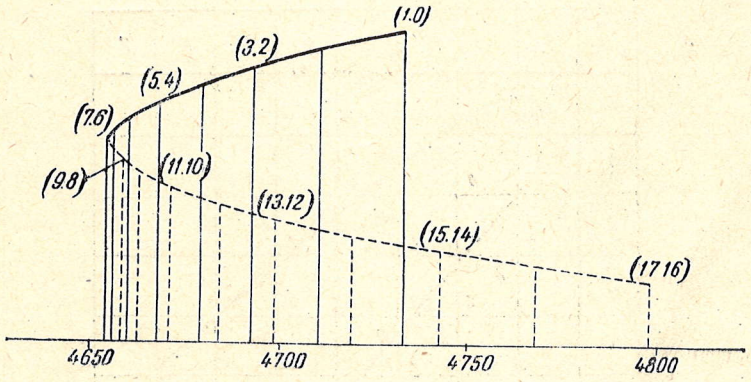

Fig. 1. Convergence limit and tail bands of the sequence +1 of C_2.

limit of the sequences +1 and 0 can form a noticeable detail in the spectrum and whether this detail can be identified with the bands 4642 and 4979 respectively, found by S h a n e (8) and S a n f o r d (9) in N and R spectra. Another question is whether the tail bands can really be of any importance in the formation of the strong depression observed in these stars in the region of the sequences +1 and 0.

To answer these questions one must firstly consider the relative intensity of bands within the given sequence. We give for the sake of illustration in Fig. 2 the band head scheme for C_2 where the numbers in ordinary type represent the laboratory intensities, according to P e a r s e and G a y d o n (10), and the numbers in italics denote the intensity estimates of bands on the Simeis spectrograms of 19 Piscium. Such estimates of intensity, especially when the bands partly overrun, are but roughly approximate. Nevertheless extrapolation allows to get some idea on the intensity of the unobserved bands with high quantum numbers. From the other part a notion of the relative intensity of bands may be got on the basis of H u t c h i s s o n ' s theory (11). In any case nobody seems to have surely observed neither in laboratory nor in stars bands with quantum numbers higher than (3, 3) and (6,5) in the sequences 0 and +1 respectively. We shall consider in the light of these and other data the gap in the continuous spectrum of about 100 A wide observed in the regions covered by the bands of the sequences +1 and 0. Whereas the limit from the longer wave-lengths at 4337 is sharp, the violet limit about 4645 is much worse defined. However the continuous absorption may be followed up to 4620 A especially in the later spectral subdivisions.

The first four vibrational bands (1,0), (2,1), (3,2) and (4,3) cover a region of about 52 A. The overlapping of these bands causes the peculiar

distribution of intensity within the limits of this sequence. The photographs, and still better the microphotograms (Fig. 3) show well the strong absorption upon which are superposed more or less distinct separate bands and other details relating mostly to blends. Besides one can mark upon the same background a wide maximum about 4668—4697. Some notion on the minimum width of at least the first band (1,0) may be got from the fact that the interval of 22 A width between (1,0) and (2,1) is filled with strong continuous absorption. This cannot obviously be ascribed neither to the influence of the isotope bands (1,0) and (2,1) nor of the tail bands, as the continuous absorption is abruptly cut off beyond the head (1,0) to longer wave-lengths. Considering the general rotational structure

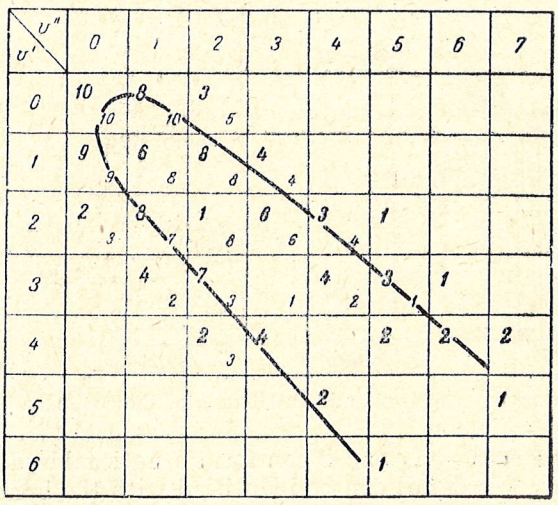

Fig. 2. Distribution of intensity within the Swan system of C_2. Numbers in ordinary type—laboratory, italics — 19 Piscium.

of the band (1,0) and especially the fact that the absorption is strong at the distance of 22 A from the head, one may think that it will be still sensible at 40—50 A from the head or even farther. There are reasons to think that the first three bands of this sequence do not differ much from one another in intensity in N type stars. This observational fact is confirmed by theory. In the light of these data one may expect that the continuous absorption is quite sensible at a distance of 100 A to the shorter wave-lengths or even more. This conception allows to interpret the general picture of the observed continuous absorption as a result of overlapping even of the four first bands (1.0), (2.1), (3.2), (4.3) only, although the bands (5.4), (6.5), no more observed as separate details, may also contribute to the absorption. There is no need to have recourse to the tail bands for the explanation of this phenomenon. In any case one cannot conclude from the observed picture of the continuous absorption upon any influence whatever of the tail bands. Undoubtebly the absorption extends beyond the convergence limit towards shorter wave-lengths and this cannot be due to the tail bands. Obviously also the overlapping of the tail bands to the red from the first band does not affect the continuous spectrum. The same considerations hold, perhaps in a much higher degree, for the sequence 0. Shortly, there is no evidence whatever in favour of any influence of the tail bands on the continuous absorption observed in the regions of the sequences +1 and 0.

If the tail bands affect in any way the observed continuous absorption or even are responsible for it, the maximum effect should be awaited about the convergence limit. As seen from Fig. 1, there must be formed a separate more or less wide band consisting from the bands (7, 6), (8, 7), (9, 8) in the sequence +1 and from (8.8), (9.9), (10.10) in the sequence 0. The computed values of the convergence limits for the sequences +1 and 0 are 4654 and 4988 (null lines), but the observed positions even of the heads of the hypothetic bands may be greater than the theoretical value in consequence of the clustering of the ordinary and tail bands about the convergence limit. Thus it is far from being evident what values properly are to

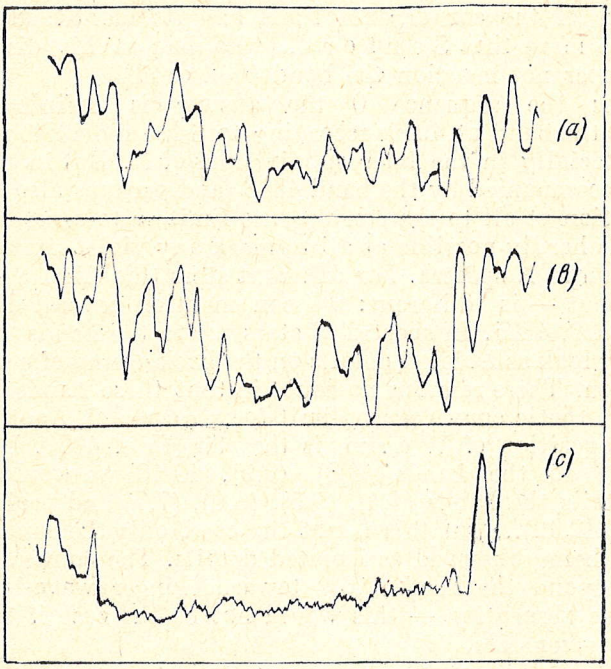

Fig. 3. Region of the sequence +1 of the Swan system.
(*a*) — 19 Piscium, (*b*) — X Cancri, (*c*) — Y Canum Venaticorum.

be compared with observations. Moreover it is not evident whether this band would be shaded to the red or to the violet, there will be rather no shading at all. The wave-length of the band observed by Shane and attributed by Wurm to the sequence +1 is 4642. It is worthy to note that Sanford, who was in possession of a far better material, does not mention of any new band in this region at all.

Wurm compared the reproductions of spectra of N type stars published by Hale, Ellerman and Parkhurst (12) with the laboratory spectrum of C_2 (Johnson) (13) and found that the sequence +1 «zeigt in Emission die gleiche Struktur, wie dieselbe Gruppe in Absorption in den ersten Unterklassen von N».

In reality the picture is as follows. For the first six of the seven stars in the above mentioned reproduction the limit of continuous absorption lies about 4646 and this detail may be regarded as the limit of continuous absorption in the earlier subdivisions of type N. As concerns Shane's band at 4642, this detail looks generally as a more or less ordinary line,

and only in the spectrum of Y Canum Venaticorum, and probably in the later subdivisions of N in general, can be considered as a band. On the Simeis spectrograms there is observed in the majority of N spectra a detail looking like the limit of absorption at 4646 and another narrow detail centered about 4640.5. Apparently, nobody identifies the detail 4646 with a band. By the way, it is rather strong in K and M type stars, but here it may be probably attributed to the low temperature line of V 4646.4 (E. P. 1.06) and possibly to other lines. One has the impression that the limit of continuous absorption can be marked at 4646 in earlier subdivisions and at 4642 in the later ones. However in both cases the continuous absorption can be traced farther towards shorter wave-lengths. Therefore one can give no definitive answer on the presence of the convergence limit and its identification with the band 4642, the more that S a n f o r d, who had at his disposal a more rich material does not mention the band 4642 or 4646.

As concerns the sequence 0 the answer is definitely negative. It is true that the band at 4979 (according to S h a n e 4976) is real and rather strong especially in the later subdivisions of N. But in these stars the band 4979 is accompanied by the band 4868 (and perhaps also by other ones) having no relation at all to the convergence limit or to separate tail bands.

Further it is hardly possible at all to mark any violet limit of the continuous absorption in N spectra. For different stars this «limit» — if one may ever speak about — is different: we can mention several «limits», for instance about 4920, 4825. In spectra of stars where the bands 4979 and 4868 are strong, they look as isolated details on the background of a sensible continuous absorption. There remains no doubt in that these bands bear no relation to the hypothetic convergence limit for sequence 0. Another argument against the supposition of W u r m is the stength of 4979. If the band at 4979 were due to the bands (8,8), (9,9), (10,10) we would also observe as separate details the bands (4,4), (5,5), (6,6), (7,7) and probably the tail bands (11,11), (12,12)... But this is not the case, only the bands (0, 0), (1,1), (2,2) and (3,3) being observed as isolated details. The continuous spectrum immediately beyond the head (0,0) towards longer wave-lengths is free from continuous absorption — this would not be the case if the tail bands were in any way sensible.

W u r m pretends to find a strong argument in favour of the existence of the convergence limit for the sequences +1 and 0 in the likeness of the general picture of the emission spectrum of C_2 (J o h n s o n) with the absorption observed in N and R stars especially near the convergence limit. This likeness is not convincing even for the sequence +1 because the limit of absorption, as shown above, is different in various subdivisions of N and moreover the absorption extends beyond the convergence limit in the later type stars.

As concerns the sequence 0, there can be hardly spoken of any likeness at all. In the laboratory spectrum (J o h n s o n) the violet limit is distinctly defined about 5070, i. e. it differs by about 90 A from the computed value of the convergence limit. W u r m ascribes this enormous difference to underexposure on the photographs by J o h n s o n. But in reality the bands look unresolved on J o h n s o n's photograph and this is rather a testimony of overexposure, which is perhaps no less, than for the sequence +1, the more that the intervals between separate bands of the 0 sequence are approximately by 1.5 greater than the respective distances in the sequence +1.

But even if in the laboratory spectrum the emission reached the convergence limit, W u r m's argument would still remain groundless as in the stellar spectra the continuous absorption extends beyond the conver-

gence limit more than by 100 A. There are definitely no indications whatever on the presence of a convergence limit and tail-bands for the sequence 0. The identification of this «convergence limit» with the observed band 4979 seems the more doubtful, if only one does not suppose the convergence limit to be masked here by the superposition of some additional absorption of unknown origin. In view of the uneven character of continuous absorption in this region one must reckon with the possibility of such an absorption. But even in this supposition we could not find any argument in favour of the identification of 4979 with the convergence limit.

The strengthening of 4979 and 4642 observed in later subdivisions of N, besides in several stars only, does not still be an argument in favour of the hypothesis under consideration. This correlation is not evident, and in any case no more evident than that between 4979 and the band 4868, bearing no relation to the convergence limit or to the tail bands. On the quite natural assumption that the advanced type corresponds to lower temperature we must expect, in consequence of Hutchisson's theory, a strengthening of the gradient within the given sequence. For instance, we must have for the first four bands of the sequence +1 in emission the ratio: 1.00 : 1.23 : 0.79 : 0.83 at $T = 3000°$ and 1.00 : 0.86 : 0.36 : 0.27 at $T = 2000°$ respectively. Thus the observed strengthening of 4979 and 4642 — if these bands are supposed to represent the convergence limits — is in contradiction with theory. However this contradiction can certainly be explained by the considerable strengthening of the bands in the later subdivisions owing to the higher abundance of the C_2 molecules in general, or owing to the lower temperature, or to both causes together. But it is to be kept in mind that the change of temperature as function of spectral subdivision in N stars remains still a rather obscure matter (see *e. g.* the classification of the carbon stars by Keenan and Morgan) (14).

One must notice by the way that in the schematic figure given by Wurm (15) the bands are represented by vertical lines, whose length is increasing with increasing quantum number; the apparent rôle of the convergence limit and tail bands becomes especially emphasized by this manner of drawing and the disproportionality of the horizonthal scale also strengthens this impression to some extent. The scheme represented in Fig. 1 of this paper gives a more correct impression of the effect of the convergence limit.

Wurm pretends also to find the convergence limit and tail bands in the violet system of CN in the R spectra. «Ganz deutlich, dass der Gruppe 3590 eine ganze Anzahl von Banden vorgelagert ist. Diese haben in ihrer Anordnung ganz den Charakter der tail Banden und sind wahrscheinlich damit identisch». (16). We recall that the five first bands of the sequence + 1 lie within 10 A approximately between 3580 and 3590. Within the same limit must be 3—4 tail bands and only the next ones 3603 (9,8), 3629 (10,9), and 3658 (11, 10) will lie outside the interval 3580—3590. Wurm's conclusion is based on the general impression from the photograph by Shane (17) which is of so low dispersion that it is difficult to mark on it any details with some certainty. Considering that this part of the spectrum contains a great number of atomic lines and that Wurm had no wave-lengths at his disposal, we must recognize his identification of the tail bands extremely unsounded. As concerns the question of the existence of the tail bands of the sequence 0 it does not arise at all. The less reasons there are to make conclusions whatever on the rôle of the tail bands in the faintening of the continuous spectrum over wide regions in the violet and ultraviolet in N and R spectra. This is, in particular, in striking contradiction with the fact that while the CN bands in N stars are at least not stronger than in R ones,

the enormous faintening of the continuous spectrum is seen only in N stars or is at least incomparable iwth what is observed in R stars.

Finally, one must note that W u r m finds possible that the effect of the convergence limit and tail bands will manifest itself in the spectra of oxydes and hydrides in M and S stars. Although the band-heads formulae for the molecule TiO, for instance, are not accurate, but if used for the computation of the quantum numbers corresponding to the convergence limit they lead for different systems of the TiO molecule to very high values of the quantum number $v' > 50$ in the far infra-red. The same holds for other oxydes and hydrides. Thus the question of the convergence limit and tail bands in M and S spectra must practically be dropped.

REFERENCES

1. L i n d b l a d. Astr. Jaktagelser och Unders. Stockholms Obs., Bd. 12, 1935.
2. W. F i n k e l n b u r g. Kontinuierliche Spektren. Berlin 1938.
3. G. S h a j n. Zs. f. Aph. **10**, p. 73, 1935.
4. K. W u r m. Zs. f. Aph. XIII, p. 179, 1937.
5. L. c., p. 180.
6. P. M e r r i l l. Spectra of long period variable stars. The University of Chicago Press, p. 42 1940.
7. F o x and H e r z b e r g P. R. **52**, 638, 1937.
8. S h a n e L. O. B. **13**, p. 123, 1928.
9. S a n f o r d. PASP, **38**, p. 177, 1926.
10. P e a r s e and G a y d o n. The identiiication oi molecular spectra N. У. 1941.
11. H u t c h i s s o n P. R. (2) **36**, p. 410, 1930; (2) **37**, p. 45, 1931.
12. Publ. Yerkes Observatory. Vol. II, pl. VIII, 1903.
13. J o h n s o n. Phil. Trans. (A) **226**, p. 157. 1926/27.
14. K e e n a n and M o r g a n. Ap. J. **94**, p. 501, 1941.
15. L. c., p. 183.
16. L. c., p. 184.
17. S h a n e. L. c.

О ПРЕДЕЛЕ СХОДИМОСТИ И ХВОСТОВЫХ ПОЛОСАХ В СПЕКТРАХ УГЛЕРОДНЫХ ЗВЕЗД

Г. Ш А Й Н и В. Г А З Е

В настоящей работе рассматривается главным образом вопрос о непрерывном поглощении в звездах N и R в связи с существованием предела сходимости и так называемых хвостовых полос у некоторых последовательностей.

Дискуссия наблюдательных и теоретических данных приводит к заключению, что ослабление непрерывного спектра, наблюдаемое в звездах типа N и R в области последовательностей +1 и 0 Свановой системы объясняется наложением обычных полос C_2. Нет никаких доказательств в пользу какого-либо заметного влияния хвостовых полос в этих областях.

Доказано, что идентификация неотождествленной полосы 4976 с пределом сходимости последовательности 0 Сванової системы, произведенная В у р м о м (K. W u r m), неправильна. Идентификация тем же автором полосы 4642 с пределом сходимости последовательности +1 также не обоснована.

В настоящее время нет данных для отождествления хвостовых полос фиолетовой системы молекулы CN в звездах типа N и R. Точно так же нет доказательства в пользу того, что хвостовые полосы CN ответственны за сильное ослабление непрерывного спектра в фиолетовой области в звездах типа N и R.

Вопрос о пределе сходимости и хвостовых полосах для окисей и гидридов в спектрах звезд типа M и S, также поднятый Вурмом, практически просто отпадает.

THE TOTAL LIGHT OF THE SOLAR CORONA OF JULY 9, 1945

V. B. NIKONOV and *E. K. NIKONOVA*

The total light of the solar corona of July 9, 1945 was determined with a special photoelectric photometer. A Kunz potassium hydride photoelectric cell was used. The measurements were referred to the sun by means of a special standardization device with a diffusing barite screen. The atmospheric extinction was accounted for from the observations of the sun on the day of the eclipse.

The total light of the observed zone of the solar corona ($1.015 R_\odot$ — $8.67 R_\odot$) proved to be

$$E_k \ (1.015;\ 8.67) = (0.43 \pm 0.03)\ 10^{-6}.$$

in terms of solar radiation.

The reduction to the zone ($1.030\ R_\odot$—$6.00\ R_\odot$), adopted as a standard one, using the mean distribution law of surface brightness in the corona (Baumbach) yields

$$E_k \ (1.030;\ 6.00) = (0.38 \pm 0.06)\ 10^{-6}.$$

The comparison of the received value with other photoelectric observations, done in the same photometric system and reduced to the standard zone, shows appreciable changes in the total light of the corona. The corona proves to be brighter in the epochs of maxima of solar activity and fainter in the epochs of minima.

INTRODUCTION

It is a current opinion now, that the total light of the corona is constant (1), although the suggestion on the dependence of the coronal radiation upon solar activity is quite natural (2). The solution of this problem meets with certain difficulties, as the separate observations, even when relating to the same eclipse, show considerable dispersion, which may conceal the real changes in the total light of the corona. The cause lies in the difficulty of accurate account of atmospheric extinction, when using the moon as a standard, in the uncertainty of extrapolation for the part of the corona eclipsed by the moon and in the heterogeneity of photometric systems used. Thus, one must use the best and homogeneous data only. Besides we find it better not to exterapolate the observations to the solar limb, but to reduce them to a standard zone corresponding to the most frequent observational conditions. The reduction error becomes thus sensibly less.

From all the numerous determinations of total light of the corona the most homogeneous group covering besides a large interval of time is formed by the photoelectric observations by J. Kunz and J. Stebbins (1918 and 1925) (3, 4), G. Briggs (1922) (5), J. Stebbins and A. Whitford (1937) (6). Unfortunately all these observations are referred to the moon (by means

of laboratory photometric standards) and only in the latter paper the account for atmospheric extinction may be considered as quite satisfactory.

The reduction of all these determinations of the total light of the corona to the zone (1.030 $R_\odot$; 6.00 $R_\odot$), adopted by us as the standard one, gave some indications on the dependence on solar activity (7). It appeared interesting to test this supposition during coming eclipses.

It was desirable to do the observations with standard outfit and in a photometric system most close to that of the authors just quoted, which used potassium hydride photoelectric cells. But as to standardization, we find it more expedient to refer the observations to the sun. This simplifies essentially the account of the extinction and is more natural from the physical point of view. The reduction of solar light by approximately 10^6 times does not present great difficulties and may be done in different ways (8, 9, 10). May be, the best method is the application of a diffusing screen.

This method was first applied by one of us during the eclipse of June 19, 1936 observed with a specially designed photocell photometer (11). Unfortunately, this observation was done with a cesium-oxyde diffusion photoelectric cell, whose spectral sensitivity curve was very accurately adapted to the visibility curve by means of a special colour filter. This causes some difficulties in the comparision with other photoelectric observations, done with potassium photocells, inasmuch as the identity of the spectral composition of the radiation of sun and corona cannot be considered as safely stated (12).

A diffusion screen was also applied, upon the advice of one of us, by N. I. Tshudovitshev and K. V. Kostilev in the construction of a photocell photometer according to a similar principle as our photometer of 1936. These authors have successfully observed the eclipse of September 21, 1941 with a Kunz potassium photocell. This observation presents special interest for the problem in question. Unfortunately, we possess only preliminary results of their work (13) based on preliminary measurement of the geometric and optical constants of the photometer and an adopted value of the coefficient of the gypsum screen used. Thus we are bound to await with interest the publication of the final results of this observations.

For observations of the eclipse of September 21, 1941 we designed in the Astronomical Institute a new photometer (based on the same principles as the 1936 apparatus), which we called the «coronal electrophotometer». The war-time conditions did not allow to apply this new photometer to the observations of the 1941 eclipse and to do the observations in parallel with Tchudovitshev and Kostilev, as it was planned. We were able to use the new photometer only for the eclipse of June 9, 1945.

THE OPTICAL SYSTEM OF THE CORONAL ELECTROPHOTOMETER

The requirements imposed to the choice of the optical scheme of the photometer were: the possibility of the most accurate comparision of the brightness of objects of different photometric structure and the possibility of reduction of the solar light by about 10^6 times. Besides, inasmuch as the photometer can be applied not only to the photometry of the corona but also to the comparison of the sun, moon and stars, we imposed a complementary condition of enlarging the range of reduction to 10^{11} times.

The optical system is represented on fig. 1; it is analogous to that of the stellar photocell photometer of the Astronomical Institute of the Academy of Sciences of the USSR (14).

In the focal plane of an achromatical objective O_1 ($F = 355$ mm; $d = 44$ mm) is placed a disc with changeable diaphragms D, limiting the

field of view the instrument (Table I). A double lens O_2 ($d = 62.5$ mm; $F = 125.8$ mm) of a condensing type projects the image of the objective O_1 on the sensitive layer of the photocell Ph. Thus the photocell is so adjusted that its layer coincides with the exit pupil of the optical system, where the illumination is always uniform, and does not depend on the photometric

TABLE 1

Diaphragm	Diameter	Notes	Diaphragm	Diameter	Notes
D1	7°.05	circular	D5	2°.00—1°.25	annular
D2	7.05—4.54	annular	D6	1.25—0.75	»
D3	4.54—3.00	»	D7	0.75	circular
D4	3.00—2.00	»	D8	0.40	»

structure of the observed object, and depends only on the total light flux passing through the diaphragm D.

In this way is secured the possibility of correct comparison of objects of different structure even if the surface sensitivity of the photocell is quite non uniform.

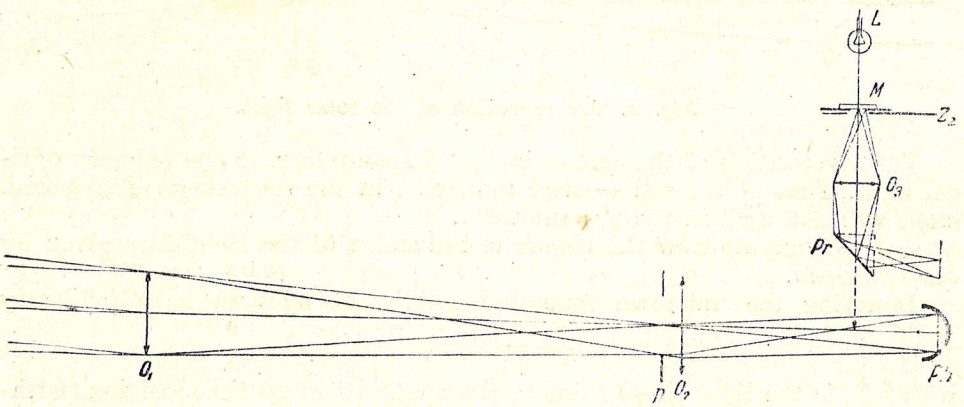

Fig. 1. Optical systems of the photometer and the photometric standard

To control the changes in the light-sensitivity of the photometer due to the changes of the filament current of the amplifier, the temperature coefficient of the grid resistor a. s. f., and to secure the reductions of observations for these changes, the instrument is supplied with a photometric standard, whose optical scheme is also given on Fig. 1. When the standardizing device is introduced as a whole in the optical path of the photometer, the image of a ground glass plate M illuminated by an incandenscence lamp L is projected by the lens O_3 on the photocell Ph. The dimensions and position of this image correspond to the exit pupil of the primary optical system.

THE STANDARDIZATION METHOD

The reduction of solar light was effectuated in the following way (Fig. 2). In the place of the photoelectric cell, strictly in the plane of the exit pupil was placed a barite screen S_1. A small changeable diaphragm d' placed on a distance r from the centre of the screen cuts out from the whole diffused light flux only a small part. The photocell is placed now behind the

diaphragm d' on such a distance that the illuminated part of its photocatode should be equal in dimensions to the exit pupil of the primary optical system. In this way are warranted equal conditions for the illumination of the cell in both positions.

To strengthen the reduction still more, with the purpose of comparison of the sun and stars, there is provided a supplementary «stage of reduction» analogous to that just described. In this case the photocell is replaced by a second barite screen S_2 and the former is transferred in the plane P, behind the second small diaphragm d''.

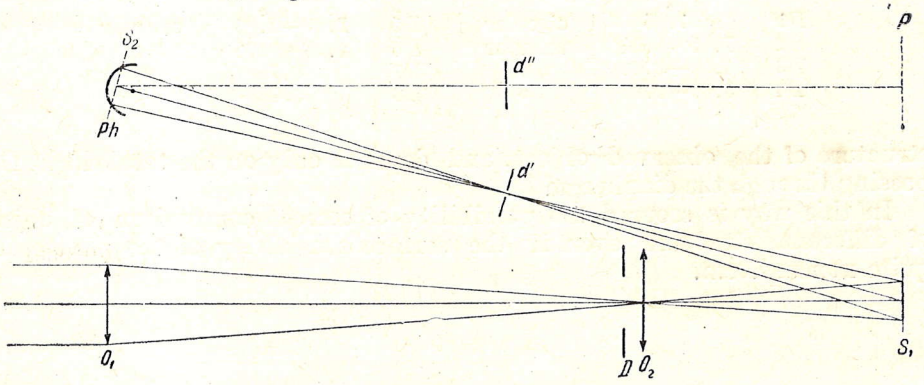

Fig. 2. The reduction of the solar light.

The observation of the corona is done immediately in the primary optical path. That of the sun — after reduction in the first stage. The second stage was not used in the present work.

Let us compute now the degree of reduction of the light flux given by our «reducer».

Denoting the unknown reduction coefficient by n we have evidently

$$n = F_0/F_1$$

where F_0 is the light flux falling on the photocell in its first position (without reduction) and F_1 — in the second one (after reduction).

Further

$$F_0 = E\sigma$$

where E is the illumination of the exit pupil of the primary optical system and σ — the area of this pupil.

The light flux F_1 which has passed through the diaphragm d' will be obviously equal to

$$F_1 = \omega B\sigma'$$

where B is brightness of the illuminated barite screen, σ' — the area of the diaphragm d' and ω — the solid angle under which the illuminated part of the screen is seen from the centre of the diaphragm d'

$$\omega = \frac{\sigma \cos \alpha}{r^2}$$

where α is the angle between the optical axes of the photometer and reducer.

If Lambert's law holds for the given screen

$$B = \frac{1}{\pi} \delta E$$

where δ is the coefficient of diffuse reflexion of the screen.

Denoting by ρ the radius of the diaphragm d' we find:

$$F_1 = \delta\sigma E \cos\alpha \left(\frac{\rho}{r}\right)^2$$

whence finally

$$n = \frac{1}{\delta}\left(\frac{r}{\rho}\right)^2 \sec\alpha. \qquad (1)$$

If the law of Lambert is not applicable to the given screen, its coefficient of diffuse reflexion must be determined for the same conditions of illumination and observation as these in the photometer.

It is seen from formula (1) that the required order of n is received at r and ρ of the order of 300 mm and 0.5 mm respectively.

PHOTOELECTRIC CELL

As it was desirable to receive the observations in the same photometric system as the above mentioned photoelectric measurements, we chose a K u n z gasfilled potassium hydride photoelectric cell.

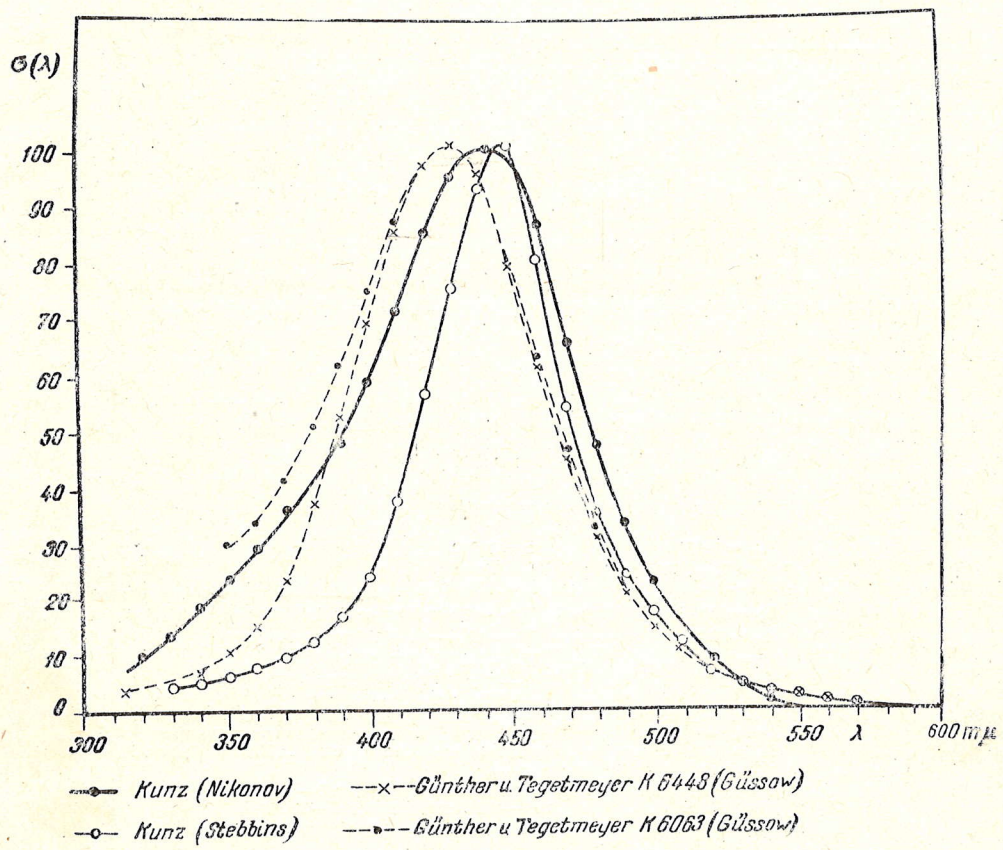

Fig. 3. Relative colour sensitivities of some potassium-hydride photoelectric cells.

The spectral sensitivity of this cell was determined by us at the Abastumani Astrophysical Observatory with the help of a Zeiss quartz monochromator. The source of light was the sun observed near the meridian.

6*

The solar light was thrown into the laboratory by means of a siderostat with an alluminium coated mirror.

The curve of spectral sensitivity received (Fig. 3) differs somewhat from that given by Stebbins (15); however many authors who worked with Kunz photoelectric cells mark their rare uniformity as concerns colour properties. In Fig.3 are shown also for comparison two curves received by M. Gussow (16) for potassium photocells by Günther & Tegetmeyer.

MEASUREMENT OF PHOTO-CURRENT

The immediate measurements of photo-current from the corona with a galvanometer may present some difficulties in field conditions, the more

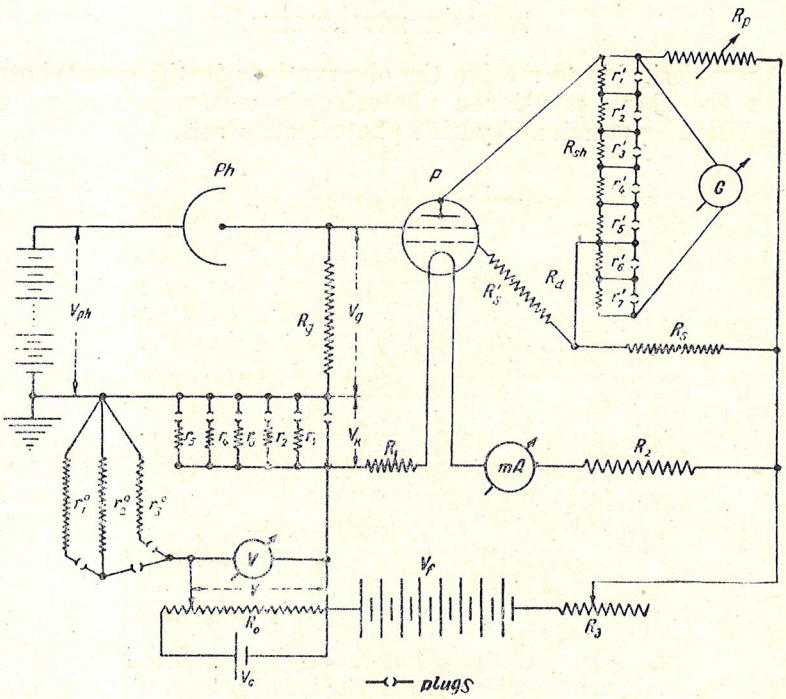

$R_g = 5.10^8\ \Omega$
$R_1 = R_2 = 50\ \Omega$
$R_3 = 21\ \Omega$
$R_S = 6000\ \Omega$
$R_S = 2000\ \Omega$
$r_1' = 200\ \Omega$
$r_2' = 500\ \Omega$
$r_3' = 1000\ \Omega$
$r_4' = r_7' = 5000\ \Omega$
$r_5' = r_6' = 10000\ \Omega$
$R_p = 15000\ \Omega$
$R_0 = 60\ \Omega$
$r_1^0 = r_2^0 = 50000\ \Omega$
$r_3^0 = 1000\ \Omega$
$r_1 = 50\ \Omega$
$r_2 = 100\ \Omega$
$r_3 = 200\ \Omega$
$r_4 = 500\ \Omega$
$r_5 = 1000\ \Omega$
V_{ph} ~100 v (dry cells battery)
V_f = 12.5—14 V (storage battery)
V_c = 1.4 V (dry cell)
Ph—Kunz' Photoelectric cell)
p — Pliotron FP—54
G — Löhle galvanometer (current sensitivity 5.10^{-9} A/d; internal resistance ca 2000 Ω; critical resistance ca 20000 Ω; period 0.5 sec.),
V—precision voltmeter 0—3V
mA—millampermeter 0—300 mA

Fig. 4. Electric circuit of the photometer.

that our photometer was designed also for the measurements of small ring zones of the corona. We chose therefore the well known one tube direct current amplifier by Du Bridge-Brown (17) with a Pliotron FP — 54 General Electric (Fig. 4).

For eclipse observations the maximum speed of work is desired. One must thus aim at maximum reduction of the time constant of the amplifier and of the period of the galvanometer. We chose a grid resistor of $5.10^8\,\Omega$ and used a Löhle galvanometer, combining high current sensitivity (5.10^{-9} A/d) with a very short period (0.5 sec.). The time of deflection of the galvanometer in the scheme of the amplifier proved to be less than one second.

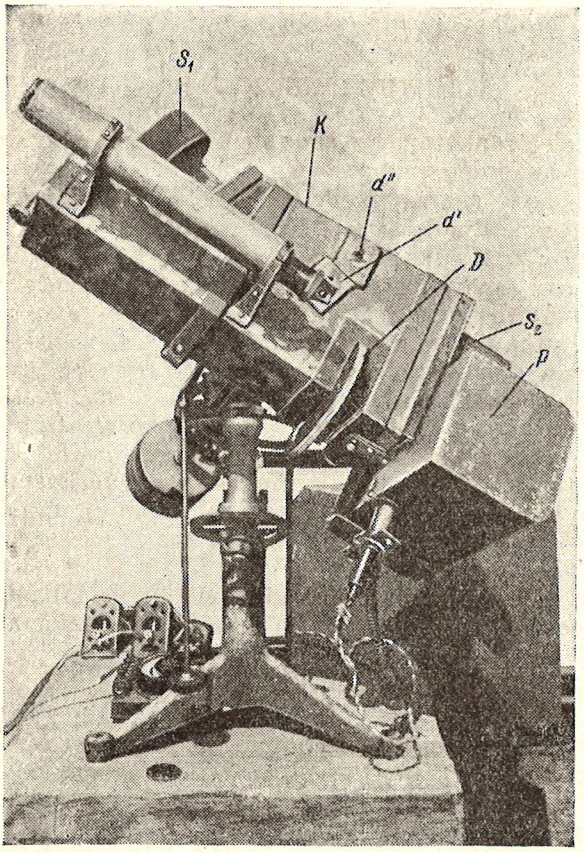

Fig. 5 Coronal electrophotometer

K—main body, *p*—photocell box, S_1, S_2—screenholders, *D*—disc with diaphragms, *d'*,*d''*—reducing diaphragms

The sensitivity of the galvanometer may be regulated by a shunt R_{sh} and an auxiliary resistance R_d. The sum of these resistances must be approximately equal to the critical resistance of the galvanometer.

The amplifier is supplied with a special device (the «Sensitivity control») for calibration, which allows to apply on the control grid of the tube known potentials of required order. As will be seen from Fig. 4 the potential applied to the grid will be

$$V_k = \frac{r_i}{r_i + r_j^0} V \qquad (i = 1, 2, 3, 4, 5; j = 1+2, 2, 3) \qquad (2)$$

where V is the potential supplied from the potentiometer R_0. If r_i is taken much less then r_j^0, V_k may be as small as necessary. The sensitivity control

may be used also for the compensation method of measurements of the photo-current.

Some data characterising the photoelectric part of the coronal electrophotometer are given in Table II.

TABLE II

Acceleration potential on the photoelectric cell	104 *V*.
Working sensitivity of the amplifier ($R_{sh}=5\,000\Omega$, $R_d=15\,000\,\Omega$)	900 d/*V*
Current amplification	7.10^3

THE PHOTOMETER

The coronal electrophotometer consists of the main body (K), photocell box (p) and screenholders (S_1) and (S_2) (Fig. 5).

In the main body are mounted: the shutter Z_1, the objective O_1, the disc with changeable diaphragms D, the condensing lens O_2 and the changeable reducing diaphragms d' and d''.

The cell box may be fastened on the main body in two positions corresponding to the observation of the corona and sun. It contains the photocell, the electrometer valve and the grid resistor. The cell box is supplied with a shutter necessary for the protection of the photocell from light when changing its position. With the shutter is mechanically connected the system of the photometric standard. When the shutter is closed, the standardization device is introduced before the photocell and the latter can be illuminated with the standard, if the supplementary shutter Z_2 (Fig. 1) is opened. The photocell box is connected with the control panel of the amplifier by means of wires enclosed in a shielded covering. The control panel is enclosed in a screened box.

The coronal electrophotometer is attached to a small parallactic mounting without clock drive; so the guiding must be done by hand.

EXAMINATION OF THE INSTRUMENT

The selective properties of the photometer must be examined, the amplifier calibrated and the reduction coefficient determined experimentally.

The spectral sensitivity of the photocell used was shown above (Fig. 3).

The calibration of the amplifier is necessary inasmuch as the electrometer valve is working on the nonlinear part of its characteristic and the deviations from the proportionality between the potential applied to the grid and the corresponding galvanometer deflections may surpass the limits of accuracy of the measurements. The calibration must be done for the working conditions of the amplifier; it was done on the eclipse day. Its result will be given below (Fig. 8).

The determination of the reduction coefficient is possible in two ways. The first is the use of formula (1). If the geometric parameters r, ρ and α are measured and the coefficient of diffuse reflection δ determined in the laboratory, we can compute the reduction coefficient n. Another way is an immediate determination of n, when the same light source is observed in both positions of the photoelectric cell. The difficulty of this method lies in the necessity of a supplementary gradation of the light source $\sim 12^m$, if even the largest diaphragm d' is used.

We have used in the present work the second method. The determination of the reduction coefficient was done in the laboratory of the Abastumani Observatory. The light source was a 100 W searchlight lamp, controlled by means of a precision ampermeter and moved along a photometric bench

of 8.5 meter length. The supplementary reduction was effectuated by means of a rotating sector, reducing the light by $4^m.99$. The total reduction of the light of the lamp reached approximately 9^m. The remaining 3^m were accounted for by the application of the compensation method of measurement of the photo-current. The «IR drop» was compensated with a potential applied to the grid from the sensitivity control [formula (2)].

The galvanometer served only as a null-instrument stating the equality

$$V_g + V_k = 0.$$

So in this method the photo-current is measured with the compensating potential and thus the influence of the amplifiers nonlinearity is completely excluded.

One could suspect some dependence of the reduction coefficient on the spectral composition of the radiation (owing to spectral selectivity of the coefficient of diffuse reflection of the screen). So there was no certitude that the determination of the reduction coefficient n, done with K u n z' photoelectric cell and artificial light source (with colour temperature $\sim 2800°$) would yield the same value as that with the solar radiation. For this reason we used an antimony-cesium photocell (characterized by a very wide spectral curve) (18) in combination with colour filters of Schott BG_3 and GG_{11} and an Ilford Daylight Filter (N 810).

TABLE III

Filters	λ_{eff}	$\Delta m = 2.5 \log n$	Filters	λ_{eff}	$\Delta m = 2.5 \log n$
BC_3	408 mμ	$12^m.08 \pm 0^m.01$	$GG_{11} + 810$	524 mμ	$12^m.08 \pm 0^m.01$
GG_{11}	544	12.04 ± 0.01	810	443	12.04 ± 0.01
$BG_3 + 810$	387	12.12 ± 0.01			

The results are shown in Table III and Fig. 6. There is really some tendency of a dependence of the reduction coefficient on spectral composition of the radiation.

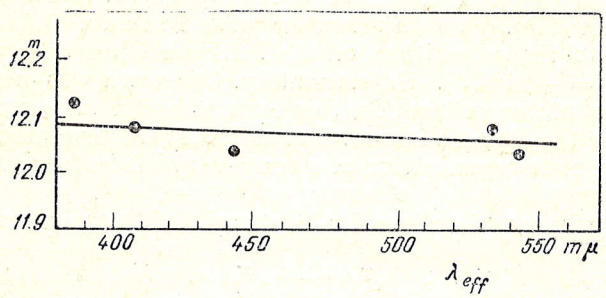

Fig. 6. Dependence of the reduction factor upon colour.

For the K u n z photoelectric cell and solar radiation we find $\lambda_{eff} = 440$ mμ, whence on the basis of Fig. 6:

$$\Delta m = 12^m.08 \pm 0^m.02.$$

The accuracy of this determination is quite sufficient for our purpose when we deal with changes of the total light of the corona by many tens of percents.

To control the value of Δm thus found we estimated it also by the first method. The measurement of the geometric parameters of the photometer gives

$$r = 302.9\text{mm};\ \rho = 1.182\text{mm};\ \alpha = 15°.1$$

We have not examined our diffusing screen in the colour system: K u n z photocell — solar radiation. But this screen was formerly examined with a thermocouple for solar radiation reflected by a silvered mirror and filtered by a water cell (19). On the basis of these measurements we find for δ a very high value 0.98. But this value was confirmed by visual measurements in the State Optical Institute. From these data we find for the reduction coefficient expressed in stellar magnitudes $\Delta m = 12^m.10$, what agrees well with

TABLE IV

Diaphragm	Diameter	Δm	n
$d'1$	0.820 ± 0.001 mm	$14^m.38$	$655. . 10^5$
$d'2$	1.265 ± 0.001	13.44	$2.38 \cdot 10^5$
$d'3$	1.774 ± 0.003	12.70	$1.20 \cdot 10^5$
$d'4$	2.363 ± 0.001	12.08	$6.79 \cdot 10^4$

the value $12^m.08$ received above. But inasmuch as we posess for the coefficient of diffuse reflexion of the screen under consideration only an approximate value (related to a quite different colour system), we chose only the first value of Δm. On the basis of this value and these of the diameters of the reduction diaphragms d' measured with a precision measuring engine, we find the following values of the reduction coefficients collected in Table IV.

THE SITE OF OBSERVATION

The eclipse of July 9, 1945 was of short duration; it reached its maximum length in USSR ($60^s.3$) on the frontier with Finland.

We joined to the expedition of the Pulkovo Observatory at Sortavala ($\lambda = 30°11'; \varphi = +61°42'$). Unfortunately, this town was not situated on the central line of the eclipse. In this respect better sites were the village Lahdenpohja or the Valaam island. But as Sortavala presented many advantages with respect to organization of a temporary laboratory a. s. f., we chose that point.

The circumstances of eclipse for Sortavala (20) are given in Table V.

TABLE V

Mean Greenwich time of beginning of totality	$T = 14^h\ 9^m.3$
Duration of totality	$\tau = 51^s$
Zenith distance of the sun	$z_\odot = 57°3$
Air mass	$F(z_\odot) = 1.848$
Ratio of the apparent diameters of moon and sun	$D_\mathbb{C}/D_\odot = 1.015$
Apparent radius of the sun	$R_\odot = 943.''9$
Distance between centres of the sun and moon	$\Delta = 0.0064 R_\odot$

In view of the short duration of totality we decided to limit ourselves with the measurements of total light of the corona.

After testing the photometer in the laboratory it was settled in a small wooden pavillion.

Training observations showed that notwithstanding that the time of deflection of the galvanometer had been less than one second, the consecutive readings could be done and written down no faster than through 3—4 sec. This defined the following program. Before totality the photometer is directed to the sun, the greatest circular diaphragm D1 set and the galvanometer read at the closed shutter. Immediately after beginning of totality the shutter is opened and the measurement done with the diaphragm D1, then without closing the shutter the greatest annular diaphragm D2 is introduced and after that consecutively the diaphragms D1 and D2; finally the determination is done through the annular diaphragm D4 and only after that the shutter closed. Then the whole series is repeated in reverse order.

We had no special device for turning the whole photometer in azimuth (by 7—8°), that seems the best method of accounting for the background effect. As known the isophotes of the sky background during totality run nearly horizontally. The shift of the instrument (by both coordinates or even by one) would take too much time for return setting on the corona. It was impossible in an eclipse of so short duration.

However, our diaphragm D2 encloses a zone so distant from the sun that we can neglect for it the effect of coronal radiation and adopt that the whole radiation passing through it comes from the sky background only. Really if B a u m b a c h's mean law of distribution of surface brightness in the corona (21) is true, the radiation of the zone extending from the solar limb to the radius R (in solar radii), will be (22)

$$E(1;R) = 1.000 - 0.189\,R^{-0.5} - 0.507\,R^{-5} - 0.304\,R^{-15} \qquad (3)$$

where the radiation from the whole corona $E(1;\infty)$ is taken as unity. Using this formula we find that the radiation passing through the diaphragm D2 amounts no more than 1.5% of the whole coronal radiation. It is easy to compute from the formula (3) that only the zone lying within 1°.5, or even 1°.0 from the sun's centre is of importance for the total light of the corona. This is confirmed by the photoelectric observations by T s h u d o v i t s h e v and K o s t i l e v (23) according to which the photometric limit of the corona lies about 1° from the sun's centre. Thus, we can admit with sufficient accuracy that we observe in the diaphragm D2 only the sky effect. But for control of this conclusion we included in our program the observation through the diaphragm D4 cutting out the zone 1°.0—1°.5.

The weather on the days preceding the eclipse was unfavourable. The morning of the eclipse day was cloudy but gradually the sky began to clear up and on 9^h30^m GMT we could begin the observations of the sun. Before the first contact some clouds were passing but during totality the sky was quite clear. The air was extremely transparent.

Immediately before the totality we made the observation of the photometric standard which gave the deflection

$$\Delta n_{s_1} = 95.1.$$

The observations of totality done in complete accord with our program are given in Table VI.

TABLE VI

T	n_0	D1	D2	D4	T	n_0	D1	D2	D4
s					s				
0	188.8				28				191.2
4		237.0			32			200.9	
8			200.4		36		236.9		
12		234.8			40			201.9	
16			200.4		44		235.4		
20				191.2	48	188.6			
24	189.2								

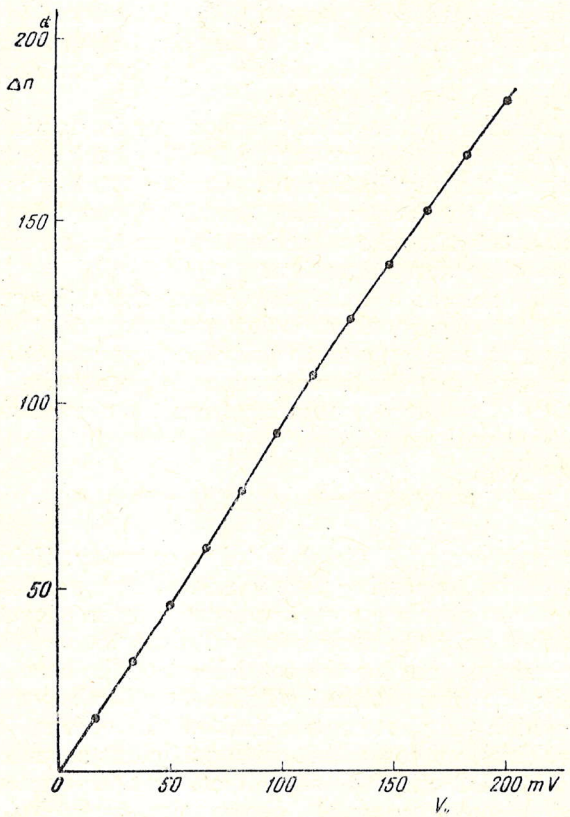

Fig. 7. Calibration curve of the amplifier for its working sensitivity ($R_{sh} = r'_4 = 5000\,\Omega$; $R_d = r'_6 + r'_7 = 15000\ \Omega$).

The observation of the photometric standard after totality gave

$$\Delta n_{s_2} = 96.6$$

whence the value corresponding to totality is

$$\Delta n_s = 95{,}8 \pm 0.8.$$

The calibration of the amplifier done shortly after the observations of the corona shows that the galvanometer deflections are proportional within the limits of the measurement errors to the potentials applied to the amplifier in their whole working diapason (Fig. 7).

There was no zero drift during totality. Thus taking the mean from the galvanometer deflections, we receive Table VII.

The mean error of one reading, as shown by Table VI, is ± 0.7.

To account for the influence of the sky background we must know the relative areas of the diaphragms used. As in the annular diaphragms the central screens are fastened on three strips, we preferred to determine the area ratio in a photometric way from the observations of the sky.

The ratios were found to be

$$D1 / D2 = 1.734 + 0.004;$$

$$D4 / D2 = 0.176 \pm 0.002$$

From these values we find that the background effect for D1 is equal

to 20.8 and consequently the deflection for the corona is

$$\Delta n_k = 26.3 \pm 0.8$$

TABLE VII

Diaph.	Δn
D1	47.1 ± 0.5
D2	12.0 ± 0.4
D4	2.3 ± 0.0

Let us see if the conclusion drawn by Tshudovitshev and Kostilev that the corona is limited by the angular diameter of 2° is correct. The background

TABLE VIII

MGT	$F(z_\odot)$	$\Delta n'_\odot$	Δm	MGT	$F(z_\odot)$	$\Delta n'_\odot$	Δm
h m			m	h m			m
9 32	1.299	127.6	+0.311	12 29	1.454	121.7	+0.260
43	1.294	127.6	+0.311	49	1.507	119.6	+0.241
59	1.293	129.0	+0.323	15 18	2.377	91.5	−0.050
11 39	1.357	124.4	+0.284	26	3.441	67.3	−0.384
42	1.359	125.3	+0.292				

effect for D4 will be obviously 2.1 ± 0.1, that within the limits of accuracy corresponds to the observed value 2.3. This confirms the correctness of our account for the sky background.

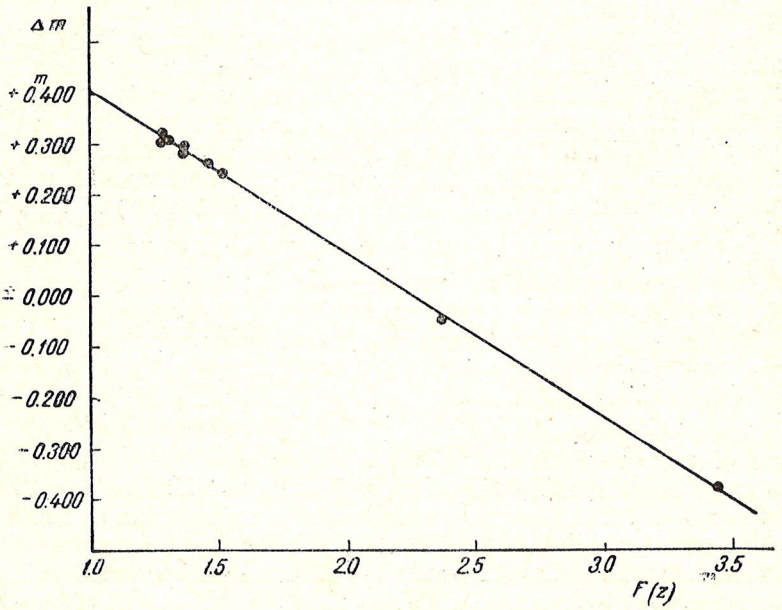

Fig. 8. Extinction on the day of the eclipse.

The observations of the sun done with the reducer before and after the eclipse are given in Table VIII and on the Fig. 8. In the first column are

given the mean Greenwich moments of observations; in the second — the air masses; in the third — the mean deflections for the sun reduced to the sensitivity of the photometer corresponding to the moment of totality; finally, in the fourth column are given the ratios of the deflections for the sun and photometric standard expressed in stellar magnitudes.

On the basis of the Table VIII a Bouguer line was drawn which is represented by the least squares method

$$\Delta m = \underset{\pm 0.006}{0.^m733} - \underset{\pm 0.003}{0.^m326}\, F(z_\odot) \qquad (4)$$

The mean error of representation of one observation of the sun equals $\pm 0.^m006$.

Interpolating by the formula (4) for the moment of the totality we find $\Delta m = +0.^m131$ whence the deflection for the sun becomes (taking in mind that for the standard $\Delta n_s = 95.8$)

$$\Delta n'_\odot = 108.1 \pm 1.4.$$

It must be noted that such an interpolation remains quite admissible also in the case of monotonous changes of the extinction. In this case the Bouguer line will remain nearly rectilinear, although it will be turned about the point corresponding to the passage through the meridian (24). Another thing will be if in the moment of totality occurred a sudden change of extinction with subsequent return to the initial value. But, as is shown by a preliminary reduction of special observations done at Sortavala by the Pulkovo expedition, no changes of extinction during totality occurred.

If the spectral composition of the radiation of the corona and sun is identical, we shall completely exclude the influence of extinction when comparing the deflection for the corona with that for the sun interpolated for totality. But if the radiation of corona and sun is of different composition, their observations must be reduced to no atmosphere with different values of extinction factors.

In the present reduction of our observations we chose the first supposition, although, as already stated above, we consider the identity of the spectral composition of the radiation of sun and corona to be still an open question (25). In any case we have as yet no trustworthy value for the colour excess of the corona, if the latter exists in reality. Assuming the colour of sun and corona to be identical and starting from the above found value for the reduction coefficient for the diaphragm $d'1$ (Table IV) we find that the deflection for the direct observation of the sun would be

$$\Delta n_\odot = (6.1 \pm 0.2) \cdot 10^7$$

whence we find for the total intensity of the observed zone of the corona $(1.015 R_\odot;\ 8.67 R_\odot)$:

$$E_k(1.015;\ 8.67) = (0.43 \pm 0.03) \cdot 10^{-6}$$

in terms of solar radiation.

One must keep in mind that Sortavala was not situated on the central line of the eclipse. The distance between the centres of sun and moon in the moment of totality was $0.006 R_\odot$ (Table V). It is easy to compute the reduction to the central line adopting some law of distribution of surface brightness in the corona. But it is more expedient first to estimate its order of magnitude. Let us see how the observed value of total light of the observed zone will change if the radius of its interior limit is reduced by $0.006 R_\odot$. Using form. (3) we find that, in this case, the total light will change only by

$0.02 \cdot 10^{-6}$. It is easily seen that this change no less than twice exceeds the reduction in question. Whence we may conclude, that this reduction will not exceed $-0.01 \cdot 10^{-6}$. There are, thus, no reasons to make detailed computations, considering the general accuracy of the determination of the total light of the corona.

Reducing the above found value for the coronal radiation to the standard zone ($1.030R_\odot$; $6.00R_\odot$) by formula (3) we find:

$$E_k\,(1.030; 6.00) = 0.38 \cdot 10^{-6}.$$

It is essential to estimate the error introduced by this reduction, which comes from the deviation of the true law of brightness distribution for the given eclipse from the adopted mean law, according to Baumbach. For this purpose, we did the reduction to the standard zone using different laws of brightness distribution, notably those based on the observations of the inner corona. For the reduction in question of greatest importance is the distri-

TABLE IX

Authors	Distr. law	E_k (1.030; 6.00)
Turner (26), Pettit and Nicholson (27)	$R_\odot{}^{-6}$	$0.41 \cdot 10^{-6}$
Young (28)	$R_\odot{}^{-8}$	0.39
Becker (29)	$(R_\odot - 0.720)^{-4}$	0.38
Balanovsky and Perepelkin; (30) Jenvall (31)	$(R_\odot - 0.854)^{-3}$	0.37

bution of brightness up to $1.060R_\odot$, i. e. only to 1′ from the limb. Thus, the well known law of fall of brightness $\sim (R_\odot - 1),^{-2}$ which obviously does not hold at the limb, must evidently be rejected.

The laws used and the results of their application are shown in Table IX.

We see that the results are very close. The difference does not exceed 10% from that received by form. (3). Thus, we adopted for the measure of the relative error of reduction to the standard zone the value 10%. Considering this, we receive finally that the total light of the standard zone of the corona of July 9, 1945 is

$$E_k\,(1.030;\ 6.00) = (0.38 \pm 0.06) \cdot 10^{-6}$$

CONCLUSION

The received value is appreciably less than has been found before from photoelectric measurements as seen from Table X (32). In this Table are

TABLE X

Date	Observers	Observed zone	Reduct. factor	E_k (1.030; 6.00)
8/I 1918	J. Kunz, J. Stebbins	1.024— 7.50	0.947	$0.91 \cdot 10^{-6}$
20/IX 1922	G. Briggs	1.056—10.25	1.147	0.62
24/I 1925	J. Kunz, J. Stebbins	1.027— 7.50	0.969	0.82
8/I 1937	J. Stebbins	1.057— 5.63	1.197	1.08
9/VII 1945	V. Nikonov, E. Nikonova	1.015— 8.67	0.885	0.38

given only photoelectric observations done with potassium photoelectric cells which warrants the homogeneity of the photometric system of the compared observations.*

On our opinion the data given in the Table X confirm the reality of changes in the total light of the corona.

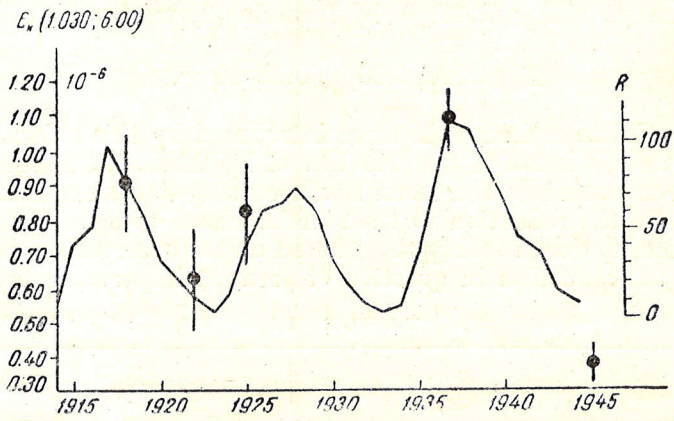

Fig. 9. Dependence of total light of the corona on solar activity

When discussing the radiometric observations of the corona of September 21, 1941 one of us suspected the dependence of total light of solar corona on solar activity. In this connection we confronted on Fig. 9 the data of Table X to the mean Wolf relative spot numbers (R). This figure does not contradict to the suggestion made. Really the 1945 corona observed a year after minimum proved to be much fainter than the corona observed during the maximum in 1937.

Thus we come to the conclusion that there are really appreciable changes in the total light of the solar corona. The corona proves to be brighter in the epochs of maxima of solar activity and fainter in epochs of its minimum.

For the further study of the dependence under consideration it seems desirable to do with our photometer systematic observations of the corona during coming eclipses, completing them with colorimetric observations.

AKNOWLEDGEMENTS

We find it a pleasant duty to express our thanks to Professors V.A. Krat and A. V. Markov of the Pulkovo Observatory for their care in the organization of the joint expedition at Sortavala.

We are much obliged to E. K. Kharadze, director of the Abastumani Astrophisical Observatory for putting at our disposal all the possibilities of the Observatory for the examination and improvement of the coronal electrophotometer during our work at Mt Kanobili.

Our thanks are due also to V. V. Vikhrov, mechanician of the Abastumani Observatory for his help in the preparation of our photometer at Mt Kanobili as well as at Sortavala.

* It must be noted that if the corona is redder than the Sun, its total light shall be even smaller, as in this case the reduction to no atmosphere shall be greater for the Sun than for the corona.

1. L. Dyson, R. v, d.R. Woolley. Eclipses of the sun and moon. p. 117, 1937.
2. S. Mitchell. Handb d. Astroph. **IV**, 338, 1929.
3. J Kunz, J. Stebbins. Ap. J. **49**, 137, 1919.
4. J. Kunz, J. Stebbins. Ap. J. **62**, 115, 1925.
5. G. Briggs. Ap. J. **60**, 273, 1924.
6. J. Stebbins, A. Whitford. Ap. J. **87**, 225, 1938,
7. V. Nikonov. Bull. Abastumani Obs. N. 7, 66, 1943.
8. G. Rougier. Ann. Obs. Strasbourg III, fsc. 5, 260, 1937.
9. E. Pettit, S. Nicholson. Ap. J. **62**, 209, 1925.
10. Calder. Harv. Ann. **105**, 445, 1937.
11. L. c., p. 63.
12. V. Nikonov. L. c., p. 68.
13. N. Tshudovitshev, K. Kostilev. Astr. Jour. Sov. Un. **20**, 8, 1942.
14. V. Nikonov, P. Kulikovsky. Astr. Journ. Sov. Un. **16**, 54, 1939.
15. J. Stebbins. Publ. Washburn Obs. XV, part 2, 219, 1934.
16. M. Güssow. Zs. Aph. **14**, 305, 1937.
17. L. Du Bridge, H. Brown. Rev. Sc. Inst. **4**, 532, 1933.
18. S. Lukjanov. Jour. Techn. Phys. (russian) 9, N. 13, 1939,
19. V. Nikonov. Bull. Abastumani Obs. № 7, 47, 1943.
20. H. Grönstrand. Medd. f. Abo Akad. Astr. Obs. N. 3, 39, 1944.
21. Baumbach A. N. **263**, 126, 1937.
22. V. Nikonov. L. c., p. 61.
23. L. c., p. 13.
24. V. Nikonov. Bull. Acad. Sc. Georgian SSR. III, N. 6, 509, 1942.
25. V. Nikonov. Bull. Absatumani Obs. N. 7, 68, 1943.
26. Turner. Proc. Roy. Soc. **68**, 36, 1901.
27. L. c., p. 219.
28. Young. Lick Obs. Bull. N. 205.
29. L. Becker. Phil. Trans. (Ser. A) **207**, 307, 1905.
30. I. Balanovsky, E. Perepelkin. M. N. **88**, 740, 1928.
31. Jenvall. Astr. Jaktagelser och Und. Stockholms Obs. **11**, 8.
32. V. Nikonov. L. c., p. 67.

ЭЛЕКТРОФОТОМЕТРИЯ СОЛНЕЧНОЙ КОРОНЫ 9 ИЮЛЯ 1945 г.

В. Б. НИКОНОВ и Е. К. НИКОНОВА

Светимость солнечной короны была определена во время полного солнечного затмения 9 июля 1945 г. посредством коронального электрофотометра, разработанного нами и построенного в Астрономическом Институте АН СССР еще в 1940 г.

Оптическая схема прибора приведена на фиг. 1, а данные о диафрагмах, ограничивающих поле зрения, в табл. I. Для стандартизации по солнцу электрофотометр имеет специальное приспособление, использующее метод рассеивающего экрана. Схема приспособления дана на фиг. 2. Коэффициенты ослабления могут определяться либо непосредственно, либо по форм. (1). Значения для этих коэффициентов, определенные первым способом, даны в табл. IV.

В качестве светоприемника был применен газополный гидрированный калийный фотоэлемент Кунца (Kunz), спектральная чувствительность которого приведена на фиг. 3. Измерение фототока велось при помощи усилителя постоянного тока Дю Бриджа-Броуна (Du Bridge-Brown) с электрометрической лампой FP-54 (фиг. 4).

Усилитель имеет приспособления для градуировки, контроля чувствительности и измерения фототоков компенсационным методом.

Результаты градуировки приведены на фиг. 7, показывающей наличие пропорциональности между отбросами гальванометра и подведенными

к усилителю потенциалами. Некоторые данные о фотоэлектрической части прибора приведены в табл. II.

Общий вид прибора дан на фиг. 5.

Затмение наблюдалось в г. Сортавала Карело-Финской ССР. Обстоятельства затмения приведены в табл. V.

Результаты наблюдений короны, выполненных при ясном небе, приведены в табл. VI. В табл. VII даются средние значения отбросов для различных диафрагм.

Солнце наблюдалось в день затмения (табл. VIII, фиг. 8), что позволило надежно исключить влияние экстинкции.

Светимость наблюдавшейся зоны короны ($1.015R_\odot$: $8.67R_\odot$), где $R_\odot$ радиус солнца, оказалась равной

$$E_k\,(1.015;\ 8.67) = (0.43 \pm 0.03)\cdot 10^{-6}.$$

Приведение к зоне ($1.030R_\odot$; $6.00R_\odot$), принимаемой нами за стандартную, выполненное на основании среднего закона падения яркости в короне, данного Баумбахом (Baumbach), дает:

$$E_k\,(1.030;\ \ 6.00) = (0.38 \pm 0.06)\cdot 10^{-6}$$

Ошибка редукции к стандартной зоне была оценена из сопоставления редукций, вычисленных по различным законам (табл. IX).

Сравнение полученного нами значения светимости с другими фотоэлектрическими наблюдениями, выполненными в той же фотометрической системе и также приведенными к стандартной зоне, показывает наличие значительных изменений светимости короны; в эпохи максимумов солнечной деятельности она выше, чем в эпохи минимумов (табл. X, фиг. 9).

RESULTS OF OBSERVATION OF THE SPECTRUM OF THE CORONA OF JUNE 19, 1936

G. SHAJN

In this paper are given mainly the results of spectrophotometric study of emission lines in the spectrum of the inner corona.

1) The total intensity of emission lines changes from one region of the corona to another, as well as from one eclipse to another (Table I).

2) The comparison of spectrophotometric measurements of the spectra taken tn 1929 and 1936 bring out a considerable difference in the intensity ratio of emission lines, for instance, for 5303, 6374 and for 3801, 3987, 4086.

3) There is no proportionality between the fall of intensity for the emission lines and the continuous background with the increasing distance from the solar limb, the intensity gradient for the former being much larger. This holds for all the lines except 4231.

4) The observed irregularities in the curves representing the change of intensity of emission lines and the continuous background with increasing distance from the limb are to be primarily ascribed to the local effect.

5) The reality of the observed delay in the increase of or even the decrease of the intensity of emission lines with the approach to the limb from the distance about 1′ is doubtful. A decrease of the intensity at the distance less than 0′.5 may be perhaps suggested only on the basis of indirect considerations.

6) The change of intensity of the continuous background as a function of distance within 1′-6′ does not seem to be sensibly dependent on wave-length.

7) The density of matter responsible for the continuous background (electrons) decreases within 1′.5-5′.5 nearly from 1.6×10^8 to 0.28×10^8; the corresponding decrease for the particles responsible for the emission lines is nearly 6—7 times more rapid.

8) The wave-lengths have been measured for the emission lines 3801, 3987, 4086, 4231.

9) There is found no trace of absorption lines K and H in the spectrum of the inner corona. The comparison with the computed profile leads to striking discrepancy with the theory of thermal motion of free electrons scattering the solar light.

INTRODUCTION

For the observation of the total solar eclipse of June 19, 1936 at Omsk, Siberia, two single-prism slit spectrographs were used. One of them was so arranged to obtain the spectrum nearly along the solar equator, the slit of the second spectrograph crossed the disc along the diameter in high latitudes.

In the expedition took part V. A. Albitzky, P. Shajn and myself. In this paper are given the results of measurement of the spectrum of the corona,

obtained with the first spectrograph giving the dispersion about 36 A per mm at H_γ.

The main purpose of our observations was to obtain the spectrum of the inner and middle corona. Because of thin clouds at the time of the eclipse the corona did not extend more than 7′—9′ from the limb even in the brightest portion of the spectrum on the spectrogram. Our spectrogram is mainly suitable for the spectrophotometric study of the emission lines in the spectrum of the inner corona.

By means of a coelostat the sunlight was thrown into a Tessar object-glass of nearly 600 mm focal distance, giving an image (nearly 5 mm) on the slit of the spectrograph. The usual slit was replaced by a new one consisting of two separate halves, so that the spectra of the east and west sides of the corona may be obtained simultaneously at different width (nearly 0.035 for east and 0.050 for west). We had in view to get the spectra of the east and west sides of different photographic density, one more suitable for the study of emission lines, the other — for the absorption lines. We also used a new plate-holder allowing to get the photographic and visual regions of the spectrum simultaneously on two different plates, the most sensitive ones for the corresponding region (Imperial 1200 and Ilford Hypersensitive Panchromatic).

The beginning of exposure was about 10 sec. after totality and the end 10 sec. before the third contact, the duration being 120 sec. A series of spectra of a lamp was taken for calibration using the same spectrograph with a step slit. A series of spectra of the sun for comparison was also obtained.

The numerous tracings of different details of the spectral lines and the background of the corona were obtained with a self-registering microphotometer, supplied with a vacuum thermoelement. Two characteristic curves were obtained, one for 3800—4300 and another for 5300—6500, both showing within the limits under consideration no sensible dependence on wave-length.

SPECTROPHOTOMETRIC-STUDY OF EMISSION LINES

§ 1. In the investigation of coronal emission lines we have paid attention mainly to the study of the intensity change of emission lines as function of distance from the solar limb and to the comparison with the corresponding change of the continuous background at the same wave-length. The main purpose was to investigate whether the density of matter responsible for the emission lines and for the continuous background changes in space proportionally to the increasing distance from the solar limb. On the other hand, the emission lines are considered from the point of view of the constancy of their intensity.

In spectrophotometric studies of the corona it is very important to account for the fog due to the scattered light. The effect in question cannot be strictly accounted for. The comparison of the clear film on the spectrogram taken from the calibration lamp with the clear film corresponding nearly to the centre of the moon's disc shows that for the majority of the measured regions of the spectrum the microphotometer tracing of the latter is only 3 mm higher, the total deflection of the galvanometer being about 60 mm. This points out that the effect of the fog due to the scattered light is generally small. However, when necessary, the correction was added according to Schwarzschild's formula, for instance for 4231, 4566 and partly for 4086, 5303 and 6374 (1). Generally the measurements of the lines and continuous background did not extend on the low photographic densities, where the corrections for the fog become sensible. For the frequencies corresponding to the strongest chromospheric lines the effect in question is great, but for many

coronal lines it is negligible and only for 4231, 5303 and 6374 we may see a very faint trace of these lines on the moon's disc closely to the limb. (Fig. 1).

The following procedure was adopted for measurement. For each line and the adjacent portion of the continuous background a series of microphotometer tracings (10—20) was obtained. For separate portions of a line we are able then to compute the equivalent width or the total intensity $W = \int J d\lambda$ expressed in A. U. of the continuous background. This way is more long, but more complete as compared with that selected by G r o t r i a n, who for the study of the relative intensities of emission lines obtained but one tracing for a definite portion of a line (2'.5 from the limb). For the study of the intensity change along the line as function of distance from the limb G r o t r i a n measured on a Hartmann microphotometer a series of very narrow strips disposed along the line in its middle (2).

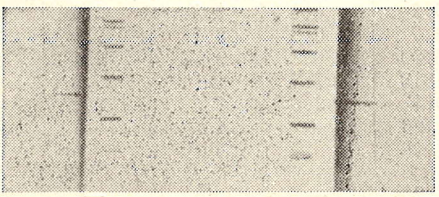

Fig. 1. The spectrum of the corona near the line 5303

For comparison of the different emission lines between them we took the mean value of the measurements of total intensity for the distance 1'.3—1'.8 from the limb of the sun (the observed distances from the moon's limb were respectively corrected). The results are represented in the second column of Table I for all the lines of the east side of the corona and for the west side only for 5303 and 6374. In order to make the lines comparable between them, the total intensities were multiplied by $F(\lambda)$, the energy distribution in the solar spectrum in arbitrary units (column 4). This seems to be plausible, since, according to current opinion, the energy distribution, at least in the inner corona, coincides with that of the sun. In the sixth column the intensity of 5303 was assumed to be equal to 100.

§ 2. The main result is that the intensity of emission lines changes absolutely and relatively within a large range. L y o t from the observations taken without eclipse has found still larger differences (3). From the comparison of the spectra of the east and west sides of the corona in 1936 and also from the comparison of the results of the 1929 and 1936 eclipses it is found that the equivalent width of emission lines expressed in units of intensity of the neighbouring continuous background changes from one region of the corona to another as well as from one eclipse to another. The changes cannot be ascribed to errors of observation.

The east side of the inner corona is brighter than the west one on our spectrogram. Taking account for the difference in the slit width for its east and west halves we can estimate that the continuous background at distances 1'.3—1'.8 from the east limb is nearly 2.6 times as bright as that at the same distance from the west limb. We were able to compare the east and west sides of the corona only with respect to the lines 5303 and 6374. From Table I it is seen that not only the absolute intensity of the same line does not remain constant, but even the intensity of the same line expressed in units of intensity of the neighbouring continuous background changes considerably when passing from one point of the corona to another.

In the light of these results it seems to be evident that when comparing the spectrograms obtained at different eclipses the intensity of the same emission lines may hardly be expected to be invariable. For instance, while in 1929 the line 5303 was 12 times as bright as 6374, the intensity ratio in 1936 is only 2.5 : 1. Further, in 1929 the line 3801 was very faint and 3987 fainter than 4086, while in 1936 the line 3987 is sensibly

TABLE I

Total intensities of emission lines

	1936 Omsk	1929 Sumatra	1936 Omsk	1929 Sumatra	1936 Omsk	1929 Sumatra
East						
3801	0.7	<0.1?	4.5	<1.0?	2.5	<0.4?
3987	1.1	0.2	8.6	1.8	4.7	0.7
4086	0.2	0.3	1.8	2.6	1.0	1.0
4231	0.7	0.8	6.4	7.0	3.5	2.6
4566	0.3[1])	0.3	3.1[1])	3.1	1.7[1])	1.1
5303	18.3	27.5	18.1	27.2	100	100
6374	9.4	2.0	7.4	2.2	40.9	8.1
6702	1.8[1])	—	1.3[1])	—	7[1])	5.4
West						
5303	5.2	—	5.1	—	28	—
6374	2.8	—	2.2	—	12.4	—

[1]) Very uncertain.

brighter than 4086, and 3801 is sufficiently intense. The fact of such large variations of absolute and especially of relative intensities of emission lines from one eclipse to another and from one point of the corona to another is of importance for the interpretation of the corona.* One may recall here the suggestion that the intensity at least of several chromospheric emission lines also undergoes to conspicuous variations. See, for instance, C i l l i é and M e n z e l s paper (4). In addition to this, one can indicate some features which are common for the coronal and chromospheric lines. It may be suggested that the same agency, probably the enormous excess of the far ultra-violet radiation is responsible for them, especially for the large variations in intensity of emission lines under consideration.

§ 3. W. G r o t r i a n measured in the spectrum of the corona of 1929 at varying distances from the limb the intensities of the lines plus the continuous spectrum and of the continuous spectrum alone. Our measurements give for different parts of the lines the equivalent width expressed in A. U. of the continuous background at the same distance from the limb. Our principal aim is at last to find the change of the density of matter in space and for this reason it is necessary to express the total intensity of different portions of a line in the same units. As such unit we have arbitrarily selected the A. U. of the continuous background about 2′.3. The total intensities of several lines in these A. U. are represented by crosses in Fig. 2—4. The circles are the corresponding values where the total intensity falls off along the line proportionally to that of the continuous background, the point of intersection of both curves being arbitrarily selected near 2′.3 (otherwise the curve drawn through the circles would represent the change of intensity of the continuous background).

* This paper was send to press already in 1938, but could be printed only after the war. The result of § 2 is in harmony with those of Lyot and Waldmeier received without eclipse in the last years.

Fig. 2—4 lead to the conclusion that the total intensity of emission lines falls off more rapidly with increasing distance from the limb than that of the continuous background. This holds for all lines except 4231. Our result with regard to the failure of the proportionality between the intensity gradient for the emission lines and the continuous background differs from

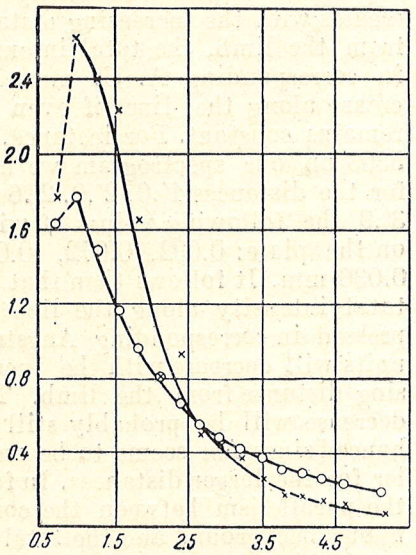

Fig. 2. The intensity of the emission line 3987(crosses) and of the continuous background (circles) as a function of the distance from the limb. The point of intersection of the curves is selected arbitrarily.

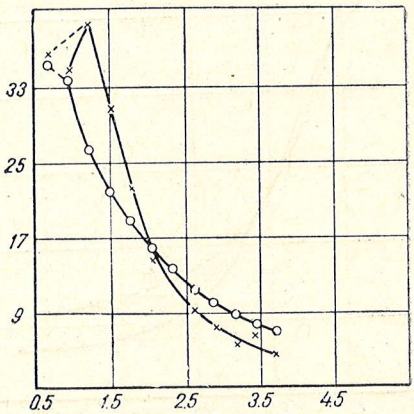

Fig. 3. The intensity of the emission line 5303 (crosses) and of the continuous background (circles) as a function of the distance from the limb. The point of intersection of the curves is selected arbitrarily.

Grotrian's one. Owing to the importance of this question we must clear up the cause of the disagreement.

Grotrian's curves (l. c., Fig. 1—11) represent the change of *J cont.* + + *J line centre* and *J cont.* with the increasing distance from the solar limb. Our observations show also an approximate parallelism between *J line centre* + *J cont.* and *J cont.* In this respect there is no sensible difference between Grotrian and myself. Basing on the observed parallelism in question, Grotrian comes to the important conclusion that the intensity of emission lines is proportional to that of the continuous background. This result is emphasized in Unsöld's «Physik der Sternatmosphären» (p. 450) and in several other textbooks. However we think, that this conclusion is undue, especially if extended on the proportionality between the density of matter responsible for the continuous background (electrons) and the emission lines (probably ions). It is obvious that in order to decide this question we must consider the change of total intensity along the line, but not of the central intensity, affected in addition by some instrumental factors. Let us assume that there is a complete parallelism between *J cont.* and *J cont.* + *J line centre* along the line, though, in reality our curves and Grotrian's ones show for many lines a decrease of Δm for the larger distances from the limb. Grotrian's equivalent width for 5303 is 27.5 A. U. at the distance 2'.5 while Δm derived from his Fig. 3 is only 1.3. Since the actual width of 5303 is about 1 A or smaller, the width of this line on the spectrogram because of the instrumental and especially of the

photographic widening must be of the order of several Angströms, at least at small distances from the limb. G r o t r i a n has cut out the central portion of the line of 0.025 mm width or somewhat more than 1 A on the plate. Our central intensity measured with the self-registering microphotometer relates to a still smaller value of $d\lambda$. Since the width of different portions of the line on the plate evidently decreases with the increasing distance from the limb, the total intensity in corresponding A. U. must decrease along the line, if even Δm remains constant. For instance, for 5303 on our spectrogram we have for the distances 1′.0, 2′.0, 2′.6 and 3′.9 the following values of width on the plate: 0.092, 0.072, 0.056, 0.036 mm. It follows then that the total intensity along the line expressed in corresponding Angström units will decrease with the increasing distance from the limb. This decrease will be probably still enhanced since Δm seems to be smaller for the larger distances. In fact, the parallelism between the continuous background and the total intensity breaks off, as it is seen on Fig. 2—4, the intensity gradient for the emission lines being more rapid. I think, that the same would be obtained from G r o t r i a n's observations, if instead of the intensities of central portions of lines, the total intensities were used. At last, only the total intensity must have here any physical meaning.

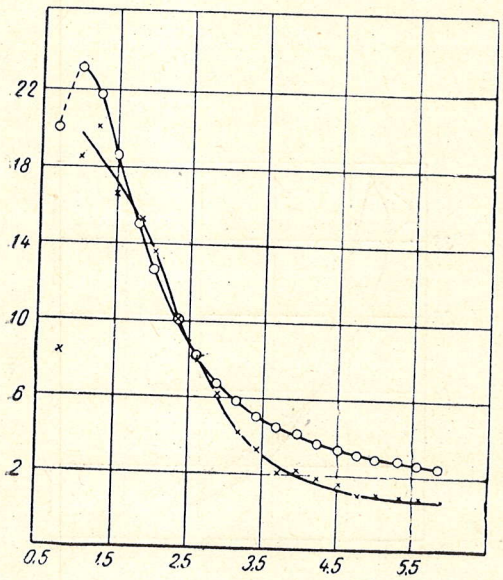

Fig. 4. The intensity of the emission line 6374 (crosses) and of the continuous background (circles) as a function of the distance from the limb. The point of intersection of the curves is selected arbirarily.

We have also another general evidence in favour of our result. A current opinion is that the emission lines appear only in the inner corona. May be, this is not quite correct, and the emission lines extend somewhat farther, at least several of them. On our spectrogram only the trace of 4231 may be seen at the distance of 8′ from the limb. On the other hand, 3987 disappears at the distance 5′—6′, though the continuous background remains to be perceptible here. According to J. H. M o o r e, the corona in 1922 extended on the spectrogram not less than to 35′, while the maximum extent of the line 5303 is about 8′ (5). The microphotometer tracing of L u d e n d o r f f' s spectrum of the 1922 corona taken by W. G r o t r i a n shows no trace of such fair emission lines as 4231, 4086 at the distance of 14′ from the limb (6). Since one may see on the same microphotogram the faint absorption lines, the photographic density seems to be suitable also for the manifestation of the emission lines. If, therefore, the emission lines merge gradually in the continuous background at the distance 5′—10′, the inevitable conclusion follows that the intensity gradient for the emission lines is greater than for the continuous background.

At the hypothesis that the matter in whole remains neutral, the proportionality or non-proportionality between the emission lines and the continuous background must lead generally to different suggestions with regard

to the stage of ionization of atoms responsible for the emission lines. This is at least of value when interpreting the chromospheric emission lines. But it is doubtful whether the presence of free electrons in the corona is controlled only by the ionization even in the inner corona.

§ 4. When approaching to the limb the curves in Fig. 2—4 mostly bring out a delay in the increase of intensity near 1′. Still stronger this is manifested on the spectrograms taken in 1929 by W. Grotrian. However it is not to be concluded, that for the distance about 1′ there is really a maximum brightness for the lines and continuous spectrum. This part of the corona was exposed less, owing to the motion of the moon, than the more distant region. In addition, near the edge some photographic effect may be sensible, especially when the emission lines are overexposed. A defect in the guiding, on the other hand, is also very dangerous, especially for the edge. It must be emphasized, that the delay in the increase or even the decrease of intensity, which is highly strong on Grotrian's curves 1—11, takes place not only for the emission lines, but also for the continuous background. Keeping in mind that the direct photographs of the inner corona taken at very short exposures do not show usually anything like, we must ascribe the measured strong decrease of the intensity of the continuous background in Grotrian's curves to some kind of occasional local effect or even to a systematic error. For this reason, the delay, or even decrease of intensity of emission lines, especially strong in Grotrian's Figures 1—11, cannot be accepted as a real behaviour of these lines near the limb.

Our curves representing the change of *J line centre* + *J cont.* and *J cont.* with the increasing distance from the limb bring out small irregularities. The latter are much stronger on Grotrian's curves (L. c., Fig. 1—11). This large difference, as well as the irregularities themselves, may be reasonably explained. The slit of our spectrograph was arranged nearly along the solar equator, while the slit in 1929 crossed the disc by a small chord and was arranged perpendicularily to the moon's motion. The former arrangement is probably more suitable for the study of the change of the intensity of emission lines and continuous background with the increasing distance from the limb. In Grotrian's arrangement, when the slit embraces a considerable range with respect to the position angle, we have properly a combined effect: the intensity change in the radial direction and the change by the position angle. The latter, owing to the presence of rays, arches and other details of different brightness, may be considerable. The local effect in the radial direction must be generally much smaller. The irregularities in question must be primarily ascribed to the local effect, especially if the slit is arranged perpendicularily to the moons motion, and in addition crosses a disturbed region, for instance, a prominence, as this occurred in 1929. For this reason our curves characterize better the fall of the intensity with the increasing distance from the limb.

§ 5. It may be suggested that the relative gradient of different lines is not the same. Particularily the gradient for 4231 seems to be slower. It is obvious that the study of the difference in the gradients in question is promising. At least, the discovery of the difference in the gradients for the chromospheric lines leads, as known, to important results. On the other hand, this may be of value from the point of view of classification of coronal emission lines.

I should like to note that the observations of 1936 favour the relationship between 3801 and 3987. As compared with the 1929 eclipse the lines 3801 and 3987, especially the first one, are increased in intensity with respect to 4086. A revision of the results of previous eclipses leads to the conclusion that

3801 and 3987 are possibly related. In fact, they are included in one group by Lockyer and Fowler, Campbell and Moore, Stratton and Davidson. Grotrian was not able to measure 3801 in view of its faintness, but 3987 is also fainter than 4086, contrary to the observations of 1936 and 1926 (7). In connection with the relative faintness of 4086 in 1936 one may mention that Mitchell, Stratton and Davidson

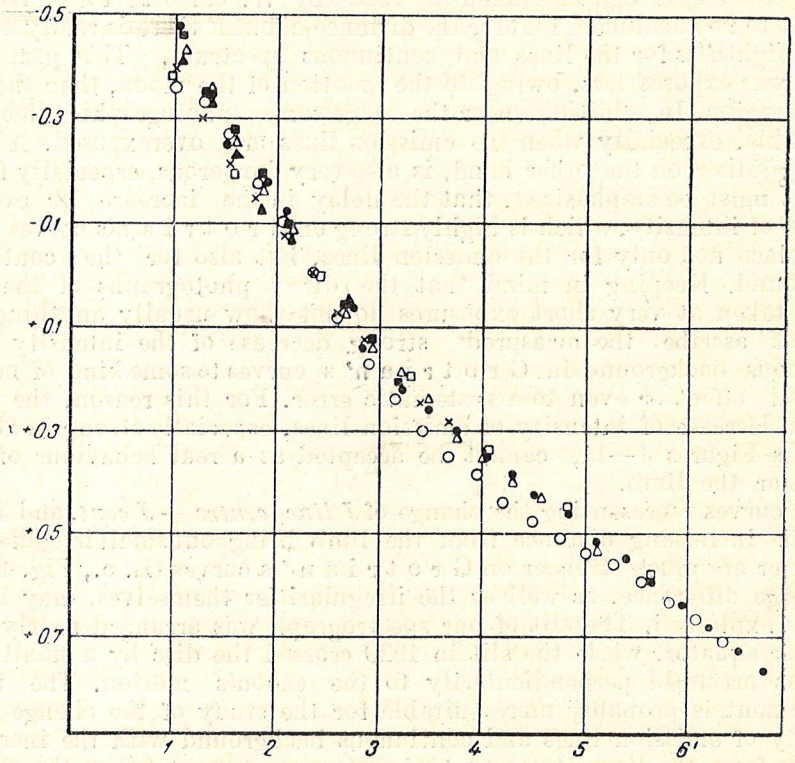

Fig. 5. The intensity of the continuous background as a function of the distance from the limb. Ordinates are log J. 6374—○, 5303—×, 4231—•, 4086—■, 3987—△, 3801—▲ Open squares are log J according to Baumbach's mean curve.

associate this line with 3601, which undergoes according to Mitchell to very sensible variations from one eclipse to another (8).

§ 6. May be it is worthy to mention that the intensity gradient for the continuous background as a function of distance within 1′—6′ from the limb does not seem to be sensibly dependent on wave-length. It is true, that a slit spectrograph is not the best instrument for this study. In Fig. 5 are plotted circles, dots, crosses, triangles a. o. representing the intensity of continuous background for different wave-lengths as function of distance from the east limb. As it is seen, the different marks lie closely, and this tests generally that within 1′—6′ our observations can reveal no sensible dependence of the gradient on wave-length.

§ 7. The comparison of the coronal and chromospheric lines presents considerable interest. The total intensity of the brightest coronal line 5303 (Table I) is equal to about 20 A. U. Let us express this value in terms of A. U. of the continuous background of the solar spectrum (centre). Using the data of the photometric measurements of the corona in past eclipses

and particularily those obtained in 1936, we may estimate that at the distance 2′ from the limb the surface brightness of the corona is nearly equal to 2×10^{-6} of the sunlight in the centre. In these new units the intensity of 5303 is nearly equal to 4×10^{-5} .. If the intensity gradient for 5303 holds with the approach to the limb, we may expect its intensity to be at the distance 5″ —10″ from the limb equal to 10^{-4}. On the other hand, the intensity of such strong chromospheric lines as H_β and D_3 at the distance about 2″ —3″ is nearly 6×10^{-2} and 2×10^{-2} respectively. The faint chromospheric lines 4713 and 4009 have at the distance 1″ —2″ the intensity of the order 2×10^{-4} and 2×10^{-5}. Therefore, if the line 5303 even does not increase in brightness with the approach to the limb from 2′, it must be probably observed among the chromospheric lines. However, there are probably no data, that the coronal lines are strong in the lower layers of the chromosphere.

Lyot found occasionally the intensity of 5303 at the distance 35″ from the limb to be equal to 1.2×10^{-4}. However, owing to the considerable variation of intensity of 5303 one cannot lay great stress upon the closeness to our value 10^{-4}. According to S. A. Mitchell, the lines 5303 and 6374 are well visible on the grating photographs even at the short exposure for the second flash, but the height is not fixed. But it is known, that H. D. and H. W. Babcock were able occasionally to find without eclipse the line 5303 only in the higher layers of the chromosphere (9). In general, on the basis of the meagre data partly of indirect character, one may suggest, that the coronal lines are to some extent weakened in the lowest layers of the solar chromosphere, or at least, are not much strenghtened with regard to the intensity at the distance near 1′—2′. May be, there is in this respect some analogy between the helium and coronal lines, since for the former the intensity decreases somewhat with the approach to the limb, or, at least increases much slower as compared with the lines of other elements.

§ 8. For the interpretation of the nature of the corona it is of importance to know the spatial distribution of the matter responsible for the continuous spectrum and the emission lines. For this purpose it is first necessary to pass from the observed intensity $J(\rho)$ to the radiation per cm^3 $F(r)$ as a function of the distance from the centre of the sun.

$$J(\rho) = \int_{-\infty}^{+\infty} F(r)\, dz$$

The solution of this Abel's integral equation leads, as known to

$$F(r) = -\frac{1}{\pi}\int_{r}^{\infty} \frac{J'(\rho)\, d\rho}{\sqrt{\rho^2 - r^2}}$$

Applying the method of numerical differentiation and integration we are able to determine the radiation per unit volume.

It is more difficult to get the density $D(r)$ from $F(r)$ since the result depends to some extent on the assumption with respect to the nature of radiation. For the emission lines we have a known relation connecting the number of atoms per cm^3 in the upper state n_k with the energy $F(r)$ radiated per cm^3:

$$F(r) = A_{k\to j}\, n_k\, h\nu$$

This formula allows to compute basing on the observed values $J(\rho)$ the

change of concentration of the matter responsible for the emission lines. Though the intensity gradient somewhat varies from one line to another, we have combined all the lines together. Owing to the lower accuracy of the measured total intensities of emission lines at the distance $<1'.5$ we do not consider them at all. The accuracy is especially low for 6374. The line 4231, showing a much smaller gradient was not accounted for. But even in this case the accuracy of the mean values of $J(\rho)$ and $F(r)$ is low.

For the continuous background $J(\rho)$ were taken from Fig. 5. The smoothed relative values of $F(r)$ for the lines and the continuous background are represented in Fig. 6.

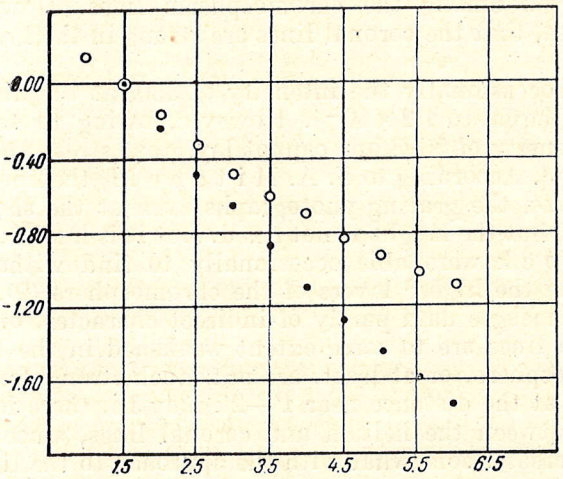

Fig. 6. The change of the radiation per cm³ with the increasing distance from the limb. Circles and dots relate to the continuous background and to the emission lines respectively. Ordinates are log $F(r)$.

For the coronal emission lines the function $F(r)$ is evidently proportional to the concentration n_k. In fact, $F(r)$ depends here on the concentration of free electrons, on the intensity of solar radiation at this point and on the angle between the falling and scattered ray. We have computed the density of electrons $D(r)$ from $F(r)$ with fair approximation, and the results are represented in Fig. 7 (circles). In the same Fig. 7 are plotted the dots representing the relative numbers for the concentration of the particles responsible for the emission lines. Ordinates to the right relate only to circles and they represent the absolute values of the density of free electrons per cm³. When computing this, we have based on the assumed number of free electrons 4×10^8 per cm³ near the solar surface.

It may be generally shown that when passing from the observed brightness $J(\rho)$ to $F(r)$, the gradient in question increases. But when passing from $F(r)$ to the density $D(r)$ for the scattering particles, the gradient decreases again and the final effect is that the gradient for $D(r)$ becomes somewhat smaller than that for $J(\rho)$. On the contrary, for the radiating particles the gradient for $D(r)$ coincides with that for $F(r)$ which is larger than that for $J(\rho)$. Therefore the observed difference between the gradient for the emission lines and the continuous background is to be only strengthened when passing to the density of the radiating particles and free electrons respectively. From Fig. 7 one may derive that, while the concentration of free electrons

within 1'.5—5'.5 from the limb decreases nearly 6 times, the corresponding decrease for the atoms is nearly 40.

It is obvious that the accuracy of the measured intensities of the emission lines is low, and the derived results cannot be exaggerated. Especially it is very difficult to escape or even to estimate the systematic error. However, the effect revealed in Fig. 7 seems to be quite real, at least qualitatively.

It is to be mentioned that our measurements may be affected by an error

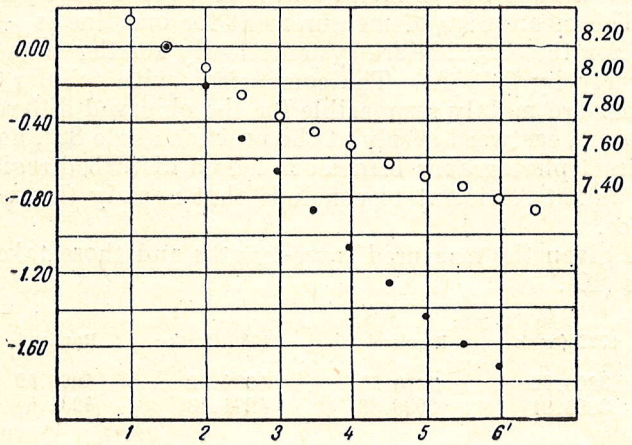

Fig. 7. The change of the density with the increasing distance from the limb. Circles and dots relate to the matter responsible for the background and the emission lines respectively. Ordinates to the left are log of relative values of the density. Ordinates to the right are log of the number of electrons per cm^3.

connected with an oversight in the adjusting of the new slit of the spectrograph (p. 98). The halves of the east portion of the slit proved to be not in the very same plane, and this produced some kind of interference effect in the spectrum. In connection with this some troubles arise when drawing the continuous background on the microphotograms. To check the effect in question we measured the ratio of intensities of several chromospheric hydrogen lines in the violet-blue part of the spectrum (their traces on the continuous background of the corona) for the east and west sides separately and did find no sensible difference. Since the spectrum of the west side is free from the effect under consideration, we think that our measurements of total intensities of coronal lines and of the relative gradients are not seriously affected by the error in question.

§ 9. Wave-lengths of emission lines. The coronal emission lines are sufficiently sharp and may be measured very accurately, but it is generally difficult to escape the systematic error. It seems to be highly desirable in addition to the iron or titanium spectrum to have here as a reference spectrum also the chromospheric lines. Still better, when the stronger chromospheric lines, owing to the scattering in the earth's atmosphere, are superposed on the continuous spectrum of the corona, resembling to some extent to coronal emission lines. We have just such a case on our spectrogram. The emission iron spectrum turned out to be not quite symmetrical with respect to the coronal spectrum, but a number of chromospheric lines superposed on the continuous spectrum of the corona allows surely to eliminate the very small systematic error in question. The wave-lengths of the chromospheric lines were taken from Rowland's Revision and for the stronger ones the laboratory values were used.

We have measured the wave-lengths of coronal emission lines only in the photographic part of the spectrum where the dispersion used is not too small (29 A per mm at H_δ). To the red from 4300 the spectrum is too overexposed and the faint emission lines are very poor or invisible. The poor line 4567 shows large disagreement in the measurement and is omitted. We have been able to measure in the photographic region under consideration 30 chromospheric lines, the height of which in the chromosphere is of the order of 2500 km or more, and four coronal lines on the east and west sides. The mean error of measurement for one line is ± 0.08 A. The wave-lengths for the east side are systematically smaller than those for the west one (nearly by 0.13 A). The comparison with tabular values shows that the former are mainly responsible for the observed difference. The slit crosses the corona eastward nearly at the position angle 82°, and the comparison with direct photographs brings out here a disturbed region. However, the accuracy is not sufficient to conclude that namely this is the cause of the divergence.

Below are given the measured wave-lengths and those taken from Rowland's Tables (10).

1936 Omsk	Rowland	1936 Omsk	Rowland
3800.72	3800.77	4086.22	4086.29
3986.91	3986.88	4231.13	4231.4

§ 10. Absorption lines. At the time of the eclipse the sky was covered with thin clouds and, probably for this reason, the maximum extent of the corona on the spectrogram is about 7′—9′ even in the brightest region of the spectrum. Just here on the very faint continuous background are seen, though not surely, several absorption lines. I tried to measure their wave-lenghts and they are probably just the strongest lines in the solar spectrum: 4045, 4077, 4226, 4383 and may be one or two others. However these lines are so faint that no conclusion can be made with respect to the displacement as well as to their intensity and width. In the inner corona is clearly seen in the visual region the telluric absorption line 6277.

As it is known, the absence of absorption lines in the spectrum of the inner corona is usually ascribed to the rapid thermal motion of free electrons scattering the solar light. The mean velocity of electrons at a surface temperature $T = 4850°$ is nearly 265 km/sec. One think, therefore, that the shallow and broad lines of the order of 10 A at λ 4000 are becoming invisible. Such an usual estimate is, however, too inaccurate. First, we must consider not the mean velocity, but the distribution of velocities of electrons, say the Maxwellian one. Secondly, we must consider a summary effect of this distribution both with reference to the sun as a source of light and with reference to the observer. In our computations we confined ourselves to a very simplified case when the line connecting the centre of unit of volume with the centre of the sun is perpendicular to the line of sight. This is a better approximation for the computation of a line profile as compared with the mere estimate of line width based on the mean thermal velocity.

It seems to be evident that the usual narrow lines in the solar spectrum in the case of thermal velocity of free electrons turn out very faint or invisible. But as the best criterion for the theory under consideration may serve such strong and wide lines as K and H, the width of which is greater than the Doppler broadening in question. In such a case the profile will be much distorted, but the line will remain prominent even in the spectrum of the inner corona. The computed profile of the K line is given in Fig. 8. When

computing the profile in question, we used an undistorted one observed in the solar spectrum taken with our spectrograph. As seen, there is a sensible difference in central intensity which increases from 0.10 to 0.30. In

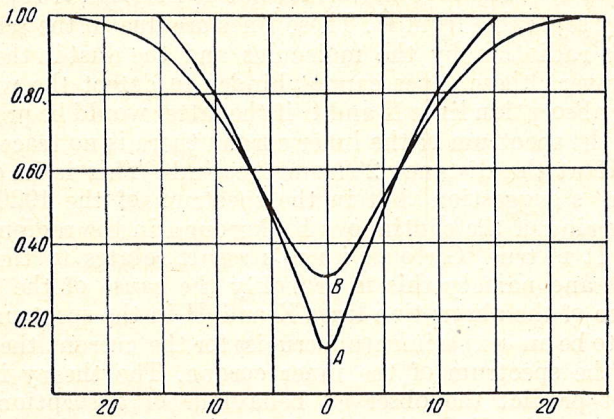

Fig. 8. A— the observed profile of the line K in the solar spectrum, *B*— the computed profile of the line K in the spectrum of the corona. Abscissae are Angströms, ordinates are intensities.

this case the K line must be easily observed in the spectrum of the inner corona, being at least as strong as, for instance, the hydrogen lines in the

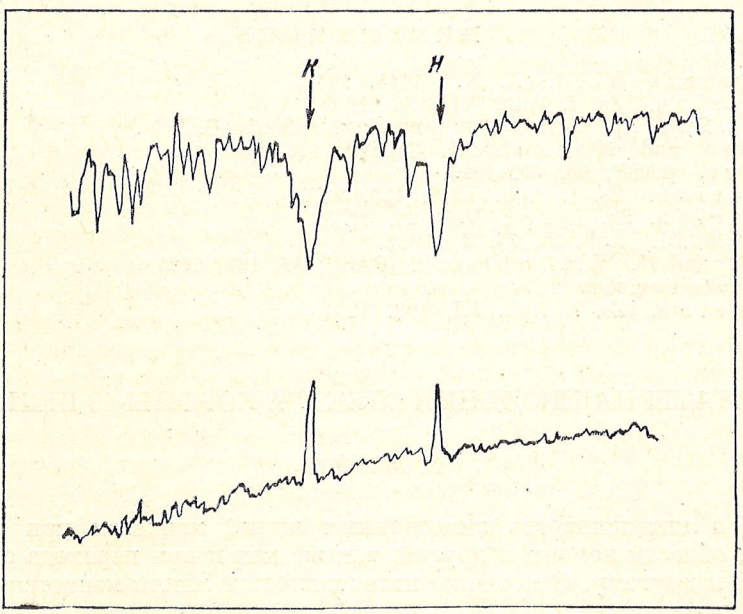

Fig. 9. Microphotometer tracing of the spectra of the Sun (top) and corona (bottom) in the region of the lines K and H.

spectrum of A type stars. The result will be not too much altered if we adopt for the electron temperature 6000 or 8000°.

The photographic density on our spectrogram at λ 3900—4000 is just suitable for the discovery of a very small lowering of the continuous background in the region of the K and H lines, if the Doppler broadening would

be even much greater than the expected one. The microphotometer tracings of the spectra of the sun and of the west side of the corona at the distance about 2′ from the limb are given in Fig. 9. On the latter we see very strong narrow emission lines K and H and somewhat to the right of H a faint emission H_ε not clearly separable from H. These lines are due to the scattering of the chromospheric radiation by the molecules and the dust in the earth's atmosphere. However these lines cannot hinder to detect the wide and sufficiently strong absorption lines K and H if the latter would be present. We may assert that in the spectrum of the inner corona there is no trace of absorption lines K and H at the distance 2′ from the limb. This is in opposition to Grotrian's suggestion that in the spectrum of the 1929 corona there is a small lowering of the continuous background in the region of the K and H lines (11). It is true, Grotrian's result relates to the distance 14′ from the limb and namely this is probably the cause of the disagreement.

The absence of the absorption lines K and H in the spectrum of the inner corona seems to be an «experimentum crucis» for the current theory of absorption lines in the spectrum of the inner corona. The theory in the present state does not predict the observed behaviour of absorption lines in the coronal spectrum. The disappearance of the lines K and H may be expected only at the mean velocity of the electrons of the order of many thousand km/sec. The supposition that the absence of absorption lines K and H in the spectrum of the inner corona is due to any motion of such high speed electrons leads to consequences which may be of importance for the problem of the corona in the whole and for allied branches of astrophysics and geophysics.

REFERENCES

1. Schwarzschild. A. N. 4614, 1912
2. Grotrian, Zs. f. Aph. VII, 26, 1933
3. Lyot. Zs. f. Ap. V, 73, 1932 (and short notes in C. R.)
4. Cillié and Menzel. H. C. **410**, 1935
5. Moore. PASP, **35**, 59, 1923
6. Grotrian. Zs. f. Aph. VIII, 129, 1934
7. Grotrian. Zs. f. Aph. VII, 26, 1933
8. Mitchell. Aph. J. **75**, 1, 1932
9. H. D. and H. W. Babcock. PASP, **46**, 132, 1934
10. Rowland's Revision, 226
11. Grotrian. Zs. f. Aph. **III**, 199, 1931

РЕЗУЛЬТАТЫ НАБЛЮДЕНИЯ СПЕКТРА КОРОНЫ 19 ИЮНЯ 1936 г.

Г. ШАЙН

Полная интенсивность эмиссионных линий меняется при переходе от одной области короны к другой, так же как и при переходе от одного затмения к другому. Отношение интенсивностей линий меняется в значительных пределах.

Градиент для эмиссионных линий больше градиента для непрерывного спектра (исключая, вероятно, линию 4231).

Наблюдаемые колебания в градиенте для эмиссионных линий и непрерывного спектра должны быть приписаны локальному эффекту.

Реальность наблюдаемого замедления в нарастании интенсивности или даже уменьшения интенсивности эмиссионных линий в пределах 0′—1′ сомнительна. Только на основании некоторых косвенных соображений можно заподозрить наличие уменьшения для расстояния 0′.5.

Изменение интенсивности непрерывного спектра в пределах 1′—6′ не обнаруживает заметной зависимости от длины волны.

Плотность материи, ответственной за непрерывный спектр (электроны), меняется от 1.6×10^8 до 0.3×10^8 в пределах 1′.5—5′.5. Соответствующее изменение для частиц, ответственных за эмиссионные линии, в 6—7 раз больше.

Измерены длины волн эмиссионных линий 3801, 3987, 4086 и 4231.

В спектре внутренней короны не обнаруживается и следов линий поглощения K и H. Сравнение с вычисленным профилем для этих линий приводит к полному разногласию с теорией теплового движения свободных электронов, рассеивающих солнечный свет.

SYSTEMATIC DISPLACEMENTS OF SPECTRAL LINES IN THE SPECTRUM OF o CETI

P. TH. SHAJN

It is shown that for the lines with E. P. < 0.20 there is a systematic negative shift reaching about 3-4 km/sec.

In this note is considered the question on the systematic displacements of spectral lines in the spectrum of o Ceti in dependence on the excitation potential. The dispersion used by us is moderate (about 36 A mm at Hγ) and the spectral lines in the overwhelming majority are blends. A great attention was paid to the selection of spectral lines available for the measurements. We hope that the main component in these blends contributes probably not less than 50 percent of the total intensity. However the lines with the excitation potential higher than 2.00 are very faint and it is very difficult to find here a predominant component. When selecting the lines in question the following sources were used: Rowland's Revision (1), Merrill's list of spectral lines for the long period variable stars (2), Miss Davis' list for α Scorpii (3), Hacker's list for α Bootis (4)

The list of spectral lines used is given in Table I (in the third column the chief contributor).

The number of the measured lines on a spectrogram usually did not surpass 50. One may hope that in the mean based on a considerable number of the measured blends the individual deviations will be after all smoothed. Three regions of the spectrum have been measured separately 3720—4020, 4000—4240, 4220—4500, and for each of them we have had 5, 7 and 10 spectrograms respectively.

Our aim was only to study the differential effect in the radial velocities for the diverse groups of spectral lines. The lines were divided into four groups 1) E. P. < 0.20, 2) E. P. between 0.20 and 1.00, 3) E. P. between 1.00 and 2.00, 4) E. P. > 2.00. The differential shift with respect to the first group is as follows:

E. P.	I	II	III	Mean (in A)	p. e.	Mean (km/sec)
0.20—1.00	+0.03	+0.05	+0.07	+0.05	±0.01	+3.5
1.00—2.00	+0.01	+0.04	+0.13	+0.06	±0.03	+4.3

TABLE I

λ	E. P.	Element	λ	E. P.	Element	λ	E. P.	Element
3859.92	0.00	Fe I	4008.94	0.02	Ti I	4226.74	0.00	Ca I
3867.63	0.04	V I	4020.40	0.00	Sc I	4232.74	0.11	Fe I
3872.51	0.99	Fe I	4023.69	0.02	Sc I	4254.35	0.00	Cr I
3875.97	0.02	V I	4024.58	0.05	Ti I	4258.33	0.09	Fe I
3878.58	0.09	Fe I	4030.77	0.00	Mn I	4260.49	2.39	Fe I
3883.29	0.98	Cr I Fe I	4033.08	0.00	Mn I	4271.78	1.48	Fe I
3886.30	0.05	Fe I	4034.49	0.00	Mn I	4274.81	0.00	Cr I
3890.20	0.04	V I	4035.74	2.13	Mn I	4289.73	0.00	Cr I Ca I ?
3892.90	0.04	V I	4045.83	1.48	Fe I	4291.48	0.05	Fe I
3895.66	0.11	Fe I	4063.61	1.55	Fe I	4294.15	1.48	Fe I Ti II
3899.72	0.09	Fe I	4077.73	0.00	Sr II	4302.54	1.89	Ca I
3902.26	0.07	V I	4090.58	1.08	V I	4325.78	1.60	Fe I
3906.49	0.11	Fe I	4105.27	0.00	V I	4330.03	0.00	V I
3920.27	0.12	Fe I	4111.79	0.30	V I	4332.83	0.02	V I
3922.92	0.05	Fe I	4115.18	0.28	V I	4344.51	1.00	Cr I
3924.54	0.02	Ti I	4116.54	0.27	V I	4347.24	0.00	Fe I
3944.02	0.00	Al I	4123.51	0.26	V I	4375.95	0.00	Fe I
3948.68	0.00	Ti I	4128.10	0.27	V I	4379.24	0.30	V I
3956.34	0.02	Ti I	4132.03	1.60	Fe I	4395.15	0.27	V I
3958.22	0.05	Ti I		0.28	V I			
3961.54	0.01	Al I	4147.68	1.47	Fe I	4404.76	1.55	Fe I
3979.53	0.10	Co I	4149.77	0.05	Fe I	4415.14	1.60	Fe I
3982.49	0.00	Ti I	4173.93	0.99	Fe I	4427.32	0.05	Fe I
3989.77	0.02	Ti I	4199.99	0.09	Fe I	4482.18	0.11	Fe I
3998.65	0.05	Ti I	4206.70	0.05	Fe I	4489.75	0.12	Fe I ?
4005.26	1.55	Fe I	4215.86	0.00	Sr I Fe I	4494.58	2.19	Fe I

For the fourth group the measured shift is about +0.1 Å, but the number of lines here is very small and this result cannot be considered as real. On the contrary, the systematic shift for the lines with low excitation potential less than 2.00 seems to be real, at least qualitatively. It is to be noted that Adams (5) using the Couder spectrograph (the dispersion 2.9 A/mm) found recently that in the spectrum of o Ceti the radial velocity increases with the increasing excitation potential, the effect being however nearly two times as small as that found at Simeis. It seems to be probable that the above mentioned effect is to be rather treated in the sense that the systematic negative shift of spectral lines increases with decreasing potential of excitation.

REFERENCES

1. Revision of Rowlands Preliminary tables, 1928.
2. P. W. Merrill Ap. J. 93 p. 380, 1941.
3. D. Davis Ap. J. 89, p. 41, 1939.
4. S. Hacker. Contr. Princeton University № 16, 1935.
5. W. S. Adams Ap. J. 93, p. 11, 1941.

СИСТЕМАТИЧЕСКИЕ СМЕЩЕНИЯ ЛИНИЙ В СПЕКТРЕ o CETI

Н. Ф. ШАЙН

В этой заметке показано, что спектральные линии с потенциалом возбуждения меньше 0.20 обнаруживают систематическое отрицательное смещение относительно линий с более высоким значением потенциала возбуждения.

ERRATA

Page	Line	Instead of	Réd
11	3 from head	$A_\lambda = \frac{\pi e^2}{Mc^2}\lambda^2.10^8.\ NHf$	$A_\lambda = \frac{\pi e^2}{mc^2}\lambda^2.\ 10^8\ NHf$
20	Fig. 5 (2 from foot)	$y^3\ G^\circ$	$z^3\ G^\circ$
37	19 from foot	+ 15 25	+ 15 35
43	11 from head	± 4. 2	4.2
	11 from head	± 2. 1	2.1
53	14 from foot	± 2. 1	2.1
	8 from head	obtained va-	obtained
54	2 from head	vsim	m_{vis}
56	20 from foot	— 2. 0	— 7. 0
57	13 from foot	± 4. 2	4. 2
	13 from foot	3. 2	+ 3. 2
	12 from foot	± 2. 1	2. 1
59	12 from head	2^3P	2^3P°
	13 from foot	still shallower	more conspicuous
89	13 from foot	524	534
90	14 from head	655	5.65
102	8 from foot	where	if
	5 from foot	would represent	represents
104	12 from foot	1922	1923
108	20 from foot	In fact $F(r)$ depends	In fact $F(r)$ for the electrons depends
112	13 from head	14′	4′
115	15 from head, col. 4	4105. 27	4105. 17
	15 from head, col. 5	0. 00	0. 27